Regulation of Opioid Receptor Trafficking and Signaling by Opioid Peptides

by

Jennifer M. Kunselman

A dissertation submitted in partial fulfillment
of the requirements for the degree of
Doctor of Philosophy
(Cellular and Molecular Biology)
in the University of Michigan
2021

Doctoral Committee:

Professor Manoj Puthenveedu, Chair
Professor Robert Fuller
Professor Carole Parent
Professor Alan Smrcka

Jennifer M. Kunselman

jkunselm@umich.edu

ORCID: 0000-0002-9772-4149

Dedication

To Mom and Dad

Acknowledgements

I am incredibly thankful for the people in my life that have supported me throughout this PhD process. First, I would like to thank my mentor, Manoj for his persistent optimism and encouragement. At the end of my first rotation at Carnegie Mellon University, Manoj told me that his lab would be moving to the University of Michigan. I am very grateful that Manoj believed in my abilities as a scientist and wanted to bring me along with him. I never expected to end up in Ann Arbor, but I am so glad that I was able to pursue my PhD here and that I was able to meet so many outstanding people at the University of Michigan. Thank you to the rest of my dissertation committee: Dr. Fuller, Dr. Parent, and Dr. Smrcka for helpful suggestions, excellent questions, and career advice. I would also like to thank our collaborators, Dr. Lakshmi Devi, Dr. Ivone Gomes, and Dr. Achla Gupta, for working together with us on exciting projects.

Next, thank you to my wonderful lab mates. I will always treasure the friendships I made while working in the Puthenveedu lab. Thank you Zara for being a supportive and inspiring mentor. I would not be the scientist I am today without your guidance, excellent chats over two hour long lunches, and your music blasting in the TC room. Thank you to the original CMU crew that moved to Michigan—Zara, Steph, and Elena—I am so glad that we had each other. Thanks to Steph for always being so helpful and a wonderful resource. Thank you Candy and Josh—I am so lucky that I got to know both of you, not only as brilliant scientists, but as incredible humans. Candy, thanks for being my coffee buddy and for always keeping me on my toes in lab. Josh, I appreciate and thank you for all of our conversations together as we navigated graduate school.

I would also like to thank the fabulous four who are now senior students –Caroline, Loyda, Ian, and Hao. Thank you for bringing fresh ideas and even more fun into the lab. Caroline, I have especially enjoyed having the chance to be your mentor—you impress me every day. I am also very lucky to have gotten to know the postdocs in our lab: Prahatha, Kasun, and Aditya. You all are so intelligent and resourceful. Special thanks to Prahatha for being such a warm and supportive friend.

Lastly, I'd like to thank my friends and family. I am so grateful for my parents. They have supported me through every stage of my life—from basketball games to Latin conventions, from college to my PhD defense. Thank you for always being there for me and encouraging me to go after my dreams. I'd also like to thank my best friend, Gina, you have been there every single day for that last eight years even when we were physically distant. Thanks for listening to anything and everything I have to say. Next I'd like to thank Elena for being an amazing friend and roommate for the last several years and for putting up with me and Marla. Thank you to Marla for being the sweetest pup and keeping me grounded during stressful times. Finally, I'd like to thank my wonderful partner, Wesley, you have made my life exponentially better, and I am so excited to continue our adventures together in this next chapter.

Table of Contents

List of Figures

List of Abbreviations

Abbreviation	Definition
β2AR	β2-adrenoreceptor
DAMGO	[D-Ala2, N-MePhe4, Gly-ol]-enkephalin
GPCR	G protein–coupled receptor
KOR	kappa opioid receptor
MOR	mu opioid receptor
mSIRK	myr-SIRKALNILGYPDYD-OH
PDZ	post-synaptic density-95/disc large tumor suppressor/zonula occludens-1
PKA	protein kinase A
PKC	protein kinase C
PLC	phospholipase C
PTX	pertussis toxin
SpH	superecliptic phluorin
WT	wild-type

Abstract

All opioids - whether they are addictive opioid analgesics or endogenous opioids like endorphins produced by our body - activate one of three receptors in our brain. However, different opioids cause different effects, including effects on pain and addiction. How opioids generate this variety in signaling has been a long-standing question in the field. My thesis tests the exciting new idea that specific opioids traffic receptors to different compartments of the cell, from where they can signal in a compartment-specific manner.

In this dissertation I review the selective mechanisms that regulate G protein-coupled receptor (GPCR) trafficking, which highlight the complex framework underlying spatial regulation of receptor function. Lipid membrane dynamics, post-translational modifications, cell-specific protein interactors, and agonist-selectivity are all key determinants for selective GPCR trafficking.

Specifically, I focus on how opioid peptides may cause distinct functional outcomes through activation of the same receptor. To address this question, I use high-resolution imaging assays to examine how different dynorphin peptides regulated kappa opioid receptor (KOR) trafficking and post-endocytic sorting. Interestingly, we observe that highly related dynorphin peptides caused distinct opioid receptor trafficking fates (recycling vs. degradation) as well as compartment-specific signaling from late endosomes and lysosomes, depending on the peptide ligand that activated the receptor. Specifically, we show that KOR activation by dynorphin A leads to receptor degradation and activation from late endosomal compartments, while KOR

activation by the highly related dynorphin B leads to receptor recycling from Rab5 and Rab11 compartments, without endosomal signaling.

Further, I investigate the dynamic relationship between receptor signaling and receptor trafficking. Initially, we observed that agonist washout caused a decrease in mu opioid receptor (MOR) recycling. This finding led us to hypothesize that signaling downstream of receptor activation regulated receptor trafficking back to the cell surface, which regulates resensitization. To test this, I used total internal reflection fluorescence (TIRF) microscopy to detect real-time exocytic fusion events in living cells. I tested various components of known signaling pathways downstream of MOR activation using pharmacological inhibitors and phosphodeficient and phosphomimetic receptor mutants to quantitate differences in MOR recycling. Our results indicate that MOR recycling is regulated via an agonist-dependent G$\beta\gamma$ signaling pathway, resulting in the phosphorylation of the receptor's C-terminal tail to increase receptor recycling. I follow up on this work by further testing the role of receptor phosphorylation in regulating MOR trafficking and signaling. By understanding the signaling pathways that regulate receptor trafficking and resensitization, this work opens new avenues for potential druggable targets.

Collectively, this work increases our understanding of opioid physiology. Further, because the opioid receptor is a prototype for GPCRs - the largest and highly conserved family of signaling receptors in humans - the principles could be relevant across many physiologically relevant members of this family.

Chapter 1 Introduction

1.1 Mechanisms of Selective G protein-coupled Receptor Localization and Trafficking

Published as Kunselman, J. M., Lott, J., & Puthenveedu, M. A. (2021). Mechanism of Selective GPCR Trafficking. Curr. Opin. Cell Biol. 71, 158-165.

Abstract

The trafficking of G protein–coupled receptors (GPCRs) to different membrane compartments has recently emerged as being a critical determinant of the signaling profiles of activation. GPCRs, which share many structural and functional similarities, also share many mechanisms that traffic them between compartments. This sharing raises the question of how the trafficking of individual GPCRs is selectively regulated. Here, we will discuss recent studies addressing the mechanisms that contribute to selectivity in endocytic and biosynthetic trafficking of GPCRs.

Introduction

The regulation of signaling by membrane trafficking has traditionally been attributed to trafficking's role in controlling the number of signaling receptors on the cell surface (Sorkin and von Zastrow, 2009). For G protein-coupled receptors (GPCRs), the largest single family of signaling receptors (Pierce et al., 2002), the removal of activated receptors from the cell surface

by endocytosis and recovery of receptors on the surface by either recycling of internalized receptors or delivery of new receptors control the strength of response to extracellular ligands (Hanyaloglu and von Zastrow, 2008; Hausdorff et al., 1990). Recent studies, however, have highlighted more complex aspects of how trafficking regulates signaling. One is that GPCRs can signal from a variety of intracellular compartments (Sposini and Hanyaloglu, 2018; Lobingier and von Zastrow, 2019). Another is that mechanisms that regulate GPCR trafficking are heterogeneous, allowing selective control over the location and trafficking of individual GPCRs (Hanyaloglu and von Zastrow, 2008). These aspects have highlighted a new idea that the primary role of trafficking might be to move specific GPCRs between specific signaling complexes on different membrane domains, as opposed to simply regulating cell surface receptors (Crilly and Puthenveedu, 2020; Calebiro and Koszegi, 2019). In this review, we will discuss recent studies on endocytic and biosynthetic trafficking of GPCRs, focusing on example mechanisms that provide specificity in the midst of shared mechanisms.

Endocytic trafficking

The mechanisms of GPCR endocytosis and post-endocytic trafficking after receptor activation, which are common features of many GPCRs, have been exhaustively addressed in several reviews (Hanyaloglu and von Zastrow, 2008; Bowman and Puthenveedu, 2015; Bahouth and Nooh, 2017; Weinberg and Puthenveedu, 2019). We will discuss recent findings on receptor interactions and signaling pathways that provide selectivity within these mechanisms.

Selectivity in endocytosis of GPCRs

How the endocytosis of GPCRs is individually controlled has been a long-standing question, considering that the general mechanism is shared broadly across most GPCRs (Weinberg and Puthenveedu, 2019). Activated GPCRs undergo specific conformational changes that, in addition to catalyzing guanosine triphosphate (GTP) exchange on G proteins, allow GPCR kinases to phosphorylate the receptor C-termini. These phosphorylated C-termini are recognized by arrestins, which act as adapters that link receptors to the clathrin endocytic machinery (Tian et al., 2014; Gurevich and Gurevich, 2019A; Caron and Barak, 2019).

One aspect of this process that could be selective is receptor phosphorylation. Many GPCRs have multiple phosphorylation sites on its C-terminal tail, which are required for receptor internalization (Patwardhan et al., 2021; Gurevich and Gurevich, 2019B). For example, in the mu-opioid receptor (MOR), a phosphorylation cluster within residues 375-379 is the primary mediator of endocytosis (Lau et al., 2011; Arttamangkul et al., 2019), which might be driven mainly by GRK2 in HEK293 cells (Bouley et al., 2020). C-terminal sites may be phosphorylated hierarchically by multiple kinases (Just et al., 2013; Duarte and Devi, 2020), suggesting that each GPCR could have a set of kinases that phosphorylate it and drives endocytosis. For example, the receptor tyrosine kinase anaplastic lymphoma kinase (ALK) associates with the dopamine D2 receptor (D2R) but not the closely related dopamine D1 receptor. An inhibitor of ALK blocks internalization of D2R but not of D1R. ALK-mediated activation of protein kinase C g (PKCg) downstream of dopamine is required and sufficient for D2R internalization in HEK293 cells (He and Lasek, 2020). The exact ALK-dependent internalization mechanism is not clear, but PKCg

may influence the phosphorylation patterns of D2R and target interactions between D2R and arrestin.

For the vasopressin 2 receptor (V2R), differences in phosphorylation at specific residues tuned the strength of arrestin interactions and regulate endocytosis. Mutation of Ser 357 or Thr 360 to alanines reduced arrestin binding as measured by co-immunoprecipitation but still retained enough binding to be visualized as membrane recruitment by microscopy. This reduced binding in the case of Ser 357 mutation was still sufficient for qualitatively similar levels of V2R and arrestin localization to endosomes. In contrast, reduced binding in the case of Thr 360 mutation abolished arrestin localization to endosomes, although its effect on V2R endocytosis was not directly measured (Dwivedi-Agnihotri et al., 2020). Similarly, a naturally occurring variant at Thr 282 for the angiotensin II receptor 1 induced a distinct conformation of arrestin upon binding, which was less stable but still supported endocytosis (Cao et al., 2020). The second aspect of endocytosis that could be selective are "checkpoints" that exist after GPCR localization to endocytic domains (Figure 1.1). GPCR C-terminal tails contain specific sequences that interact with several components of the endocytic machinery. For example, a type I PDZ ligand on the C-terminus of the beta 2 adrenergic receptor indirectly links receptors to the actin cytoskeleton in clathrin-coated pits. This link delays the recruitment of dynamin, a GTPase that is required for membrane scission during endocytosis (Puthenveedu and von Zastrow, 2006). In contrast, PDZ-mediated interaction of mGluR1 and mGluR5, two metabotropic glutamate receptors, with the scaffold protein tamalin is essential for receptor endocytosis (Pandey et al., 2020). In this case, tamalin might link the receptors to motors via a scaffold protein S-SCAM, suggesting that it acts at a late step. An unrelated "bileucine" sequence on the C-terminal tail of MOR delays scission even after dynamin is recruited (Weinberg et al., 2017). The same receptor

might contain multiple discrete sequences that regulate endocytosis. The first intracellular loop of MOR contains specific lysines that are ubiquitinated by the ubiquitin ligase Smurf2. This ubiquitination, recognized by the endocytic accessory protein Epsin1, is required for endocytic scission (Henry et al., 2012). For the protease-activated receptor 1, ubiquitination- dependent recruitment of Epsin1 and the endocytic adapter AP-2 can induce receptor endocytosis in the absence of arrestins (Chen et al., 2011). The third intracellular loop of the beta 1 adrenergic receptor (B1AR) recruits endophilin, a BAR domain-containing protein that generates membrane curvature as part of the endocytic machinery, when linked to Giant Unilamellar Vesicles. Endophilin, once recruited via interactions of the third loop with the endophilin SH3 domain, can generate membrane curvature on these vesicles (Mondal et al., 2021). Specific local protein interactions of individual GPCRs might therefore delay or facilitate their own endocytosis by modulating endocytic components.

Figure 1.1

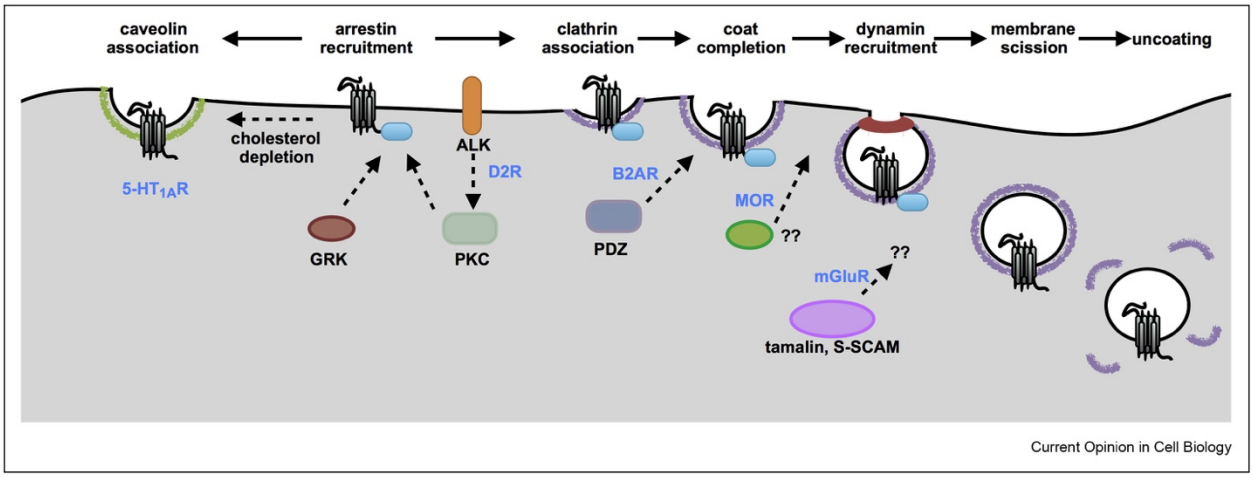

Figure 1.1 GPCR endocytosis is regulated by selective mechanisms. GPCR endocytosis from the plasma membrane can be regulated at multiple steps. The 5-HT1AR can switch between clathrin-dependent or caveolin-dependent endocytosis depending on cholesterol levels in the plasma membrane, which suggests that GPCR endocytosis can be regulated by the local

membrane environment. GPCR interactions with arrestin, a shared endocytic adapter, could be regulated by the slate of kinases that determine the phosphorylation patterns on the GPCR C-termini. The GPCR C-termini and cytoplasmic loops contain additional sequences that regulate later steps in endocytosis by interacting with structural scaffold proteins such as PDZ proteins or tamalin. Although these mechanisms are still not fully understood, newer methods including high resolution live cell microscopy and single molecule tracking may help us decipher the interplay between these factors, GPCRs, and the endocytic machinery.

A third aspect is the selective interaction of GPCRs with membrane lipids. The third intracellular loop of the B1AR, described previously, electrostatically interacts with anionic phospholipids, which interfere with SH3 recruitment (Mondal et al., 2021). GPCRs might localize to micro- domains, such as lipid rafts or caveolae on the surface, often in a regulated manner (Patel et al., 2008; Briddon et al., 2018). Activation of the glucagon-like peptide-1 receptor (GLP-1R) in pancreatic beta cells redistributes the receptors to membrane nanodomains that contain the lipid raft marker flotillin (Buenaventura et al., 2019). When cholesterol was depleted by methyl-b-cyclodextrin, GLP-1R failed to redistribute to nano- domains and to internalize. Receptor palmitoylation and different agonists regulated this redistribution, raising the possibility that the process could be regulated by signaling. The role that cholesterol interactions play could be specific for each GPCR. When cholesterol was depleted by statin drugs, 5-HT1A receptors (5-HT1AR) internalized, but the pathway switched from clathrin-mediated to caveolin-mediated endocytosis (Kumar and Chattopadhyay, 2020). Interestingly, when cholesterol was depleted to similar levels using methyl-b-cyclodextrin, 5-HT1AR still internalized via a clathrin-mediated pathway, although post-endocytic sorting was altered (Kumar and Chattopadhyay, 2021).

Several cholesterol-binding motifs, termed cholesterol consensus motifs, cholesterol recognition amino acid consensus (CRAC) motifs, or CARC motifs when they exist in reverse, have been identified in GPCRs (Fantini et al., 2016; Fatakia et al., 2019). In many cases, the

motifs have been functionally confirmed as being required for normal GPCR trafficking. A recent analysis of structural data across available GPCR structures, however, concluded that CRAC motifs are not predictive of cholesterol binding (Taghon et al., 2021). One potential way to reconcile these observations is that the motifs reflect potential hot spots of interactions (Sarkar and Chattopadhyay, 2020). Another way is to consider that lipid binding might be hierarchical, where allosteric changes caused by lipid binding on one site increases or decreases the affinity of other lipid-binding sites. In this context, it is important to note that the structural informatics (Taghon et al., 2021) was based largely on structures generated under conditions using synthesized lipids or detergents, which are different from in vivo environments where a full complement of lipids and proteins are present. Overall, much less is known about how lipids interact with GPCRs, compared with how proteins interact with GPCRs.

Selectivity in post-endocytic trafficking of GPCRs

Internalized GPCRs typically have two fates once they are internalized and trafficked to the endosomal system. They may recycle back to the cell surface or may be degraded in the lysosome (Bowman and Puthenveedu, 2015; Bahouth and Nooh, 2017). Nutrient receptors such as the transferrin receptor are recycled largely by bulk membrane flow (Mayor et al., 1993), but GPCR recycling requires specific sequences on receptors. These sequences both restrict GPCRs from recycling by bulk flow and direct GPCRs to sequence-dependent recycling or degradation (Hanyaloglu and von Zastrow, 2008; Bahouth and Nooh, 2017). Mutating two protein kinase A (PKA) phosphorylation sites on B2AR converts the receptor into a bulk recycling protein, suggesting that bulk sorting is hierarchically above sorting between sequence-dependent

recycling and degradation (Vistein and Puthenveedu, 2013). At present, the factors that restrict GPCRs from accessing the bulk recycling pathway are not known.

Spatial segregation of GPCRs in the endocytic pathway.

The endolysosomal system is now recognized as a complex mix of partially overlapping membrane systems that constantly mature along the endocytic pathway (Figure 1.2). The current model is that endocytosed GPCRs pass through the very early endosome (VEE) to the early endosome (EE). The VEE is marked by APPL1 but devoid of Rab5 and EEA1, which mark the EE. The luteinizing hormone receptor (LHR) and the follicle- stimulating hormone receptor (FSHR) are localized to the VEE after activation (Jean-Alphonse, et al., 2014). Many other GPCRs such as the prototypical B2AR are localized mainly to EE after activation (Puthenveedu et al., 2010).

Figure 1.2

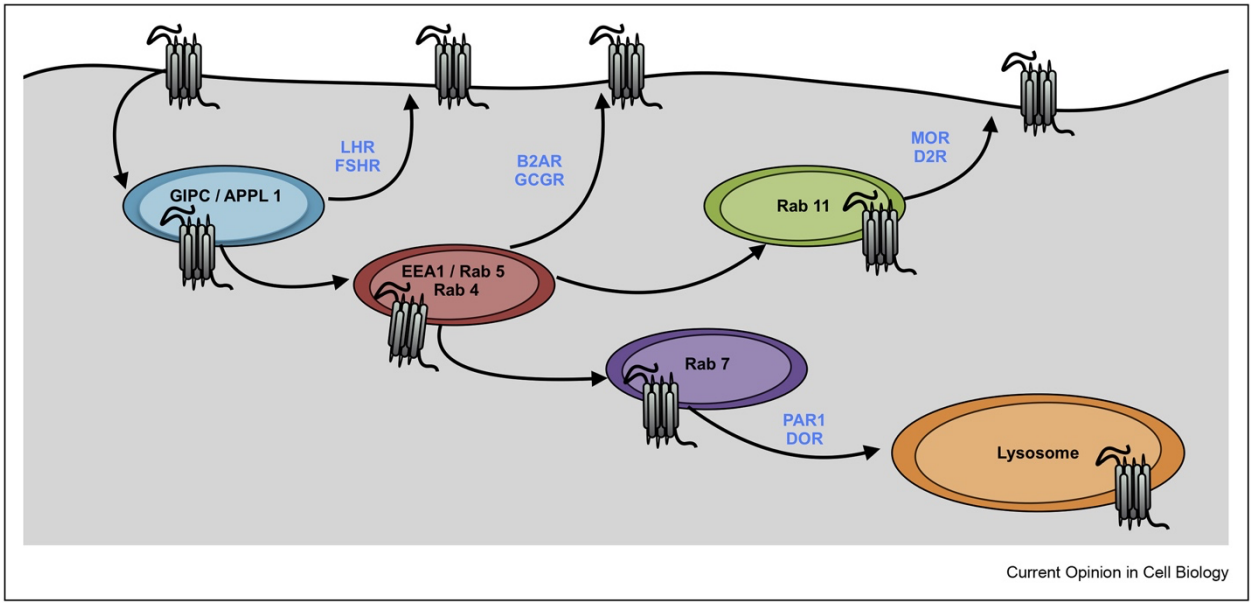

Figure 1.2. A sequential model for GPCR sorting throughout the endolysosomal network. After internalization from the plasma membrane, GPCRs are sequentially transported through the VEE and EE, at which point they are sorted into the RE or the late endocytic/degradative pathway. These compartments are marked by specific biochemical components. GPCRs can interact with specific recycling trafficking proteins in these compartments that direct them to the recycling pathway. Selected examples of markers for compartments and GPCRs that recycle from them are shown. It is important to note that these compartments are depicted separately to denote where the majority of components are at steady state. In vivo, these compartments are likely to overlap significantly because of dynamic membrane exchange and maturation.

The steady-state segregation of GPCRs in distinct compartments likely represents receptor recycling from that compartment. LHR and FSHR are rapidly recycled from the VEE via interactions of receptor C-termini with the PDZ-containing protein GIPC. Disrupting PDZ-GIPC interactions decreases recycling and shifts the steady state distribution of LHR to the EE and later compartments (Jean-Alphonse, et al., 2014). Similarly, B2AR is recycled from the EE by interactions of a PDZ ligand on its C-terminal tail with proteins in the actin-sorting nexin-retromer tubular domains of endosomes. Disrupting PDZ interactions decreases recycling and drives B2AR into the late endosomal pathway to be degraded (Cao et al., 1999). For the atypical chemokine receptor 3, overexpression of RAMP3, a PDZ-containing member of a family of single-transmembrane proteins that associate with GPCRs, and NSF qualitatively changes receptor localization from Rab7 late endosomes to Rab4 early endosomes, after an hour of agonist treatment and 4 h of washout (Mackie et al., 2019). GPCRs in the EE may also be trafficked to a dedicated recycling endosome marked by Rab11, from which they can recycle. Receptor interactions with these specific components and localization depend on a slate of posttranslational modifications on the receptor, such as phosphorylation or ubiquitination (Patwardhan et al., 2021).

Regulation of GPCR sorting by signaling

Signaling pathways downstream of the same receptor (homologous) or other receptors (heterologous) could selectively regulate the rates of sorting and recycling of GPCRs by inducing posttranslational modifications on select GPCRs. B2AR activity reduces the rate of B2AR recycling via receptor phosphorylation by PKA (Vistein and Puthenveedu, 2013). MOR activity, however, increases MOR recycling independent of PKA via phosphorylation at Ser 363 and Thr 370 by PKC downstream of receptor activation (Kunselman et al., 2019). The same sites on MOR can also be phosphorylated by PKC downstream of neurokinin-1 signaling to increase MOR recycling and resensitization, allowing for cross- talk between these signaling pathways (Bowman et al., 2015). For the chemokine receptor CXCR4, however, PKC activation drives receptor degradation, suggesting that the same signaling pathway can affect different receptors differently (Caballero et al., 2019). PKC phosphorylation of CXCR4 at Ser 324/ 325 recruits the ubiquitin ligase AIP4. PKC was sufficient but not necessary for CXCR4 degradation, suggesting that another kinase might phosphorylate one of these residues and recruit AIP4 (Caballero et al., 2019). Importantly, post-endocytic sorting mechanisms might be leveraged by physiological systems to fine tune the effects of receptor activation. Two endogenous ligands regulated the post-endocytic fate of the kappa opioid receptor (KOR) differently (Kunselman et al., 2021). Dynorphin B caused KOR to rapidly recycle via Rab11, whereas Dynorphin A caused KOR to be degraded in the lysosomes. Interestingly, KOR localized to the lysosomes was able to signal from there, causing a sustained signaling compared with when KOR was recycled.

Biosynthetic trafficking

The folding and export of GPCRs from the endoplasmic reticulum is regulated by a variety of interacting proteins and by exogenous drugs that act as chaperones (Zhang and Wu, 2019; Doly and Marullo, 2015). In contrast, whether and how GPCR trafficking after ER export is regulated is less well understood. In this section, we will discuss recent data describing the heterogeneous mechanisms that regulate GPCRs transport from compartments after ER export (Figure 1.3).

Figure 1.3

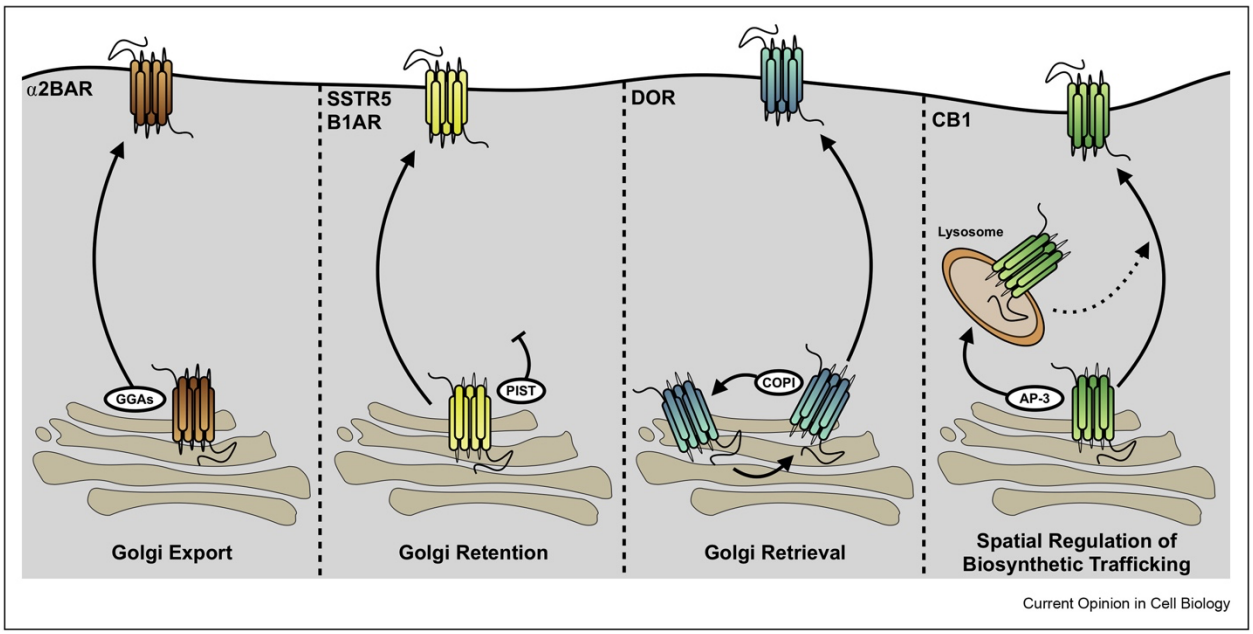

Figure 1.3. Post-Golgi trafficking of GPCRs can be regulated by diverse mechanisms. Example pathways by which GPCR export can be regulated. GPCRs such as the α-2B adrenergic receptor and angiotensin II receptor type I are exported by interactions with GGA proteins. SSTR5 and B1AR are retained in the Golgi via interactions with PIST, a PDZ-binding protein. DOR, on the other hand, is kept in the Golgi by constant retrieval via COPI interactions. CB1 is routinely trafficked to lysosomal compartments via AP-3 interactions, and disrupting these interactions redirects receptors to the plasma membrane. It is possible that additional pathways exist and that these pathways and interactions are relevant to different receptors in different cell types based on expression of components.

Many “general” trafficking proteins, such as small monomeric GTPases and their interactors, have been implicated in GPCR export from the Golgi apparatus (Zhang and Wu, 2019). For example, the trafficking of a2B-adrenergic receptors depends on the Golgi-localizing, gamma-adaptin ear homology domain, ARF-binding (GGA) family of proteins and Rab26 (Zhang et al., 2016A; Zhang et al., 2016B; Wei et al., 2019). GGA1, 2, and 3 all interact with the third intracellular loop of a2B-adrenergic receptor, although by different mechanisms. Depleting any one of the GGAs causes a partial reduction in surface delivery of a2B-adrenergic receptor, suggesting that each of them is partially required. GGA3 binds an RRR motif in the loop, whereas GGA1 and 2 do not. GGA3 depletion reduces export also of a2C-adrenergic receptors, but not of a2A-adrenergic receptors. Rab26 also binds the same intracellular loop in a GTP-dependent manner, regulated by the putative GAP TBC1D6 (Wei et al., 2019). Unlike for GGA3, linear motifs on the receptor required for GGA1, GGA2, or Rab26 could not be identified by deletion studies, suggesting that they may bind a multipartite motif based on a specific conformation of the loop. Interestingly, an alternatively spliced variant of GGA1 lacks the hinge region of GGA1 that interacts with the a2B-adrenergic receptor, suggesting that isoform expression could provide selectivity (Zhang et al., 2019). As another example, the export of PAR2 from the Golgi requires the activation of protein kinase D (PKD). In this case, PKD is activated by G$\beta\gamma$ translocation to the Golgi after PAR activation, causing a feedback loop for repopulating the surface after receptor downregulation (Zhao et al., 2019). G$\beta\gamma$ and PKD are required for general TGN export (Diaz Anel and Malhorta, 2005), and whether other cargo molecules are also regulated downstream of PAR2 activation is not clear. Nevertheless, it is clear that some GPCRs use the predominant TGN export pathways to traffic to the cell surface.

Selective mechanisms that localize specific GPCRs without affecting trafficking in general have also been recently identified. The Leukotriene B4 Receptor Type 2 (BLT2) contains an unidentified sequence on its C- terminal tail, which enables it to interact with the scaffold protein LIN7C (Hara et al., 2021). A truncated BLT2 without this tail accumulates in the Golgi. But when LIN7C is depleted, BLT2 accumulates in intracellular compartments not restricted to the Golgi. In contrast, over- expression of the PDZ protein PIST localizes somatostatin receptor 5 and B1AR to the Golgi (Wente et al., 2005; Koliwer et al., 2015), presumably by interacting with the C-terminal PDZ ligand on the receptor.

The delta opioid receptor (DOR) provides a unique and interesting example of a GPCR whose Golgi localization is cell type specific and highly regulated. In neurons, newly synthesized DOR is retained in intracellular compartments that overlap with the Golgi, but in nonneuronal cells, DOR is efficiently expressed on the surface (Shiwarski et al., 2017A; Gendron et al., 2016). This Golgi localization is highly regulated by signaling. In the neuroendocrine PC12 cells, DOR is normally expressed at the cell surface, but a short exposure to Nerve Growth Factor, which inhibits phosphoinositide 3 kinase class 2 and reduces PI(3,4)P levels, induces Golgi localization of DOR (Shiwarski et al., 2017B). The current model for this retention is that in neurons or in NGF-treated PC12 cells, DOR is constantly retrieved to earlier compartments in the Golgi by regulated interactions with the coatomer protein 1 (COPI) complex. DOR contains two atypical COPI-binding RXR motifs in its C-terminal tail (Shiwarski et al., 2019), which are required and sufficient for regulated Golgi localization. DOR contains additional canonical COPI-binding motifs in the second and third intracellular loops (St. Louis et al., 2017), which could contribute to a basal level of intracellular DOR. At present, whether these interactions are regulated is not known.

In contrast to DOR, endogenous cannabinoid receptor 1 (CB1R) is localized to the late endosomal compartments and axonal surface in hippocampal neurons (Rozenfeld and Devi, 2008; Fletcher-Jones et al., 2019). The late endosomal localization could be because of the shunting of CB1R in the TGN to an adaptor protein 3demediated export pathway (Rozenfeld and Devi, 2008). The deletion of helix 9 (H9) in the C-terminus caused CB1R to lose axonal polarization, but it was still delivered to the surface (Fletcher-Jones et al., 2019). This suggests that the receptor might be able to access multiple export pathways out of the TGN. The mechanism by which H9 regulates export is not known. The amphipathic nature of the helix might play a role, as amphipathicity of H8 was required for the export of apelin receptor from intracellular compartments and for efficient surface expression (Pandey et al., 2019).

Outside of specific adapters and interacting proteins, receptor oligomerization is an exciting possibility that could provide specificity to trafficking. For example, the transport protein RTP4 interacts with MOR and DOR and selectively increases expression of heteromers on the surface (Decaillot et al., 2008), without affecting individually expressed MOR and DOR or CB1R or dopamine 2 receptors (Fujita et al., 2019). Overall, the diversity of mechanisms that regulate Golgi retention and export suggest that GPCR delivery via the secretory pathway could be selectively regulated for individual GPCRs.

Conclusions

The subcellular location of GPCRs could be a master regulator of GPCR function, as the list of GPCRs capable of signaling from intracellular compartments is rapidly growing (Sposini and Hanyaloglu, 2018; Lobingier and von Zastrow, 2019; Crilly and Puthenveedu, 2020). Modulating signals from specific compartments, by either relocating receptors to the plasma

membrane (Bowman et al., 2015; Shiwarski et al., 2017A) or specifically targeting signaling from endosomes (Jimenez-Vargas et al., 2020), has clear effects on signaling and behavior. As we develop sophisticated tools to study both the mechanisms of selective trafficking and localized signaling of GPCRs (Calebiro and Grimes, 2020; Halls and Canals, 2018; Maziarz et al., 2020), we will be able to generate a more precise understanding of spatial patterns of signaling for each member of this important family of signaling receptors.

1.2 References

Arttamangkul S, Leff ER, Koita O, Birdsong WT, Williams JT: Separation of acute desensitization and long-term tolerance of m-opioid receptors is determined by the degree of C-terminal phosphorylation. Mol Pharmacol 2019, 96: 505 – 514.

Bahouth SW, Nooh MM: Barcoding of GPCR trafficking and signaling through the various trafficking roadmaps by com- partmentalized signaling networks. Cell Signal 2017, 36: 42–55.

Bouley RA, Weinberg ZY, Waldschmidt HV, Yen YC, Larsen SD, Puthenveedu MA, Tesmer JJ: A new paroxetine-based GRK2 inhibitor reduces internalization of the m-opioid receptor. Mol Pharmacol 2020, 97:392–401.

Bowman SL, Puthenveedu MA: Postendocytic sorting of adrenergic and opioid receptors: new mechanisms and functions. Pro Mol Biol Trans Sci 2015, 132:189–206.

Bowman SL, Soohoo AL, Shiwarski DJ, Schulz S, Pradhan AA, Puthenveedu MA: Cell-autonomous regulation of Mu-opioid receptor recycling by substance P. Cell Rep 2015, 10: 1925 – 1936.

Briddon SJ, Kilpatrick LE, Hill SJ: Studying GPCR pharma- cology in membrane microdomains: fluorescence correlation spectroscopy comes of age. Trends Pharmacol Sci 2018, 39: 158 – 174.

Buenaventura T, Bitsi S, Laughlin WE, Burgoyne T, Lyu Z, Oqua AI, Norman H, McGlone ER, Klymchenko AS, Corrêa Jr IR, Walker A: Agonist-induced membrane nanodomain clustering drives GLP-1 receptor responses in pancreatic beta cells. PLoS Biol 2019, 17, e3000097.

Caballero A, Mahn SA, Ali MS, Rogers MR, Marchese A: Heter- ologous regulation of CXCR4 lysosomal trafficking. J Biol Chem 2019, 294:8023–8036.

Calebiro D, Grimes J: G protein – coupled receptor pharmacology at the single-molecule level. Annu Rev Pharmacol Toxicol 2020, 60:73–87.

Calebiro D, Koszegi Z: The subcellular dynamics of GPCR signaling. Mol Cell Endocrinol 2019, 483:24–30.

Cao TT, Deacon HW, Reczek D, Bretscher A, von Zastrow M: A kinase-regulated PDZ-domain interaction controls endocytic sorting of the b2-adrenergic receptor. Nature 1999, 401: 286 – 290.

Cao Y, Kumar S, Namkung Y, Gagnon L, Cho A, Laporte SA: * Angiotensin II type 1 receptor variants alter endosomal receptor–b-arrestin complex stability and MAPK activation. J Biol Chem 2020, 295:13169–13180.

Caron MG, Barak LS: A brief history of the b-arrestins. Methods Mol Biol 2019, 1957:3–8. 2019.

Chen B, Dores MR, Grimsey N, Canto I, Barker BL, Trejo J: Adaptor protein complex-2 (AP-2) and epsin-1 mediate protease-activated receptor-1 internalization via phosphorylation-and ubiquitination-dependent sorting sig- nals. J Biol Chem 2011, 286:40760–40770.

Crilly SE, Puthenveedu MA: Compartmentalized GPCR signaling from intracellular membranes. J Membr Biol 2020, https://doi.org/10.1007/s00232-020-00158-7.

Décaillot FM, Rozenfeld R, Gupta A, Devi LA: Cell surface targeting of mu-delta opioid receptor heterodimers by RTP4. Proc Natl Acad Sci USA 2008, 105:16045–16050.

Díaz Añel AM, Malhotra V: PKCeta is required for beta1- gamma2/beta3gamma2- and PKD-mediated transport to the cell surface and the organization of the Golgi apparatus. J Cell Biol 2005, 169:83 – 91.

Doly S, Marullo S: Gatekeepers controlling GPCR export and function. Trends Pharmacol Sci 2015, 36:636 – 644.

Duarte ML, Devi LA: Post-translational modifications of opioid receptors. Trends Neurosci 2020, 43:417 – 432.

Dwivedi-Agnihotri H, Chaturvedi M, Baidya M, Stepniewski TM, Pandey S, Maharana J, Srivastava A, Caengprasath N, Hanyaloglu AC, Selent J, Shukla AK: Distinct phosphorylation sites in a prototypical GPCR differently orchestrate b-arrestin interaction, trafficking, and signaling. Sci Adv 2020, 6, eabb8368.

Fantini J, Di Scala C, Baier CJ, Barrantes FJ: Molecular mechanisms of protein-cholesterol interactions in plasma mem- branes: functional distinction between topological (tilted) and consensus (CARC/CRAC) domains. Chem Phys Lipids 2016, 199:52 – 60.

Fatakia SN, Sarkar P, Chattopadhyay A: A collage of cholesterol interaction motifs in the serotonin1A receptor: an evolutionary implication for differential cholesterol interaction. Chem Phys Lipids 2019, 221:184–192.

Fletcher-Jones A, Hildick KL, Evans AJ, Nakamura Y,Wilkinson KA, Henley JM: The C-terminal helix 9 motif in rat cannabinoid receptor type 1 regulates axonal trafficking and surface expression. eLife 2019, 8, e44252.

Fujita W, Yokote M, Gomes I, Gupta A, Ueda H, Devi LA: Regulation of an opioid receptor chaperone protein, RTP4, by morphine. Mol Pharmacol 2019, 95:11–19.

Gendron L, Cahill CM, von Zastrow M, Schiller PW, Pineyro G: Molecular pharmacology of d-opioid receptors. Pharmacol Rev 2016, 68:631–700.

Gurevich VV, Gurevich EV: GPCR signaling regulation: the role of GRKs and arrestins. Front Pharmacol 2019B, 10:125.

Gurevich VV, Gurevich EV: The structural basis of the arrestin binding to GPCRs. Mol Cell Endocrinol 2019, 484:34 – 41.

Halls ML, Canals M: Genetically encoded FRET biosensors to illuminate compartmentalised GPCR signalling. Trends Pharmacol Sci 2018, 39:148–157.

Hanyaloglu AC, Zastrow MV: Regulation of GPCRs by endo- cytic membrane trafficking and its potential implications. Annu Rev Pharmacol Toxicol 2008, 48:537–568.

Hara T, Saeki K, Jinnouchi H, Kazuno S, Miura Y, Yokomizo T: The c-terminal region of BLT2 restricts its localization to the lateral membrane in a LIN7C-dependent manner. Faseb J 2021, 35, e21364. official publication of the Federation of American Societies for Experimental Biology.

Hausdorff WP, Caron MG, Lefkowitz RJ: Turning off the signal: desensitization of b-adrenergic receptor function. Faseb J 1990, 4:2881–2889.

He D, Lasek AW: Anaplastic lymphoma kinase regulates internalization of the dopamine D2 receptor. Mol Pharmacol 2020, 97:123 – 131.

Henry AG, Hislop JN, Grove J, Thorn K, Marsh M, von Zastrow M: Regulation of endocytic clathrin dynamics by cargo ubiq- uitination. Dev Cell 2012, 23:519–532.

Jean-Alphonse F, Bowersox S, Chen S, Beard G, Puthenveedu MA, Hanyaloglu AC: Spatially restricted G protein-coupled receptor activity via divergent endocytic compartments. J Biol Chem 2014, 289:3960–3977.

Jimenez-Vargas NN, Gong J, Wisdom MJ, Jensen DD, Latorre R, Hegron A, Teng S, DiCello JJ, Rajasekhar P, Veldhuis NA, Carbone SE, Yu Y, Lopez-Lopez C, Jaramillo-Polanco J,

Canals M, Reed DE, Lomax AE, Schmidt BL, Leong KW, Vanner SJ, ... Poole DP: Endosomal signaling of delta opioid receptors is an endogenous mechanism and therapeutic target for relief from inflammatory pain. Proc Natl Acad Sci USA 2020, 117:15281–15292.

Just S, Illing S, Trester-Zedlitz M, Lau EK, Kotowski SJ, Miess E, Mann A, Doll C, Trinidad JC, Burlingame AL, von Zastrow M: Differentiation of opioid drug effects by hierar- chical multi-site phosphorylation. Mol Pharmacol 2013, 83: 633 – 639.

Koliwer J, Park M, Bauch C, von Zastrow M, Kreienkamp HJ: The golgi-associated PDZ domain protein PIST/GOPC stabilizes the b1-adrenergic receptor in intracellular compartments after internalization. J Biol Chem 2015, 290:6120 – 6129.

Kumar GA, Chattopadhyay A: Membrane cholesterol regulates endocytosis and trafficking of the serotonin1A receptor: in- sights from acute cholesterol depletion. Biochim Biophys Acta Mol Cell Biol Lipids 2021:158882.

Kumar GA, Chattopadhyay A: Statin-induced chronic cholesterol depletion switches GPCR endocytosis and trafficking: insights from the serotonin1A receptor. ACS Chem Neurosci 2020, 11:453 – 465.

Kunselman JM, Gupta A, Devi LA, Puthenveedu MA: Compart- ment-specific opioid receptor signaling is selectively modu- lated by dynorphin subtypes. eLife 2021, 10, e60270, https://doi.org/10.7554/eLife.60270.

Kunselman JM, Zajac AS, Weinberg ZY, Puthenveedu MA: Homologous regulation of mu opioid receptor recycling by G$\beta\gamma$, protein kinase C, and receptor phosphorylation. Mol Pharmacol 2019, 96:702–710.

Lau EK, Trester-Zedlitz M, Trinidad JC, Kotowski SJ, Krutchinsky AN, Burlingame AL, von Zastrow M: Quantitative encoding of the effect of a partial agonist on individual opioid receptors by multisite phosphorylation and threshold detec- tion. Sci Signal 2011, 4. ra52-ra52.

Lobingier BT, von Zastrow M: When trafficking and signaling mix: how subcellular location shapes G protein-coupled re- ceptor activation of heterotrimeric G proteins. Traffic 2019, 20: 130 – 136.

Mackie DI, Nielsen NR, Harris M, Singh S, Davis RB, Dy D, Ladds G, Caron KM: RAMP3 determines rapid recycling of atypical chemokine receptor-3 for guided angiogenesis. Proc Natl Acad Sci USA 2019, 116:24093–24099.

Mayor S, Presley JF, Maxfield FR: Sorting of membrane com- ponents from endosomes and subsequent recycling to the cell surface occurs by a bulk flow process. J Cell Biol 1993, 121:1257 – 1269.

Maziarz M, Park JC, Leyme A, Marivin A, Garcia-Lopez A, Patel PP, Garcia-Marcos M: Revealing the activity of trimeric G-proteins in live cells with a versatile biosensor design. Cell 2020, 182:770–785.

Mondal S, Narayan KB, Powers I, Botterbusch S, Baumgart T: Endophilin recruitment drives membrane curvature generation through coincidence detection of GPCR loop interactions and negative lipid charge. J Biol Chem 2021: 100 – 140.

Pandey A, LeBlanc DM, Parmar HB, Phạm TTT, Sarker M, Xu L, Duncan R, Liu XQ, Rainey JK: Structure, amphipathy, and topology of the membrane-proximal helix 8 influence apelin receptor plasma membrane localization. Biochim Biophys Acta Biomembr 2019, 1861:183036.

Pandey S, Ramsakha N, Sharma R, Gulia R, Ojha P, Lu W, Bhattacharyya S: The post-synaptic scaffolding protein Tamalin regulates ligand-mediated trafficking of metabotropic glutamate receptors. J Biol Chem 2020, 295:8575–8588. jbc-RA119.

Patel HH, Murray F, Insel PA: G-protein-coupled receptor- signaling components in membrane raft and caveolae microdomains. Protein-Protein Interactions as New Drug Tar- gets 2008:167 – 184.

Patwardhan A, Cheng N, Trejo J: Post-translational modifications of G protein–coupled receptors control cellular signaling dynamics in space and time. Pharmacol Rev 2021, 73:120 – 151.

Pierce KL, Premont RT, Lefkowitz RJ: Seven-transmembrane receptors. Nat Rev Mol Cell Biol 2002, 3:639–650.

Puthenveedu MA, Lauffer B, Temkin P, Vistein R, Carlton P, Thorn K, Taunton J, Weiner OD, Parton RG, von Zastrow M: Sequence-dependent sorting of recycling proteins by actin-stabilized endosomal microdomains. Cell 2010, 143: 761 – 773.

Puthenveedu MA, von Zastrow M: Cargo regulates clathrin-coated pit dynamics. Cell 2006, 127:113–124.

Rozenfeld R, Devi LA: Regulation of CB1 cannabinoid receptor trafficking by the adaptor protein AP-3. Faseb J 2008, 22: 2311–2322. official publication of the Federation of American Societies for Experimental Biology.

Sarkar P, Chattopadhyay A: Cholesterol interaction motifs in G protein-coupled receptors: slippery hot spots? Wiley Inter- disciplinary Rev: Sys Biol Med 2020, 12, e1481.

Shiwarski DJ, Crilly SE, Dates A, Puthenveedu MA: Dual RXR motifs regulate nerve growth factor-mediated intracellular retention of the delta opioid receptor. Mol Biol Cell 2019, 30: 680 – 690.

Shiwarski DJ, Darr M, Telmer CA, Bruchez MP, Puthenveedu MA: PI3K class II a regulates d-opioid receptor export from the trans-Golgi network. Mol Biol Cell 2017B, 28:2202 – 2219.

Shiwarski DJ, Tipton A, Giraldo MD, Schmidt BF, Gold MS, Pradhan AA, Puthenveedu MA: A PTEN-regulated checkpoint controls surface delivery of d opioid receptors. J Neurosci 2017A, 37:3741 – 3752. the official journal of the Society for Neuroscience.

Sorkin A, von Zastrow M: Endocytosis and signalling: inter- twining molecular networks. Nat Rev Mol Cell Biol 2009, 10: 609 – 622.

Sposini S, Hanyaloglu AC: Evolving view of membrane traf- ficking and signaling systems for G protein-coupled re- ceptors. Endocytos Signal 2018:273–299.

St-Louis É, Degrandmaison J, Grastilleur S, Génier S, Blais V, Lavoie C, Parent JL, Gendron L: Involvement of the coatomer protein complex I in the intracellular traffic of the delta opioid receptor. Mol Cell Neurosci 2017, 79:53–63.

Taghon GJ, Rowe JB, Kapolka NJ, Isom DG: Predictable cholesterol binding sites in GPCRs lack consensus motifs. Structure 2021, https://doi.org/10.1016/j.str.2021.01.004.

Tian X, Kang DS, Benovic JL: b-arrestins and G protein- coupled receptor trafficking. Handb Exp Pharmacol 2014, 219: 173 – 186.

Vistein R, Puthenveedu MA: Reprogramming of G protein- coupled receptor recycling and signaling by a kinase switch. Proc Natl Acad Sci USA 2013, 110:15289–15294.

Wei Z, Zhang M, Li C, Huang W, Fan Y, Guo J, Khater M, Fukuda M, Dong Z, Hu G, Wu G: Specific TBC domain-containing proteins control the ER-golgi-plasma membrane trafficking of GPCRs. Cell Rep 2019, 28:554 – 566. e4.

Weinberg ZY, Puthenveedu MA: Regulation of G protein- coupled receptor signaling by plasma membrane organiza- tion and endocytosis. Traffic 2019, 20:121–129.

Weinberg ZY, Zajac AS, Phan T, Shiwarski DJ, Puthenveedu MA: Sequence-specific regulation of endocytic lifetimes modu- lates arrestin-mediated signaling at the m opioid receptor. Mol Pharmacol 2017, 91:416–427.

Wente W, Stroh T, Beaudet A, Richter D, Kreienkamp HJ: In- teractions with PDZ domain proteins PIST/GOPC and PDZK1 regulate intracellular sorting of the somatostatin receptor subtype 5. J Biol Chem 2005, 280:32419–32425.

Zhang M, Davis JE, Li C, Gao J, Huang W, Lambert NA,
Terry Jr AV, Wu G: GGA3 interacts with a G protein-coupled receptor and modulates its cell surface export. Mol Cell Biol 2016, 36:1152 – 1163.

Zhang M, Huang W, Gao J, Terry AV, Wu G: Regulation of a2B- adrenergic receptor cell surface transport by GGA1 and GGA2. Sci Rep 2016, 6:37921.

Zhang M, Wu G: Mechanisms of the anterograde trafficking of GPCRs: regulation of AT1R transport by interacting proteins and motifs. Traffic 2019, 20:110 – 120 (Copenhagen, Denmark).

Zhang M, Xu X, Li C, Huang W, Xu N, Wu G: A naturally occurring splice variant of GGA1 inhibits the anterograde post-golgi traffic of a2B-adrenergic receptor. Sci Rep 2019, 9:10378.

Zhao P, Pattison LA, Jensen DD, Jimenez-Vargas NN, Latorre R, Lieu T, Jaramillo JO, Lopez-Lopez C, Poole DP, Vanner SJ, Schmidt BL, Bunnett NW: Protein kinase D and G$\beta\gamma$ mediate sustained nociceptive signaling by biased agonists of protease-activated receptor-2. J Biol Chem 2019, 294:10649 – 10662.

Chapter 2: Compartment-specific Opioid Receptor Signaling is Selectively Modulated by Different Dynorphin Peptides

Published as Kunselman, J. M., Gupta, A., Gomes, I., Devi, L. A., & Puthenveedu, M. A. (2021). Compartment-specific opioid receptor signaling is selectively modulated by different Dynorphin peptides. Elife, 10, e60270.

Abstract

Many signal transduction systems have an apparent redundancy built into them, where multiple physiological agonists activate the same receptors. Whether this is true redundancy, or whether this provides an as-yet unrecognized specificity in downstream signaling, is not well understood. We address this question using the kappa opioid receptor (KOR), a physiologically relevant G protein-coupled receptor (GPCR) that is activated by multiple members of the Dynorphin family of opioid peptides. We show that two related peptides, Dynorphin A and Dynorphin B, bind and activate KOR to similar extents in mammalian neuroendocrine cells and rat striatal neurons, but localize KOR to distinct intracellular compartments and drive different post-endocytic fates of the receptor. Strikingly, localization of KOR to the degradative pathway by Dynorphin A induces sustained KOR signaling from these compartments. Our results suggest that seemingly redundant endogenous peptides can fine-tune signaling by regulating the spatiotemporal profile of KOR signaling.

2.1 Introduction

The endogenous opioid system provides an excellent and physiologically relevant example to study redundancy in signaling systems in our body. Over 20 endogenous opioids have been identified, all of which preferentially activate one of three opioid receptors – delta, kappa, and mu opioid receptors – which are all members of the G protein-coupled receptor (GPCR) family of proteins (Gendron et al., 2016; Chavkin, 2013; Williams et al., 2013). All these opioid peptides activate their cognate GPCRs broadly at similar levels in most of the readouts that have been used to measure activation (Sternini et al., 2013). Whether all these opioid peptides are truly redundant or whether they contribute to signaling diversity beyond the initial signaling has been a long-standing question in the field.

Signaling from intracellular compartments, after the initial signaling from the surface, is emerging as a key determinant of the downstream consequences of receptor activation (Irannejad et al., 2013; Yarwood et al., 2017; Eichel and von Zastrow, 2018). While this is still an emerging field, a growing body of evidence suggests that GPCRs are active in endosomes and other intracellular compartments, and that receptors in endosomes can cause distinct signaling outcomes compared to receptors on the cell surface (Vilardaga et al., 2014; Bowman et al., 2016; Stoeber et al., 2018). Receptors rapidly and dynamically move between intracellular compartments and the surface by trafficking. Trafficking could therefore act as a master regulator of GPCR signaling by selectively amplifying signals from specific locations (Weinberg et al., 2019; Hanyaloglu, 2018). Whether physiological systems take advantage of trafficking to localize receptors to different compartments and dictate location-biased signaling, however, is still unanswered.

Here we bridge both questions by asking whether different endogenous opioid peptides can sort receptors to distinct intracellular compartments and drive different location-biased signaling outcomes. Using the kappa opioid receptor (KOR) as a model GPCR, we show that although related Dynorphin peptides can activate KOR on the surface to a similar extent, they induce different trafficking fates and endosomal localization of the receptor. Dyn B predominantly localized KOR to Rab11 recycling endosomes and caused KOR recycling, while Dyn A predominantly localized KOR to late endosomes and caused KOR degradation. Strikingly, Dyn A-activated KOR, but not Dyn B-activated KOR, was in an active conformation in lysosomes and induced cAMP signaling from intracellular compartments. The differences are likely a result of differences in how the peptides activate KOR, as opposed to peptide stability. Our results show that seemingly redundant opioid peptides, which activate receptors on the surface to similar levels, can drive spatially and temporally different signaling outcomes by differentially sorting receptors to distinct endosomal compartments after internalization.

2.2 Results

To examine activation and internalization of KOR by Dynorphin peptides we first focused on four physiologically relevant endogenous peptides – Dynorphin A17 (Dyn A), Dynorphin A8 (Dyn A8), Dynorphin B (Dyn B), and a-neoendorphin (a-neo). These peptides differ mainly in their length and C-terminal peptide sequence (Figure 2.1A). We carried out our studies using neuroendocrine PC-12 cells stably expressing KOR tagged with a pH-sensitive GFP (SpH-KOR) (Sankaranarayanan et al., 2000) that facilitates visualization of agonist-mediated KOR trafficking, and CHO cells stably expressing Flag epitope tagged KOR (CHO-KOR). Consistent

with previous findings, we find that in these cells Dyn A, Dyn A8, Dyn B, and a-neo bind KOR at relatively comparable affinities (Table 1).

Next, we measured the inhibition of cAMP levels and KOR endocytosis induced by these peptides. Dose–response curves with Dyn A and Dyn B in SpH-KOR cells showed maximal inhibition ~1 mM (Supplemental Figure 2.1A). At this concentration, Dyn A8 and a-neo inhibited whole cell cAMP to levels comparable to that of Dyn A and Dyn B (Figure 1B). Measurement of cell surface levels of KOR by ELISA show that Dyn A and Dyn B endocytose the receptor to a similar extent in SpH-KOR cells and in CHO-KOR cells (Supplemental Figure 2.1B and C; Gupta et al., 2016), with maximal endocytosis at ~1 mM. Examination of surface SpH-KOR fluorescence by live cell imaging using Total Internal Reflection Microscopy (TIR-FM) shows similar extent of agonist-mediated KOR clustering into endocytic domains and receptor endocytosis by the four Dynorphin peptides (1 mM) (Figure 2.1C and D). Together these results indicate that different Dynorphin peptides activate KOR and induce KOR internalization to similar levels.

Figure 2.1

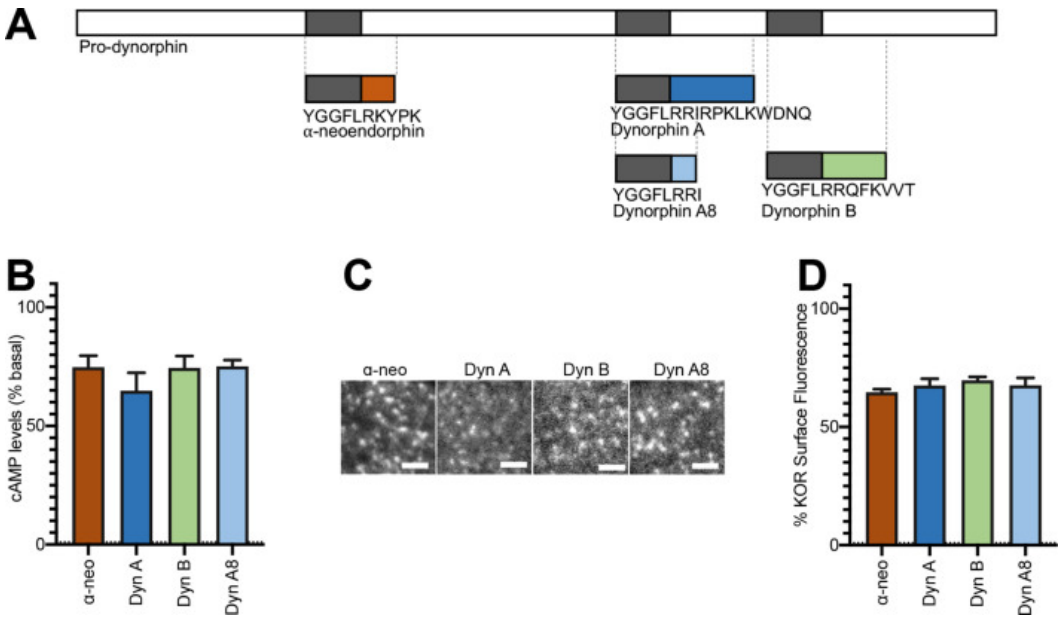

Figure 2.1 . Initial activation and internalization of KOR by Dynorphins are comparable. (**A**) Schematic of the regions of Pro-dynorphin from which Dynorphin A8 (Dyn A8), Dynorphin A (Dyn A), Dynorphin B (Dyn B), and α-neoendorphin (α-neo) peptides are generated, showing that Dyn A and Dyn B are processed from adjacent regions. (**B**) Dyn A8, Dyn A, Dyn B, and α-neo (1 μM) inhibit intracellular cAMP levels to a similar extent in PC12 cells stably expressing SpH-KOR. Values were normalized to basal cAMP measurements in the absence of peptide, which were set as 100% (mean ± SEM shown). (**C**) Representative TIR-FM images of PC12 cells stably expressing SpH-KOR treated with Dyn A8, Dyn A, Dyn B, and α-neo (1 μM) show roughly similar agonist-mediated receptor clustering at the cell surface following 1 min treatment. Scale bar = 2 μm. (**D**) Quantitation of the loss of surface SpH-KOR fluorescence, as an index of internalization, after 5 min of treatment with each peptide (1 μM), normalized to surface fluorescence before agonist treatment, show similar levels of internalization for all four peptides (mean ± SEM shown, Dyn A: n = 10 cells; Dyn B: n = 10 cells; Dyn A8: n = 10 cells; α-neo: n = 11 cells).

Table 1

Displacement binding parameters for Dynorphin peptides at PC12 SPH-KOR and CHO-KOR cells.

	PC12 SpH-KOR cells				CHO-KOR cells			
Ligand	**Low K_i (nM)**	**High K_i (nM)**	**% B_{max} at 10 μM**	**n_H**	**Low K_i (nM)**	**High K_i (nM)**	**% B_{max} at 10 μM**	**n_H**
Dyn A8	56.9 ± 0.3	0.020 ± 1.90	18.30 ± 1.48	36.9%	563 ± 0.1	0.41 ± 0.15	21.51 ± 1.54	41.6%
Dyn A17 (Dyn A)	52.4 ± 0.3	0.016 ± 0.47	15.22 ± 1.56	39.1%	119 ± 0.2	0.26 ± 0.54	18.72 ± 1.09	29.4%
Dyn B13 (Dyn B)	37.8 ± 0.2	0.010 ± 0.31	11.13 ± 1.07	33.4%	355 ± 0.1	0.38 ± 0.11	17.16 ± 0.82	42.2%
a-neo-endorphin	39.1 ± 0.1	0.011 ± 0.20	13.32 ± 1.84	38.7%	591 ± 0.1	0.18 ± 0.34	20.55 ± 1.57	21.4%

Supplemental Figure 2.1

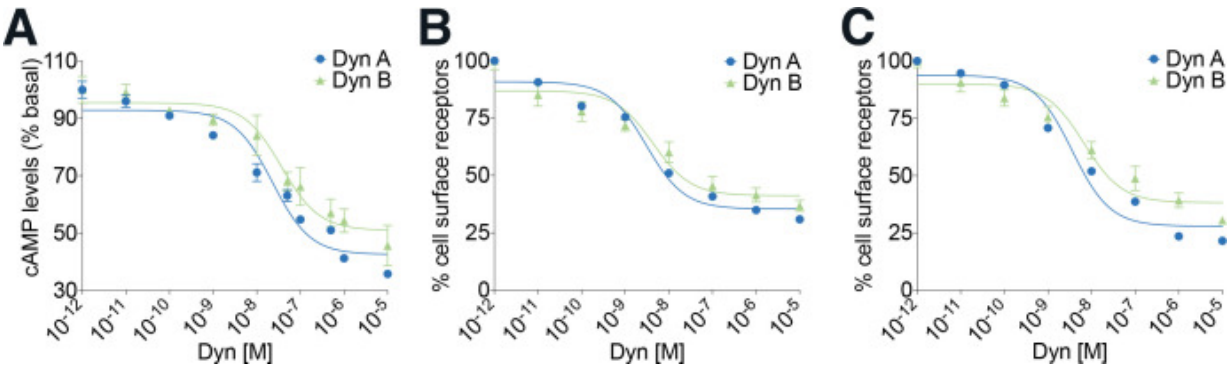

Supplemental Figure 2.1. Ligand-mediated decreases in intracellular cAMP levels and endocytosis of KOR saturates at 1 μM for Dyn A and Dyn B.

(**A**) Dyn A- and Dyn B-mediated decreases in intracellular cAMP levels were measured by carrying out doseresponse curves (0–10 μM) in PC12 cells stably expressing SpH-KOR treated for 30 min at 37°C. (**B**) Dyn A- and Dyn B-mediated changes in surface receptor levels were measured by ELISA by carrying out dose–response curves (0–10 μM) in PC12 cells stably expressing SpH-KOR treated for 30 min at 37°C. (**C**) Dyn A- and Dyn B-mediated changes in surface receptor levels were measured by ELISA by carrying out dose–response curves (0–10 μM) in CHO cells stably expressing Flag-KOR treated for 60 min at 37 °C.

We next examined if different Dynorphins selectively regulate the fate of KOR after initial activation and internalization, by adapting a discrete-event imaging method to quantitate the rate of individual KOR recycling events over unit time. SpH-KOR fluorescence is quenched in acidic endosomal compartments and is rapidly dequenched when receptors recycle back to the cell surface and are exposed to the extracellular media. This dequenching can be visualized as single events using Total Internal Reflection Fluorescence microscopy (TIR-FM), where the recycling events appear as distinctive sudden spikes in fluorescence followed by an exponential decay as the receptors diffuse on the cell membrane (Figure 2.2A–C). This method allows us to quantitate individual recycling events in the same cells over time without the confounding effects of continuing endocytosis (Kunselman et al., 2019). When the number of SpH-KOR recycling events were quantitated and normalized to time and cell area, a significantly higher number of recycling events was seen 5 min after Dyn B-induced KOR internalization , compared to Dyn A, Dyn A8, or a-neo (Figure 2.2D).

To test whether this increase in the rate of discrete recycling events corresponded to an increase in receptor levels at the cell surface, we measured ensemble changes in surface KOR levels by two different methods – whole-cell fluorescence and ELISA-based methods. We focused on Dyn A and Dyn B as a highly relevant and interesting pair, as both are processed from adjacent regions of prodynorphin and are often co-expressed in physiologically relevant brain regions (Nikoshkov et al., 2005; Corder et al., 2018). When SpH-KOR fluorescence was

followed by live confocal imaging, surface fluorescence decreased after Dynorphin addition, as was expected with receptor internalization. The fluorescence decrease reached a plateau at 10 min, suggesting an equilibrium between endocytosis and recycling at this time point (Figure 2.2E). When agonist was removed by washing out the media and replacing with fresh media containing antagonist (naltrexone; 10 mm), to specifically measure recycling without the contribution of endocytosis, the fluorescence recovery rate was higher with Dyn B than with Dyn A at the 30 min time point (Figure 2.2F and G).

A potential reason for the differences we observe could be differences in the rate of proteolytic degradation of the peptides (Mzhavia et al., 2003; Fricker et al., 2020). Therefore, we directly tested whether inhibiting proteolysis abolishes the difference between Dyn A and Dyn B. We first used a protease inhibitor cocktail in the media to inhibit general proteolysis. When discrete recycling events were quantitated as in Figure 2D, Dyn B showed a higher number of KOR recycling events even in the presence of protease inhibitors (Supplemental Figure 2.2A). When the recovery of surface KOR levels after agonist washout were measured by an independent ELISA-based method, Dyn B-treated cells showed a higher rate of recovery compared to Dyn A, even in the presence of protease inhibitors (Figure 2.2H). These experiments indicate that differences in general proteolysis of the peptides did not contribute to the increased KOR recycling we observe with Dyn B. Because Dyn B, but not Dyn A, can be cleaved by Endothelin Converting Enzyme 2 (ECE2) in vitro, we next tested whether this differential proteolysis by ECE2 could contributes to the differences between Dyn A and Dyn B-induced KOR recycling. We used S136492, which inhibits ECE2 relatively selectively in vitro in purified systems (Mzhavia et al., 2003), to test whether ECE2 activity was required for Dyn B to drive increased recycling. S136492 significantly reduced recycling for both Dyn A and Dyn B,

indicating that the differences in trafficking between Dyn B and Dyn A cannot be explained solely by ECE2 sensitivity (Supplemental Figure 2.2B). Together, these results suggest that intrinsic differences between Dyn A and Dyn B contribute to differences in KOR recycling when activated by these peptides.

Because KOR did not recycle efficiently when activated by Dyn A, we next asked whether Dyn A-activated KOR was sorted into the degradative pathway. To test this, PC12 cells expressing SpHKOR were pretreated with cycloheximide (3 mg/ml) 2 hr before agonist addition to inhibit any new protein synthesis and to measure agonist-mediated turnover of KOR. Total KOR levels were determined through immunoblotting, after Dyn A or Dyn B treatment for 30 min or 2 hr (Figure 2.2I). When total receptor levels were quantified, 2 hr treatment with Dyn A caused a loss of 50% of KOR, while Dyn B treatment caused no loss (Figure 2.2J). These results suggest that, after endocytosis, Dyn A preferentially sorts KOR into the degradative pathway, while Dyn B sorts KOR into the recycling pathway.

Figure 2.2

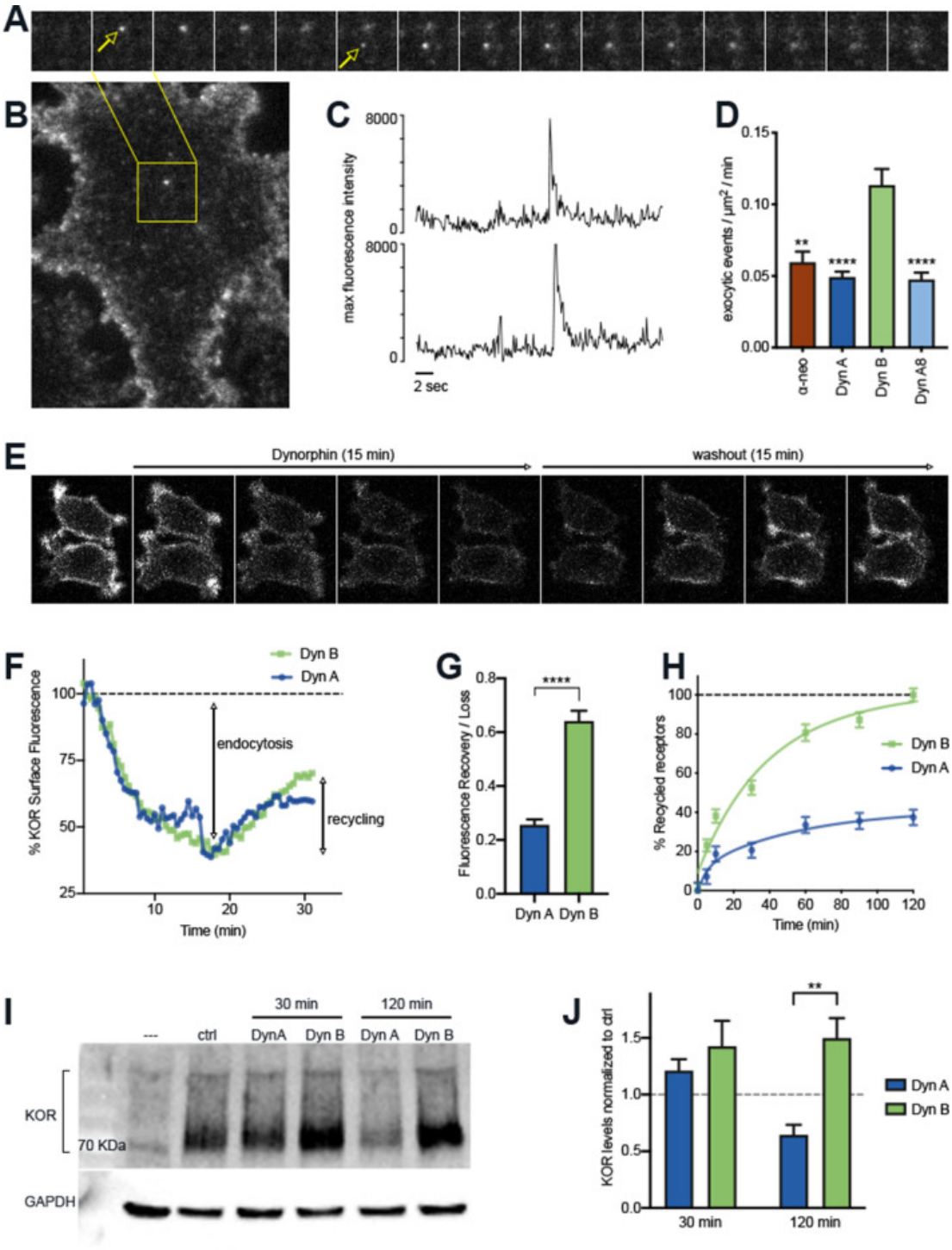

Figure 2.2. The post-endocytic fate of KOR is determined by the specific Dynorphin that activates it.

(**A**) Frames from a time lapse movie of a representative region of a PC12 cell stably expressing SpH-KOR (SpH-KOR cells) shown in (**B**), treated for 5 min with Dyn B (1 µM) and imaged in

TIR-FM, showing two examples of exocytic events (white arrows in **A**) associated with KOR recycling. (**C**) Fluorescence traces of the two exocytic events, arbitrary units, showing a characteristic abrupt increase in maximum fluorescence intensity followed by exponential decay. (**D**) Quantitation of the number of exocytic events/μm^2/min showing a significant increase for Dyn B compared to the other peptides (mean ± SEM, **p<0.01, ****p<0.0001 in multiple comparisons after ANOVA, n = 14, 39, 52, and 33 cells for α-neo, Dyn A, Dyn B, and Dyn A8, respectively). (**E**) Ensemble SpH-KOR surface fluorescence measured over time using confocal microscopy shows a decrease in fluorescence upon agonist addition because of quenching of internalized SpH-KOR, and an increase upon peptide washout as receptors recycle to the surface and SpH-KOR is dequenched. (**F**) Quantification of change in ensemble surface fluorescence over 30 min following treatment with Dyn A or Dyn B (1 μM), normalized to fluorescence before agonist addition, showing the loss during endocytosis and increase during recycling. (**G**) Quantitation of the amount of SpH-KOR recycled, normalized to the amount endocytosed after Dyn A or Dyn B treatment B (1 μM), shows that a higher amount of receptor is recycled after Dyn B washout (mean ± SEM, ****p<0.0001 by Mann–Whitney; n = 33 and 30 fields for Dyn A and Dyn B, respectively). (**H**) Recycling of SpH-KOR to the cell surface after treatment with 100 nM Dyn A or Dyn B measured by ELISA shows a much higher rate and extent of recycling after Dyn B washout. (**I**) Representative immunoblot of total receptor levels in SpH-KOR cells treated with cycloheximide (3 μg/ml) for 2 hr prior to Dyn A or Dyn B treatment (1 μM) for the indicated times show receptor loss after 120 min of Dyn A but not Dyn B treatment. GAPDH is used as a control. (**J**) Quantification of total receptor levels normalized to untreated control cells under each condition (**p<0.01 by post hoc comparison after two-way ANOVA; n = 5).

Supplemental Figure 2.2

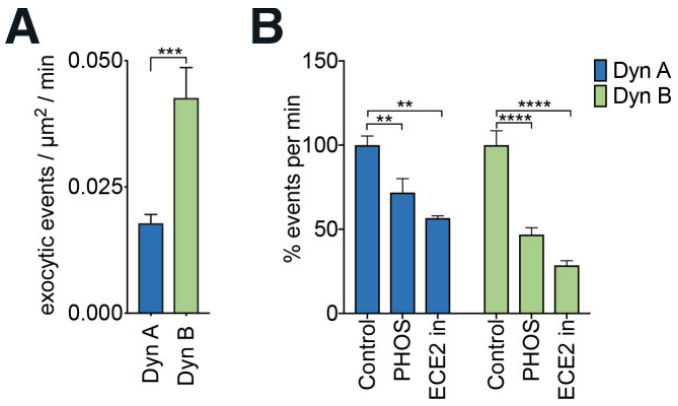

Supplemental Figure 2.2. The differences in KOR recycling between Dyn A and Dyn B cannot be explained entirely by peptide degradation.
(**A**) Quantitation of the number of exocytic events/μm^2/min in SpH-KOR PC12 cells shows a significantly higher number of events for Dyn B compared to Dyn A (1 μM) in the continued presence of protease inhibitors (***p<0.001, in unpaired t-test n = 9 and 6 cells for Dyn B and Dyn A, respectively). (**B**) Quantitation of the percent change of exocytic events in PC12 SpH-KOR cells treated with Dyn A or Dyn B in the presence or absence of 10 μM phosphoramidon (PHOS), a neprilysin/ECE inhibitor, or 20 μM S136492, an ECE2 inhibitor (ECE2 inh). Both

inhibitors decreased % events/minute for both Dyn A and Dyn B, suggesting that ECE2 inhibition on its own cannot explain the differences between the peptides.

Considering the emerging importance of spatial encoding in diversifying the outcomes of GPCR signaling (Eichel and von Zastrow, 2018; Weinberg et al., 2019; Hanyaloglu, 2018), we next asked whether Dyn A or Dyn B generated distinctive intracellular localization patterns of KOR at steady state. Because Dyn A drove KOR degradation, we first tested whether Dyn A-activated KOR was differentially localized to the late endosomal pathway. When PC12 cells expressing FLAG-KOR and Rab7-GFP, to mark the late endocytic pathway, were treated with 1 mM Dyn A for 20 min and imaged live, KOR colocalized predominantly with Rab7 (example in Figure 2.3A). To quantitate the distribution of KOR in the endosomal pathway more comprehensively, we treated cells expressing SpH-KOR with 1 mM Dyn A or Dyn B for 20 min, and fixed and stained for APPL1 (very early endosomes), EEA1 and Rab5 (early endosomes), Rab11 (recycling endosomes), Rab7 (late endosomes), and Lamp1 (lysosomes), as markers for the biochemically distinct compartments along the early, recycling, and late endosomal pathway. Using automated object-picking, we then quantitated the fraction of KOR that colocalized with each endosomal marker under these conditions. KOR localized mainly to compartments marked by Rab7 and Lamp1 when activated by Dyn A, but to compartments marked by EEA1, Rab5, and Rab11 when activated by Dyn B (Figure 2.3B and C). These results show that KOR is concentrated in different endosomal compartments based on the Dynorphin that activates it.

The agonist-selective localization of KOR to specific endosomes raised the exciting possibility that different Dynorphins could generate distinct subcellular spatial patterns of KOR signaling. To test this possibility, we combined conformation-selective biosensors and high-resolution imaging of FLAG-KOR to ask whether KOR was active in endosomes. A nanobody (Nb39) that specifically recognizes the active conformation of KOR (Che et al., 2018), when co-

expressed with FLAG-KOR in PC12 cells, localized efficiently to endosomes that also contained Dyn A-activated KOR. In contrast, Nb39 localized less to endosomes containing Dyn B-activated KOR (Figure 2.3D and E). When the fraction of total number of KOR endosomes/cell that colocalized with Nb39 was quantitated by analyzing 3D stacks, endosomes containing Dyn A-activated KOR recruited Nb39 at a significantly higher level (Figure 2.3F and G), suggesting that KOR was in an active conformation in the endosomes specifically after activation by Dyn A. Nb39 recruitment to endosomes required KOR endocytosis, as recruitment was abolished when cells were treated with agonist in the presence of 40 μM Dyngo4A, an endocytosis inhibitor (Supplemental Figure 2.3A and B). To directly examine whether Dyn A-activated KOR in lysosomes was in an active conformation, we used three-color live cell imaging of FLAG-KOR, Nb39, and LysoTracker. In cells treated with 1 μM Dyn A, a subset of KOR endosomes colocalized with both Nb39 and Lysotracker. In cells treated with 1 mM Dyn B, however, virtually no KOR endosomes colocalized with both Nb39 and Lysotracker (Figure 2.3H). When the colocalization was quantitated in Dyn A-treated cells, ~15% of all KOR endosomes colocalized with both markers, suggesting that a subset of Dyn A-activated KOR in the lysosome was in the active conformation (Figure 2.3I). In contrast, in cells treated with 1 mM Dyn B, virtually no KOR endosomes colocalized with both Nb39 and Lysotracker (Figure 2.3H).

To test whether the subset of Dyn A-activated KOR in the active conformation in late endosomes and lysosomes was capable of signaling, we measured cAMP inhibition under conditions where the agonist was washed out to avoid continued signaling from the surface. Twenty-five minutes after agonist washout, Dyn A-activated KOR was still localized predominantly to Rab7-labeled late endosomal compartments, while Dyn B-activated KOR was localized predominantly to Rab11-labeled recycling endosomes (Supplemental Figure 2.3C–H).

This distribution was comparable to that observed in the continued presence of agonist, and at this time point, there was little to no KOR degradation (Figure 2.2I and J). Strikingly, Dyn A, but not Dyn B, caused sustained decrease in cAMP levels under conditions where the majority of KOR was in late endosomes and lysosomes (Figure 2.3J). Together, our results suggest that Dyn A, but not Dyn B, specifically coordinates activation and cAMP inhibition by KOR in late endosomes and lysosomes.

Figure 2.3

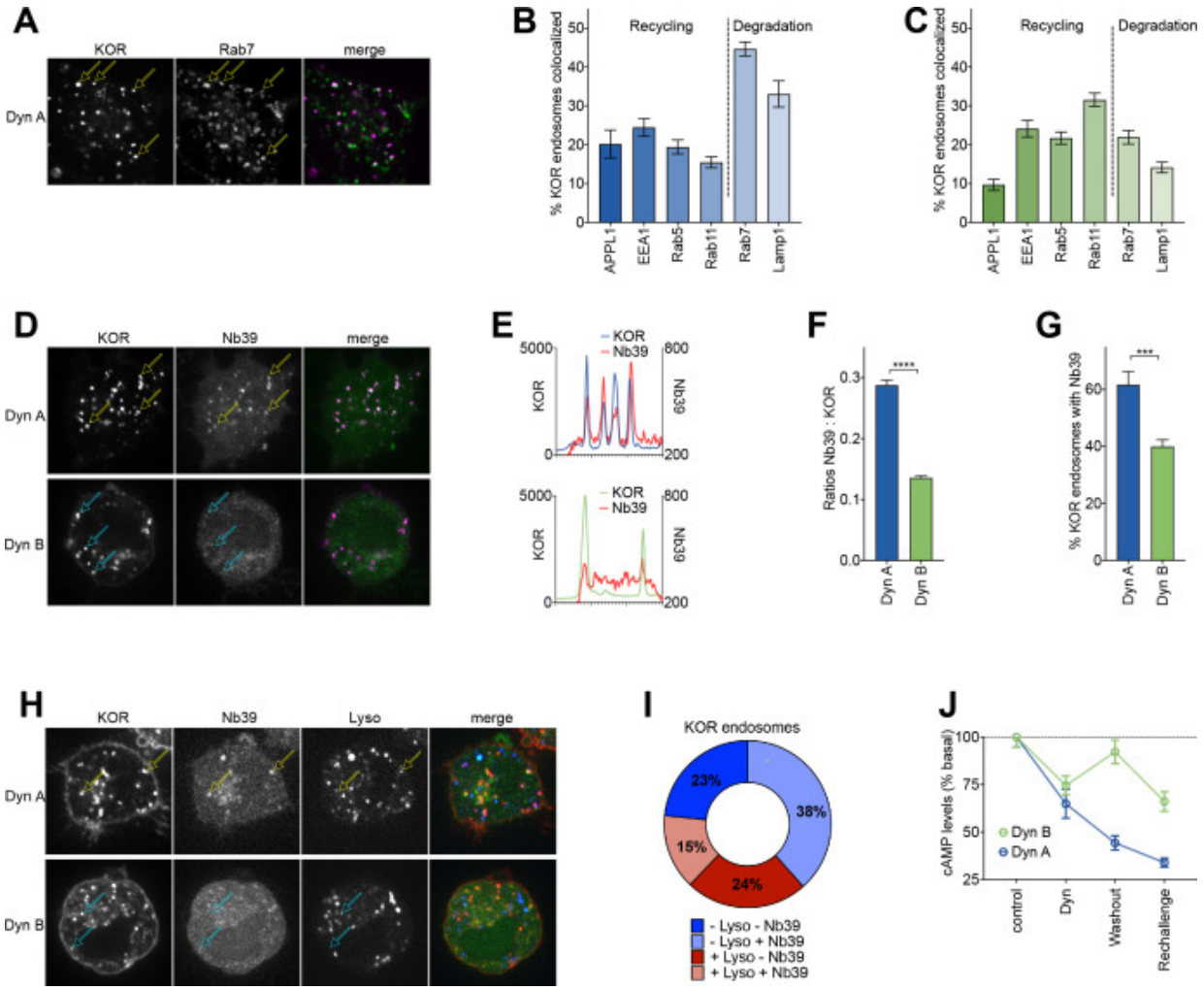

Figure 2.3. Dyn A selectively drives KOR signaling from late endosomal compartments.

(**A**) Representative image of a PC12 cell expressing FLAG-KOR and Rab7-GFP, treated with 1 μM Dyn A for 20 min. Yellow arrows denote KOR endosomes that colocalize with Rab7. (**B**) SpH-KOR cells treated with 1 μM Dyn A for 20 min were fixed and processed for immunofluorescence with the noted markers. Quantitation, across multiple cells, of the percentage of KOR containing endosomes that colocalize with each of the endosomal markers is noted. KOR primarily localizes in Rab7 and Lamp1 positive late endosomes after Dyn A (n = 8, 10, 9, 11, 20, and 17 cells for APPL1, EEA1, Rab5, Rab11, Rab7, and Lamp1, respectively). (**C**) A similar quantitation of immunofluorescence images after Dyn B treatment (1 μM for 20 min) shows that KOR localizes less with late endosomes, and more with markers of early/recycling endosomes (n = 18, 16, 15, 18, 23, and 29 cells for APPL1, EEA1, Rab5, Rab11, Rab7, and Lamp1, respectively). (**D**) Representative images of PC12 cells expressing FLAG-KOR and Nb39, imaged live after treatment with 1 μM Dyn A or Dyn B for 20 min. Yellow arrows in Dyn A show KOR endosomes that recruited Nb39, while cyan arrows in Dyn B show KOR endosomes that do not show obvious recruitment of Nb39. (**E**) Linear profile plots of fluorescence of KOR and Nb39, measured along lines drawn across regions of the cell with KOR endosomes after treatment with 1 μM Dyn A or Dyn B for 20 min, show that Nb39 fluorescence increases along with KOR in Dyn A, but less noticeably with Dyn B. (**F**) Ratios of integrated fluorescence of Nb39:KOR in endosomes identified by 3D object analysis show higher amounts of Nb39 relative to KOR in Dyn A-treated cells (****$p<0.0001$ by Mann–Whitney, n = 766 and 800 endosomes for Dyn A and Dyn B, respectively). (**G**) Quantitation of the percentage of KOR endosomes per cell with a noticeable increase in Nb39 fluorescence above background shows a higher fraction of KOR endosomes recruited Nb39 in 1 μM Dyn A-treated cells (***$p<0.001$ by Mann–Whitney, n = 11 and 14 cells for Dyn A and Dyn B, respectively). (**H**) Representative images of PC12 cells expressing FLAG-KOR and Nb39 and labeled with LysoTracker imaged live after treatment with 1 μM Dyn A or Dyn B for 20 min. Yellow arrows in Dyn A show KOR endosomes that recruited Nb39 that were also labeled with Lysotracker, while cyan arrows in Dyn B show KOR endosomes that do not show obvious labeling with Nb39 and Lysotracker. (**I**) The average composition of total KOR endosomes that are positive for ±Nb39 and ±Lysotracker after 20 min treatment with Dyn A (1 μM). n = 10 cells. −Lyso/−Nb39 = 23.4 ± 8.1%; −Lyso/+Nb39 = 38.4% ± 17.4%; +Lyso/−Nb39 = 23.7 ± 11.4%; +Lyso/+Nb39 = 14.6 ± 5.1%. (**J**) cAMP levels after initial Dynorphin treatment (1 μM) for 5 min, washout for 25 min, or a Dynorphin rechallenge (1 μM) at end of the washout, show comparable initial cAMP inhibition by both Dyn A and Dyn B, but persistent signaling by Dyn A after agonist washout.

Supplemental Figure 2.3

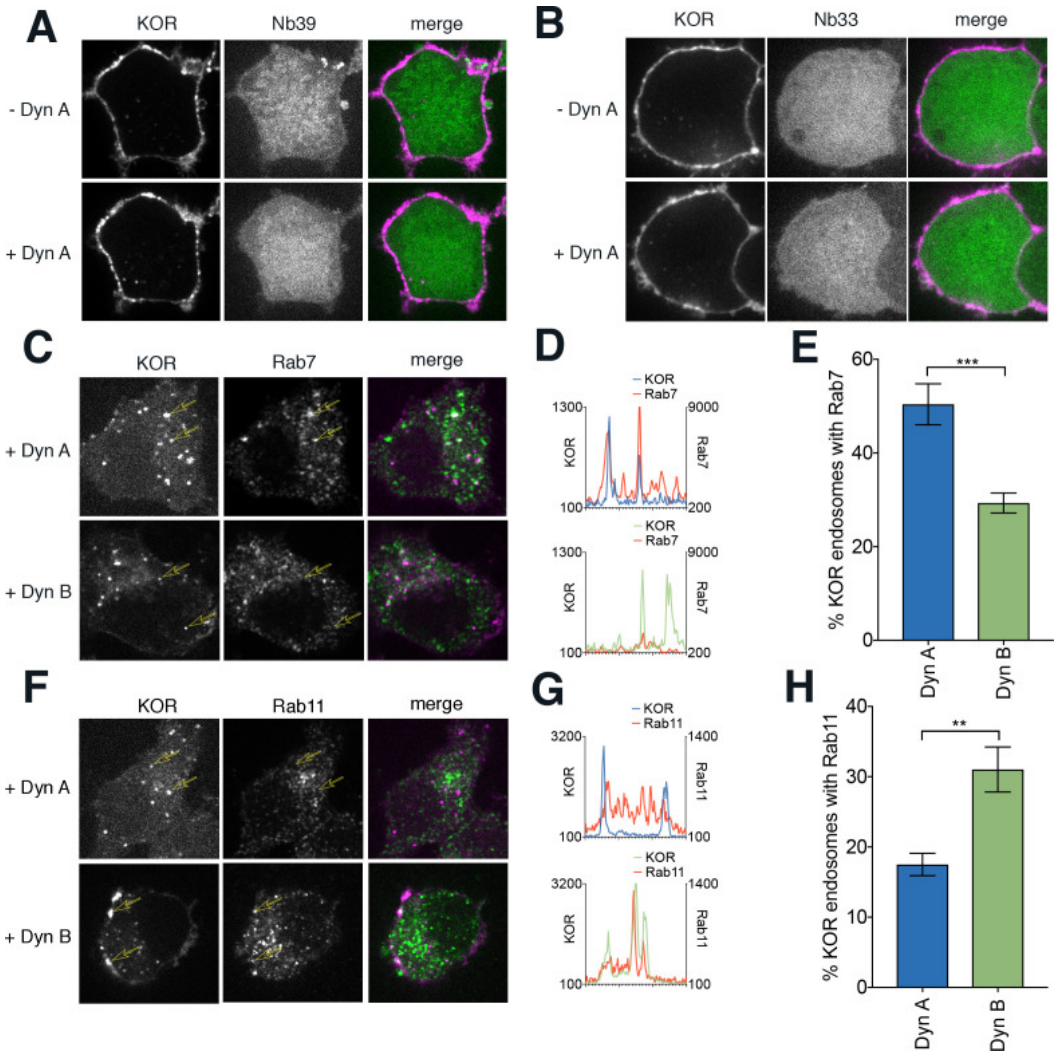

Supplemental Figure 2.3. Differential receptor sorting between Dyn A and Dyn B persists even after agonists are washed out from the surface.
(**A**) Representative images of PC12 cells expressing FLAG KOR treated with Dyn A in the presence of 40 µM Dyngo4A for 30 min to block endocytosis. KOR (magenta in merge) fluorescence is restricted to the surface with little endosomal KOR after 20 min Dyn A (1 µM), and no recruitment of Nb39 (green) to internal endosomes. (**B**) A similar Dyngo4a treatment blocked recruitment of Nb33 to internal endosomes after 20 min Dyn A (1 µM). (**C**) Representative images of cells labeled live with anti-FLAG antibodies for surface KOR, treated for 5 min with 1 µM Dyn A or Dyn B followed by a 25 min washout, then fixed and stained for Rab7 to mark late endosomes. (**D**) Linear profile plots of fluorescence for KOR and Rab7, measured along lines drawn across regions of the cells in **C**, show that Rab7 fluorescence spikes correlate with KOR spikes in Dyn A, but less with Dyn B. (**E**) Quantitation of the percentage of KOR endosomes/cell colocalizing with Rab7 shows a higher fraction of KOR endosomes recruited Rab7 in Dyn A-treated cells (***$p<0.001$ by Mann–Whitney, n = 10 and 11 cells for Dyn A and Dyn B, respectively). (**F**) Representative images of cells labeled live with anti-FLAG antibodies for surface KOR, treated for 5 min with 1 µM Dyn A or Dyn B followed by a 25 min

washout, then fixed and stained for Rab11 to mark recycling endosomes. (**G**) Linear profile plots of fluorescence for KOR and Rab11, measured along lines drawn across regions of the cells in **F**, show that Rab11 fluorescence increases along with KOR in Dyn B, but less noticeably with Dyn A. (**H**) Quantitation of the percentage of KOR endosomes/cell colocalizing with Rab11 shows a higher fraction of KOR endosomes recruited Rab11 in Dyn B-treated cells (**$p<0.01$ by Mann–Whitney, n = 9 and 10 cells for Dyn A and Dyn B, respectively).

Importantly, this Dynorphin-selective coordination of KOR recycling and endosomal activation was conserved in striatal neurons. To directly measure KOR recycling, E18 rat primary embryonic striatal neurons were transfected with SpH-KOR, and individual recycling events were imaged using TIRFM. The number of individual exocytic events, when quantified per minute and normalized to cell area, was significantly lower in neurons treated for 30 min with 1 mM Dyn A compared to Dyn B (Figure 2.4A). This suggested that Dyn B, but not Dyn A, preferentially sorted KOR to recycling endosomes in neurons. We directly tested this by detecting the steady-state localization of KOR in endosomes after Dyn A or Dyn B treatment. KOR colocalized predominantly with Rab7 when activated by Dyn A, and with Rab11 when activated by Dyn B (Figure 2.4B and C). To test whether this differential localization correlated with differential location-based activation of KOR in endosomes, we expressed Nb33, a distinct nanobody that recognizes the active conformation of opioid receptors (Manglik et al., 2017), fused to GFP in neurons. Endosomes containing Dyn A-activated KOR recruited Nb33, while endosomes containing Dyn B-activated KOR recruited Nb33 to a noticeably lesser extent. This recruitment was readily apparent in dendritic projections, where endosomes were distinctly visible (Figure 2.4D). The percentage of KOR endosomes that recruited Nb33 was significantly higher for Dyn A-activated KOR than for Dyn B (Figure 2.4E), showing that dynorphin-selective spatial activation of KOR was conserved in neurons.

Figure 2.4

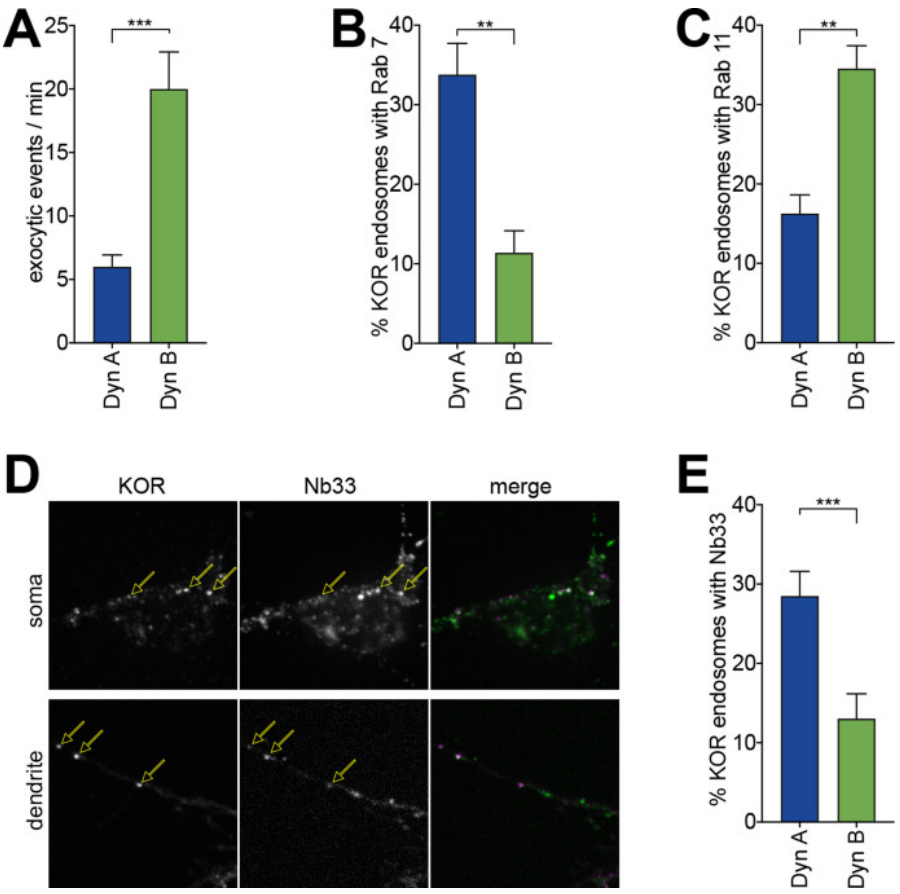

Figure 2.4. Dyn A-specific late endosomal localization and signaling is conserved in striatal neurons.
(**A**) The number of discrete exocytic events quantitated in rat medium spiny neuron (MSN) expressing SpH-KOR shows increased recycling for 1 μM Dyn B compared to Dyn A (***$p<0.001$, n = 8 cells). (**B**) Quantification of the percentage of KOR endosomes colocalized with Rab7 in MSN expressing SpH-KOR treated with 1 μM Dyn A or Dyn B for 30 min (**$p<0.01$, n = 5 cells for both). (**C**) Quantification of the percentage of KOR endosomes colocalized with Rab11 in MSN expressing SpH-KOR treated with 1 μM Dyn A or Dyn B for 30 min (**$p<0.01$, n = 5 and 9 cells for Dyn A and Dyn B, respectively). (**D**) Colocalization of FLAG-KOR and Nb33-GFP in the soma and in dendrites of MSNs treated with 1 μM Dyn A for 30 min, seen by confocal microscopy. Yellow arrows show KOR endosomes that recruit Nb33. (**E**) Quantitation of the percentage of KOR endosomes/cell with a noticeable increase in Nb33 fluorescence above background shows that a higher fraction of KOR endosomes recruited Nb33 in Dyn A-treated cells (1 μM for 30 min; ***$p=0 < 0.001$, n = 10 cells). All p-values were from non-parametric Mann–Whitney tests.

Supplemental Figure 2.4

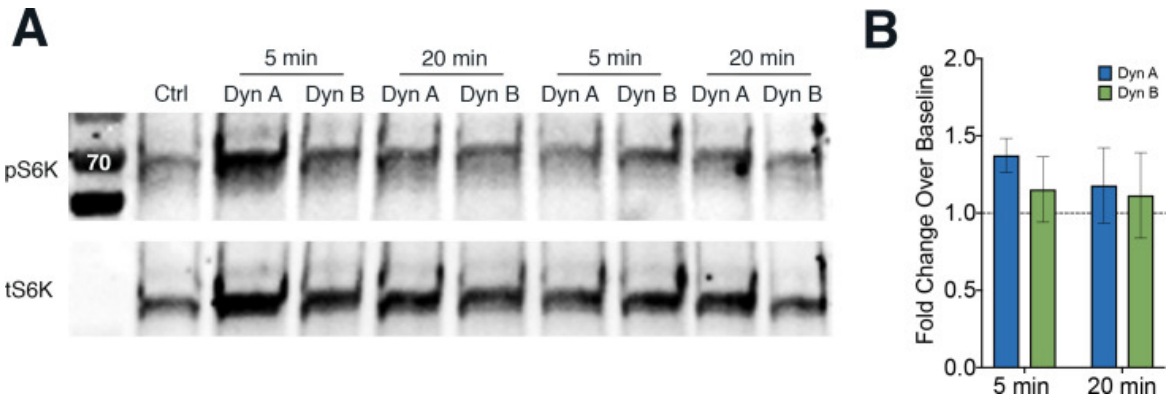

Supplemental Figure 2.4. mTOR signaling does not show significant differences between Dyn A and Dyn B.
(**A**) Representative blots showing phosphorylated (pS6K) and total (tS6K) S6K levels in PC12 cells stably expressing SpH-KOR treated with 1 μM Dyn A or Dyn B for 5 and 20 min. (**B**) Quantitation of the fold change over Ctrl baseline to measure mTOR activation: pS6K signal divided by tS6K signal in cells treated with Dyn A or Dyn B for 5 or 20 min. n = 5 biological replicates.

2.3 Discussion

Together, our results reveal an unanticipated difference between physiologically important endogenous opioid peptides in encoding the subcellular spatial patterns of KOR signaling. Peptidases localized to endosomes, like endothelin-converting enzymes (ECEs) may provide another level of regulation for agonist-dependent KOR trafficking (Padilla et al., 2007; Roosterman et al., 2007; Gupta et al., 2015). However, our results do not suggest that ECE peptide-sensitivity is the only or primary factor that determines agonist-dependent KOR localization (Supplemental Figure 2.2). Ubiquitination of KOR may also regulate its ability to traffic to and signal from late endosomal and lysosomal compartments (Li et al., 2008; Henry et al., 2011; Dores and Trejo, 2019).

The exact mechanism by which KOR is localized to different compartments is not clear. Because the post-endocytic sorting of GPCRs is usually mediated by specific interactions of the

unstructured cytoplasmic tail of the receptors with trafficking proteins, KOR sorting probably involves interactions with PDZ-interacting protein NHERF1/EBP50 (Liu-Chen, 2004). In this context, different Dynorphin peptides could lock KOR into conformations that selectively allow or inhibit interactions with trafficking and signaling proteins, essentially defining the receptor interactome in an agonist-specific manner. This conformational lock could require the presence of the ligand that is co-internalized with the receptor, although an exciting possibility is that the ligands provide a 'conformational memory' to KOR that is sustained through the endocytic trafficking pathway. At present it is not clear what could provide such a conformational memory. It is possible that different Dynorphins could cause agonist specific post-translational modifications, which is a general emerging theme for opioid receptors (Chiu et al., 2017; Mann et al., 2019). In any case, the differential subcellular localization and trafficking of KOR by two physiologically important ligands that we show here are important to underscore the physiological relevance of receptor sorting, which has been studied largely using receptor mutants or by depleting key components of the trafficking machinery (Bowman et al., 2016; Weinberg et al., 2019; Zhao et al., 2013; Sposini et al., 2017).

One striking aspect of our results is that Dyn A-bound KOR activates Gi in the late endosomal pathway on its way to being degraded. This is surprising because early endosomes are the main compartments that support endosomal signaling for most other canonical GPCRs. For example, other Gi-coupled receptors such as the mu opioid receptor can exist in an active conformation in earlier endosomal compartments (Stoeber et al., 2018). Internalization is required for sustained inhibition of cAMP for many receptors, such as for the class B S1P receptor (Willinger et al., 2014). However, Gi is likely present on late endosomal and lysosomal compartments, as cannabinoid receptors trafficking from the Golgi can activate Gi on lysosomes

(Rozenfeld and Devi, 2008). Further, the binding of peptides to opioid receptors does not change dramatically at lower pH (Gupta et al., 2015). Therefore, it is possible that Gi could be activated at multiple endosomal compartments based on the specific opioid receptor and ligand, leading to distinct early and late phases of endosomal signaling.

Post-translational modifications such as phosphorylation or ubiquitination could provide regulatory handles for this late phase of signaling. For example, three lysine residues on the C-terminus of KOR are required for normal levels of degradation of KOR, but not for internalization from the surface (Li et al., 2008). Ubiquitination, however, plays complex roles in receptor trafficking and signaling at the endosome, controlling transport of receptors to lysosomes, entry of receptors into intralumenal vesicles, and recruitment of signaling scaffolds that could initiate non-canonical signaling pathways (Patwardhan et al., 2021). In this context, Dyn A-activated KOR could also activate alternate pathways, such as mTOR signaling, on late endosomes and lysosomes. Interestingly, mTOR signaling is involved in potentially deleterious effects of KOR, leading to efforts to generate agonists bypassing this signaling pathway (Che and Roth, 2018; Liu et al., 2018; Liu et al., 2019). However, under the conditions we tested, we did not see a significant increase in p70S6 phosphorylation, as a readout for mTOR activation, upon activation of KOR with either Dyn A or Dyn B. This could potentially be due to the high baseline of p70S6 phosphorylation in the PC12 cells (Supplemental Figure 2.4). However, it is possible that KOR could activate mTOR signaling from late endosomes or lysosomes in a subset of neurons yet to be identified, that could mediate aversive effects of KOR.

Physiological systems could leverage receptor sorting to fine-tune both spatial and temporal aspects of GPCR signaling. KOR is activated by many opioid peptides that are generated from multiple precursor peptides, some of which bias signaling from the cell surface to

different outputs (Gomes et al., 2020). Our results suggest that, even for peptides where there are no obvious differences in surface signaling, there are differential effects in endocytic sorting and signaling from endosomes. Receptor sorting in cells is a dynamic and incomplete process. The fractions of receptors we see at steady state likely represent an equilibrium of many rounds of rapid iterative sorting as the endosome matures, where only a small fraction is recycled back to the surface in the case of Dyn A, while a large fraction is recycled in the case of Dyn B. Because Dyn A drives little KOR to recycle and promotes endosomal KOR activation, the net effect would be to cause a sustained cAMP inhibition from endosomes after a single exposure. Because Dyn B drives KOR recycling and induces endosomal signaling only to small amounts, the net effect would be short-lived cAMP inhibition primarily from the surface. On the other hand, the rapid recycling and resensitization caused by Dyn B would sensitize cells to repeated pulses of ligand release, unlike with Dyn A. This difference in steady-state localization, however, is enough to cause a difference in endosomal receptor activation and cAMP signaling, suggesting that small differences in steady-state localization can cause relevant changes in signaling.

Whether these different Dynorphins are always co-released in the nervous system, or whether different brain regions selectively release specific Dynorphins, is still unclear. Dyn A and Dyn B are generated from prodynorphin likely in the late stages of dense core vesicle maturation and could be predominantly co-released, but there could be mechanisms that actively segregate or selectively release individual Dynorphins. In the case of co-released peptides, it is possible that one or more of the peptides could be dominant in dictating the conformational states in which receptors spend most of their time, in which case the signaling and trafficking fates would be determined primarily by these dominant peptides. In any case, our results that

highly related opioid peptides regulate spatial encoding of KOR suggest an unanticipated layer of granularity to the anatomical and functional maps of the brain.

2.4 Materials and Methods

Reagents, constructs, and cells

Dynorphin A17 (Dyn A), Dynorphin B13 (Dyn B), Dynorphin A (Dyn A8), and a-neoendorphin (a-neo) were purchased from Tocris Bioscience and/or Phoenix Pharmaceuticals. Naltrexone, protease inhibitor cocktail (Cat. No. P2714), anti-Flag M2 antibody (Cat. No. F3165) were purchased from Sigma Aldrich (St. Louis, MO). Anti-APPL1, -EEA1, -Rab5, -Rab11, -Rab7, -Lamp1 rabbit monoclonal antibodies were purchased from Cell Signaling Technology. Anti-GFP rabbit polyclonal antibodies (Cat. No. A10260) were from Thermo Fisher Scientific. Nb39 and Nb33 constructs were provided by Dr. Bryan Roth (UNC Chapel Hill) and Dr. Mark von Zastrow (UCSF) respectively. Cell lines used were validated, and cells were purchased from ATCC. Cells in the lab are routinely tested for mycoplasma contamination. Stable non-clonal PC12 cells expressing KOR N-terminally tagged with superecliptic phluorin (SpH) (SpH-KOR cells) were selected in puromycin (Gibco) and grown in F12K media supplemented with 10% horse serum and 5% fetal bovine serum (Gibco) in collagen coated flasks. PC12 cells were also transiently transfected with KOR fused to FLAG on its N-terminus using Lipofectamine 2000 as per manufacturer's protocol (ThermoFisher). Transfected cells were imaged 2–3 days after transfection. CHO cells stably expressing Flag epitope tagged KOR generated as described previously (Gupta et al., 2016) were grown in F12 media supplemented with 10% fetal bovine serum and 1% penicillin–streptomycin. E18 rat striatal neurons were obtained from BraintBits LLC and cultured on poly-d-lysine (Sigma) coated coverslips for 1

week in Neurobasal media (Gibco) supplemented with B27 (Gibco), 1% Glutamax (Gibco), and 1% penicillin–streptomycin (Gibco) before transfection with SpH-KOR or Flag-KOR and Nb33-GFP using Lipofectamine 2000 as per manufacturer's protocol (ThermoFisher). Antibodies used are listed below.

Displacement binding assays

Displacement binding assays were carried out using membranes from PC12 cells stably expressing SpH-KOR (SpH-KOR cells) (100 mg) and CHO-KOR (15 mg) cells. Membranes were prepared as described previously (Gomes et al., 2003). Displacement binding assays were carried out as described previously (Gomes et al., 2004; Gomes et al., 2011) by incubating membranes with [3H] diprenorphine (3 nM) without or with different concentrations (1012to 105 M) of Dyn A8, Dyn A17, Dyn B13, or a-neo-endorphin in 50 mM Tris-Cl buffer pH 7.4 containing 100 mM NaCl, 10 mM MgCl2, 0.2 mM EGTA, and protease inhibitor cocktail (Sigma-Aldrich; cat No. P2714) for 1 hr at 37˚ C. Non-specific binding was determined in the presence of 10 mM cold diprenorphine. Specific Bound Counts obtained in the absence of peptides was taken as 100%. Data presented are mean ± SE of three independent experiments in triplicate.

Live cell imaging

Cells were plated onto poly-D-lysine (Sigma) coated 25 mm coverslips. Cells were imaged 2 days later in Leibovitz L15 imaging medium (Gibco) and 1% fetal bovine serum at 37˚C in a CO-controlled imaging chamber, using a Nikon Eclipse Ti automated inverted microscope with a 60 or a 100 1.49 N.A. TIRF objective or a 20 0.75 N.A. objective. Images

were acquired with an iXon +897 electron-multiplying charge-coupled device camera with a solid state laser of 488 nm or 647 nm as a light source. Images were analyzed using FIJI (Schindelin et al., 2012).

Quantification of individual recycling events

PC12 cells stably expressing SpH-KOR (SpH-KOR cells) were treated with KOR agonists: Dyn A17, Dyn B13, Dyn A8, or a-neo endorphin (1 mM) for 5 min to induce receptor clustering and internalization at 37˚C. Receptor clustering was visualized using TIRF microscopy. Images were acquired every 3 s for a total of 5 min. Following internalization, a recycling movie was recorded at 10 Hz for 1 min in TIRF. The number of exocytic recycling events were manually scored in FIJI (Fiji Is Just Image J) to determine the recycling rate for each agonist. Recycling events were counted throughout the 1 min movie and the total number of events were normalized by the cell area to determine a recycling rate. Recycling events were also recorded using the same method in primary striatal rat medium spiny neurons transfected with the SpH-KOR plasmid. Recycling movies were taken 30 min after agonist addition in neurons. Statistical significance was determined using a one-way ANOVA

Ensemble recycling assay

Receptor surface levels were measured in PC12 cells stably expressing SpH-KOR (SpH-KOR cells) by using confocal microscopy on a 20 objective and 488 nm laser. Images were collected in 30 s intervals across 20 different cell fields. After 2 min of baseline an agonist (1 mM Dyn A17 or Dyn B13) was added to imaging media. Following agonist addition, images were collected for 15 min. After 15 min, agonist was removed, and the imaging media was

replaced with fresh media containing antagonist (naltrexone; 10 mm). Images were then collected for another 15 min. Fluorescence intensities were corrected by a background threshold and normalized by the average fluorescence of the baseline frames before agonist treatment. Surface fluorescence analysis was conducted using an ImageJ Macro automated script (National Institutes of Health) (Weinberg et al., 2019). Fluorescence recovery/loss ratios after washout were quantified by normalizing the fluorescence values after washout to the total fluorescence lost before washout. Cell fields that did not respond to Dynorphin treatment were excluded from analysis. Statistical significance was determined by using Student's paired t-test comparing the endpoints between agonist treatment.

ELISA internalization assays

CHO cells expressing Flag-epitope tagged KOR (CHO-KOR cells) or PC12 cells stably expressing SpH-KOR (SpH-KOR cells) were seeded in complete growth media into 24-well plates (2 105 cells per well). Next day, cells were rinsed with PBS followed by labeling with mouse anti-Flag antibodies for CHO-KOR cells or chicken anti-GFP antibodies for SpH-KOR cells (1:1000 in PBS containing 1% BSA) for 1 hr at 4˚C, followed by treatment with 0–10 mM of Dyn A or Dyn B in growth media containing protease inhibitor cocktail (Sigma-Aldrich; Cat. No. P2714) for 60 min at 37˚C. Cells were briefly fixed (3 min) with 4% paraformaldehyde followed by three washes (5 min each) with PBS, and incubation with anti-mouse or anti-chicken antibody coupled with horse-radish peroxidase (1:1000 in PBS containing 1% BSA) for 90 min at 37˚C. Cells were washed three times with 1% BSA in PBS (5 min each wash), and color was developed by the addition of the substrate o-phenylenediamine (5 mg/10 ml in 0.15 M citrate buffer [pH 5] containing 15 ml of H2O2). Absorbance at 490 nm was measured with a Bio-Rad

ELISA reader. Values obtained with secondary antibody in the absence of primary antibody were taken as non-specific and subtracted from all points. The percentage of internalized receptors was calculated by taking total cell surface receptors before agonist treatment for each individual experiment as 100% and subtracting percent surface receptors following agonist treatment. Data presented are mean ± SE of three independent experiments in triplicate.

ELISA recycling assays

CHO cells expressing Flag-epitope tagged human KOR (CHO-KOR cells) or PC12 cells stably expressing SpH-KOR (SpH-KOR cells) were seeded in complete growth media into 24-well plates (2 105 cells per well). Next day, cells were rinsed with PBS followed by labeling with mouse anti-Flag antibodies for CHO-KOR cells or chicken anti-GFP antibodies for SpH-KOR cells (1:1000 in PBS containing 1% BSA) for 1 hr at 4˚C, followed by treatment with 100 nM Dyn A, Dyn B, or BAM-22 in growth media containing protease inhibitor cocktail (Sigma-Aldrich; Cat. No. P2714) for 30 min to elicit receptor internalization. The cells were washed to remove the agonist and incubated with medium without or with the ECE2 inhibitor (S136492, 20 mM) for 0–120 min to allow for receptor recycling. At the end of the incubation period, cells were chilled to 4˚C and then fixed briefly (3 min) with 4% paraformaldehyde followed by three washes (5 min each) with PBS and incubation with antimouse or anti-chicken antibody coupled with horse-radish peroxidase (1:1000 in PBS containing 1% BSA) for 90 min at 37˚C. Cells were washed three times with 1% BSA in PBS (5 min each wash), and color was developed by the addition of the substrate o-phenylenediamine (5 mg/10 ml in 0.15 M citrate buffer [pH 5] containing 15 ml of H2O2). Absorbance at 490 nm was measured with a Bio-Rad ELISA reader. Values obtained with secondary antibody in the absence of primary antibody were taken as non-

specific and subtracted from all points. % recycled receptors were calculated by subtracting receptors at t = 0 (30 min internalization) from each recycling time point; this represents 0% recycled receptors. Data presented are mean ± SEM of three independent experiments in triplicate.

Immunofluorescence of endosomal markers

PC12 cells stably expressing SpH-KOR were plated on poly-d-lysine (Sigma Aldrich) coverslips and grown for 24–48 hr at 37˚C. Cells were then incubated with different agonists (Dyn A, Dyn B, Dyn A8, or a-neo) for 20 min at 37˚C. Cells were then fixed with 4% paraformaldehyde (PFA), pH 7.4, for 20 min. Cells were then rinsed with complete PBS twice and then blocked in PBS containing calcium, magnesium, with 5% FBS, 5% 1M glycine, and 0.75% Triton X-100. SpH-KOR cells were then incubated with an antibody for one of the endosomal markers for 1 hr. Cells were washed three times with PBS containing calcium and magnesium and then labeled with Alexa 647 goat anti-rabbit secondary antibody (1:1000) in a blocking buffer for 1 hr. Confocal imaging of cells was performed using spinning disk confocal microscope (Andor) and 100 objective. Representative images were taken across 10–20 fields for each agonist treatment and endosomal marker. Three biological replicates were performed in each condition.

Endosomal KOR colocalization in live cells with nanobodies and lysotracker

PC12 cells were transiently transfected with FLAG-KOR and Nb39-YFP or (Nb33-GFP). Cells were labeled with M1-647 for 10 min prior to imaging 3 days after transfection. Images were taken before and after cells were treated with 1 mM Dyn A or Dyn B for 20 min. Confocal

imaging of cells was performed using spinning disk confocal microscope (Andor) and 100 objective. Representative images were taken across 10–20 fields for each agonist treatment. In the experiments with Dyngo4A, cells were pretreated with 40 mM Dyngo4a for 30 min prior to imaging. In the Lysotracker experiments, cells were labeled with 25 nM Lysotracker-561 for 5 min prior to imaging.

Endosomal colocalization quantification

The percent colocalization of the endosomal marker with the total number of receptor positive endosomes was determined using an ImageJ Macro: Object.picker (Weinberg, 2020; doi.10.5281/ zenodo.3811031) to identify the total number of endosomes containing receptor in one channel and determine the colocalization with an endosomal marker in another channel. The Image J macro: 3D Object Counter was used as another method of quantification for colocalization. Integrated density values for each object detected in both the receptor and endosome marker channels were used to determine a ratio of endosomal colocalization by dividing the endosomal marker signal by the receptor signal.

Immunoblotting

PC12 cells stably expressing SpH-KOR were grown in a PDL coated 12-well plate for 2 days at 37˚C. Cells were treated with cycloheximide (3 mg/ml) for 2 hr before agonist incubation. Cells were treated with Dyn A17 or Dyn B13 for 30 min or 2 hr. A non-agonist treated well of PC12 cells stably expressing SpH-KOR and a well of PC12 cells not expressing SpH-KOR were used as controls. Following agonist treatments, cells were placed on ice and rinsed twice with PBS containing calcium and magnesium. Cells were directly lysed in the plate

using 2 RSB (Bio-Rad, Hercules, CA). Lysates were placed on ice for 30 min and then sonicated in 5 s pulses. Following sonication, lysates were incubated at 37˚C for 1 hr. Lysates were run on 10% stain-free gels (BioRad), which were then transferred to nitrocellulose membrane overnight. Membranes were blocked in 5% milk and then probed with anti-GFP Chicken pAB (Abcam) to detect total receptor levels in each condition. Blots were developed using the iBright imager for chemiluminescence signal and quantified using FIJI software. Receptor signal for each condition was normalized to the no treatment control. Five biological replicates were performed. Statistical analysis was performed using two-way ANOVA across time and drug treatment. To test for mTOR activation, PC12 cells stably expressing SpH-KOR were grown in a PDL coated 12-well plate for 2 days at 37˚C. Cells were starved overnight in serum-free media and then treated with 1 mM Dyn A or Dyn B for 5 min or 20 min. Cells were placed on ice and rinsed twice with PBS containing calcium and magnesium. Cells were directly lysed in the plate using 2 RSB (Bio-Rad, Hercules, CA). Lysates were placed on ice for 5 min and then placed at 95˚C for 5 min. Lysates were run on 10% stain-free gels (BioRad), which were then transferred to nitrocellulose membrane overnight. Membranes were blocked in 5% BSA and then probed with phospho-p70 S6K (CST) to detect phosphorylated S6K levels in each condition. Blots were developed using the iBright imager for chemiluminescence signal and quantified using FIJI software. Membrane was stripped and probed with total p70 S6K (CST) to determine total levels of S6K present in the samples. The phospho-p70 S6K signal was normalized to the total p70 S6K signal for each condition. All samples were then normalized to the no treatment control to determine the fold change over baseline for each condition. Five biological replicates were performed. Statistical analysis was performed using two-way ANOVA across time and drug treatment.

cAMP assays

PC12 cells stably expressing SpH-KOR (SpH-KOR cells) or CHO cells stably expressing Flag epitope tagged human KOR (CHO-KOR cells) cells (10,000/well) were treated with Dyn A, Dyn B, Dyn A8, or a-neo (1 mM) for 30 min at 37˚C in HBSS assay buffer containing 10 mM HEPES, 20 mM forskolin, and protease inhibitor cocktail (Sigma-Aldrich; Cat. No. P2714) and cAMP levels were quantified using the HitHunter cAMP detection kit from DiscoveRx according to the manufacturer's protocol. In a separate set of experiments dose–response curves were carried out with Dyn A or Dyn B (0–10 mM). In another set of experiments cells were treated Dyn A or Dyn B (1 mM) for 5 min, after which peptides were washed out and cells were incubated in assay buffer for 25 min. Cells were then given a second 5 min treatment with Dyn A or Dyn B (1 mM) and cAMP levels measured. Values obtained in the absence of peptide were taken as 100%. Data presented are mean ± SEM of three independent experiments in triplicate.

2.5 References

Bowman SL, Shiwarski DJ, Puthenveedu MA. 2016. Distinct G protein–coupled receptor recycling pathways allow spatial control of downstream G protein signaling. Journal of Cell Biology 214:797–806. DOI: https://doi.org/ 10.1083/jcb.201512068

Chavkin C. 2013. Dynorphin–still an extraordinarily potent opioid peptide. Molecular Pharmacology 83:729–736. DOI: https://doi.org/10.1124/mol.112.083337, PMID: 23152558

Che T, Majumdar S, Zaidi SA, Ondachi P, McCorvy JD, Wang S, Mosier PD, Uprety R, Vardy E, Krumm BE, Han GW, Lee MY, Pardon E, Steyaert J, Huang XP, Strachan RT, Tribo AR, Pasternak GW, Carroll FI, Stevens RC, et al. 2018. Structure of the Nanobody-Stabilized active state of the kappa opioid receptor. Cell 172:55–67. DOI: https://doi.org/10.1016/j.cell.2017.12.011, PMID: 29307491

Che T, Roth BL. 2018. Phosphoproteomics illuminates opioid actions. Biochemistry 57:5505–5506. DOI: https:// doi.org/10.1021/acs.biochem.8b00809, PMID: 30179451

Chiu YT, Chen C, Yu D, Schulz S, Liu-Chen LY. 2017. Agonist-Dependent and -Independent k opioid receptor phosphorylation: distinct phosphorylation patterns and different cellular outcomes. Molecular Pharmacology 92:588–600. DOI: https://doi.org/10.1124/mol.117.108555, PMID: 28893975

Corder G, Castro DC, Bruchas MR, Scherrer G. 2018. Endogenous and exogenous opioids in pain. Annual Review of Neuroscience 41:453–473. DOI: https://doi.org/10.1146/annurev-neuro-080317-061522, PMID: 2 9852083

Dores MR, Trejo J. 2019. Endo-lysosomal sorting of G-protein-coupled receptors by ubiquitin: diverse pathways for G-protein-coupled receptor destruction and beyond. Traffic 20:101–109. DOI: https://doi.org/10.1111/tra. 12619, PMID: 30353650

Eichel K, von Zastrow M. 2018. Subcellular organization of GPCR signaling. Trends in Pharmacological Sciences 39:200–208. DOI: https://doi.org/10.1016/j.tips.2017.11.009

Fricker LD, Margolis EB, Gomes I, Devi LA. 2020. Five decades of research on opioid peptides: current knowledge and unanswered questions. Molecular Pharmacology 98:96–108. DOI: https://doi.org/10.1124/mol. 120.119388, PMID: 32487735

Gendron L, Cahill CM, von Zastrow M, Schiller PW, Pineyro G. 2016. Molecular pharmacology of d-Opioid receptors. Pharmacological Reviews 68:631–700. DOI: https://doi.org/10.1124/pr.114.008979, PMID: 27343248

Gomes I, Filipovska J, Devi LA. 2003. Opioid receptor oligomerization. Detection and functional characterization of interacting receptors. Methods in Molecular Medicine 84:157–183. DOI: https://doi.org/10.1385/1-59259- 379-8:157, PMID: 12703323

Gomes I, Gupta A, Filipovska J, Szeto HH, Pintar JE, Devi LA. 2004. A role for heterodimerization of mu and Delta opiate receptors in enhancing morphine analgesia. PNAS 101:5135–5139. DOI: https://doi.org/10.1073/ pnas.0307601101, PMID: 15044695

Gomes I, Ijzerman AP, Ye K, Maillet EL, Devi LA. 2011. G protein-coupled receptor heteromerization: a role in allosteric modulation of ligand binding. Molecular Pharmacology 79:1044–1052. DOI: https://doi.org/10.1124/ mol.110.070847, PMID: 21415307

Gomes I, Sierra S, Lueptow L, Gupta A, Gouty S, Margolis EB, Cox BM, Devi LA. 2020. Biased signaling by endogenous opioid peptides. PNAS 117:11820–11828. DOI: https://doi.org/10.1073/pnas.2000712117, PMID: 32393639

Gupta A, Fujita W, Gomes I, Bobeck E, Devi LA. 2015. Endothelin-converting enzyme 2 differentially regulates opioid receptor activity. British Journal of Pharmacology 172:704–719. DOI: https://doi.org/10.1111/bph. 12833, PMID: 24990314

Gupta A, Gomes I, Bobeck EN, Fakira AK, Massaro NP, Sharma I, Cave´ A, Hamm HE, Parello J, Devi LA. 2016. Collybolide is a novel biased agonist of k-opioid receptors with potent

antipruritic activity. PNAS 113:6041– 6046. DOI: https://doi.org/10.1073/pnas.1521825113, PMID: 27162327

Hanyaloglu AC. 2018. Advances in membrane trafficking and endosomal signaling of G Protein-Coupled receptors. International Review of Cell and Molecular Biology 339:93–131. DOI: https://doi.org/10.1016/bs. ircmb.2018.03.001, PMID: 29776606

Henry AG, White IJ, Marsh M, von Zastrow M, Hislop JN. 2011. The role of ubiquitination in Lysosomal trafficking of d-opioid receptors. Traffic 12:170–184. DOI: https://doi.org/10.1111/j.1600-0854.2010.01145.x, PMID: 21106040

Irannejad R, Tomshine JC, Tomshine JR, Chevalier M, Mahoney JP, Steyaert J, Rasmussen SG, Sunahara RK, ElSamad H, Huang B, von Zastrow M. 2013. Conformational biosensors reveal GPCR signalling from endosomes. Nature 495:534–538. DOI: https://doi.org/10.1038/nature12000, PMID: 23515162

Kunselman JM, Zajac AS, Weinberg ZY, Puthenveedu MA. 2019. Homologous regulation of mu opioid receptor recycling by G bg , Protein Kinase C, and Receptor Phosphorylation. Molecular Pharmacology 96:702–710. DOI: https://doi.org/10.1124/mol.119.117267, PMID: 31575621

Li JG, Haines DS, Liu-Chen LY. 2008. Agonist-Promoted Lys63-Linked polyubiquitination of the human k-Opioid receptor is involved in receptor Down-Regulation. Molecular Pharmacology 73:1319–1330. DOI: https://doi. org/10.1124/mol.107.042846, PMID: 18212250

Liu JJ, Sharma K, Zangrandi L, Chen C, Humphrey SJ, Chiu YT, Spetea M, Liu-Chen LY, Schwarzer C, Mann M. 2018. In vivo brain GPCR signaling elucidated by phosphoproteomics. Science 360:eaao4927. DOI: https://doi. org/10.1126/science.aao4927, PMID: 29930108

Liu JJ, Chiu YT, DiMattio KM, Chen C, Huang P, Gentile TA, Muschamp JW, Cowan A, Mann M, Liu-Chen LY. 2019. Phosphoproteomic approach for agonist-specific signaling in mouse brains: mtor pathway is involved in k opioid aversion. Neuropsychopharmacology 44:939–949. DOI: https://doi.org/10.1038/s41386-018-0155-0, PMID: 30082888

Liu-Chen LY. 2004. Agonist-induced regulation and trafficking of kappa opioid receptors. Life Sciences 75:511– 536. DOI: https://doi.org/10.1016/j.lfs.2003.10.041, PMID: 15158363

Manglik A, Kobilka BK, Steyaert J. 2017. Nanobodies to study G Protein-Coupled receptor structure and function. Annual Review of Pharmacology and Toxicology 57:19–37. DOI: https://doi.org/10.1146/annurevpharmtox-010716-104710, PMID: 27959623

Mann A, Moule´ dous L, Froment C, O'Neill PR, Dasgupta P, Gu¨ nther T, Brunori G, Kieffer BL, Toll L, Bruchas MR, Zaveri NT, Schulz S. 2019. Agonist-selective NOP receptor phosphorylation correlates in vitro and in vivo and reveals differential post-activation signaling by chemically diverse agonists. Science Signaling 12:eaau8072. DOI: https://doi.org/10.1126/scisignal.aau8072, PMID: 30914485

Mzhavia N, Pan H, Che FY, Fricker LD, Devi LA. 2003. Characterization of endothelin-converting enzyme-2. implication for a role in the nonclassical processing of regulatory peptides. The Journal of Biological Chemistry 278:14704–14711. DOI: https://doi.org/10.1074/jbc.M211242200, PMID: 12560336

Nikoshkov A, Hurd YL, Yakovleva T, Bazov I, Marinova Z, Cebers G, Pasikova N, Gharibyan A, Terenius L, Bakalkin G. 2005. Prodynorphin transcripts and proteins differentially expressed and regulated in the adult human brain. The FASEB Journal 19:1543–1545. DOI: https://doi.org/10.1096/fj.05-3743fje, PMID: 16014400

Padilla BE, Cottrell GS, Roosterman D, Pikios S, Muller L, Steinhoff M, Bunnett NW. 2007. Endothelin-converting enzyme-1 regulates endosomal sorting of calcitonin receptor-like receptor and b-arrestins. Journal of Cell Biology 179:981–997. DOI: https://doi.org/10.1083/jcb.200704053

Patwardhan A, Cheng N, Trejo J. 2021. Post-Translational modifications of G Protein-Coupled receptors control cellular signaling dynamics in space and time. Pharmacological Reviews 73:120–151. DOI: https://doi.org/10. 1124/pharmrev.120.000082, PMID: 33268549

Roosterman D, Cottrell GS, Padilla BE, Muller L, Eckman CB, Bunnett NW, Steinhoff M. 2007. Endothelinconverting enzyme 1 degrades neuropeptides in endosomes to control receptor recycling. PNAS 104:11838– 11843. DOI: https://doi.org/10.1073/pnas.0701910104, PMID: 17592116

Rozenfeld R, Devi LA. 2008. Regulation of CB1 cannabinoid receptor trafficking by the adaptor protein AP-3. FASEB Journal : Official Publication of the Federation of American Societies for Experimental Biology 22:2311– 2322. DOI: https://doi.org/10.1096/fj.07-102731, PMID: 18267983

Sankaranarayanan S, De Angelis D, Rothman JE, Ryan TA. 2000. The use of pHluorins for optical measurements of presynaptic activity. Biophysical Journal 79:2199–2208. DOI: https://doi.org/10.1016/S0006-3495(00)76468- X, PMID: 11023924

Schindelin J, Arganda-Carreras I, Frise E, Kaynig V, Longair M, Pietzsch T, Preibisch S, Rueden C, Saalfeld S, Schmid B, Tinevez JY, White DJ, Hartenstein V, Eliceiri K, Tomancak P, Cardona A. 2012. Fiji: an open-source platform for biological-image analysis. Nature Methods 9:676–682. DOI: https://doi.org/10.1038/nmeth.2019, PMID: 22743772

Sposini S, Jean-Alphonse FG, Ayoub MA, Oqua A, West C, Lavery S, Brosens JJ, Reiter E, Hanyaloglu AC. 2017. Integration of GPCR signaling and sorting from very early endosomes via opposing APPL1 mechanisms. Cell Reports 21:2855–2867. DOI: https://doi.org/10.1016/j.celrep.2017.11.023, PMID: 29212031

Sternini C, Duraffourd C, Anselmi L. 2013. Opioids. In: Sternini C (Ed). Handbook of Biologically Active Peptides. Elsevier. p. 1283–1288. DOI: https://doi.org/10.1016/C2010-0-66490-X

Stoeber M, Jullie´ D, Lobingier BT, Laeremans T, Steyaert J, Schiller PW, Manglik A, von Zastrow M. 2018. A genetically encoded biosensor reveals location Bias of opioid drug action. Neuron 98:963–976. DOI: https:// doi.org/10.1016/j.neuron.2018.04.021, PMID: 29754753

Vilardaga JP, Jean-Alphonse FG, Gardella TJ. 2014. Endosomal generation of cAMP in GPCR signaling. Nature Chemical Biology 10:700–706. DOI: https://doi.org/10.1038/nchembio.1611, PMID: 25271346

Weinberg ZY, Crilly SE, Puthenveedu MA. 2019. Spatial encoding of GPCR signaling in the nervous system. Current Opinion in Cell Biology 57:83–89. DOI: https://doi.org/10.1016/j.ceb.2018.12.006, PMID: 30708280

Weinberg Z. 2020. IJMacros: object-picker. Zenodo. https://doi.org/10.5281/zenodo.3811031

Williams JT, Ingram SL, Henderson G, Chavkin C, von Zastrow M, Schulz S, Koch T, Evans CJ, Christie MJ. 2013. Regulation of m-opioid receptors: desensitization, phosphorylation, internalization, and tolerance. Pharmacological Reviews 65:223–254. DOI: https://doi.org/10.1124/pr.112.005942, PMID: 23321159

Willinger T, Ferguson SM, Pereira JP, De Camilli P, Flavell RA. 2014. Dynamin 2–dependent endocytosis is required for sustained S1PR1 signaling. Journal of Experimental Medicine 211:685–700. DOI: https://doi.org/ 10.1084/jem.20131343

Yarwood RE, Imlach WL, Lieu T, Veldhuis NA, Jensen DD, Klein Herenbrink C, Aurelio L, Cai Z, Christie MJ, Poole DP, Porter CJH, McLean P, Hicks GA, Geppetti P, Halls ML, Canals M, Bunnett NW. 2017. Endosomal signaling of the receptor for calcitonin gene-related peptide mediates pain transmission. PNAS 114:12309– 12314. DOI: https://doi.org/10.1073/pnas.1706656114, PMID: 29087309

Zhao P, Canals M, Murphy JE, Klingler D, Eriksson EM, Pelayo J-C, Hardt M, Bunnett NW, Poole DP. 2013. Agonist-biased trafficking of somatostatin receptor 2A in enteric neurons. Journal of Biological Chemistry 288: 25689–25700. DOI: https://doi.org/10.1074/jbc.M113.496414

Chapter 3: Homologous Regulation of Mu Opioid Receptor Recycling

Published as Kunselman, J. M., Zajac, A. S., Weinberg, Z. Y., & Puthenveedu, M. A. (2019). Homologous regulation of mu opioid receptor recycling by Gβγ, Protein Kinase C, and receptor phosphorylation. Molecular Pharmacology, 96(6), 702-710.

Abstract

Membrane trafficking and receptor signaling are two fundamental cellular processes that interact constantly. Although how trafficking regulates signaling is well studied, how signaling pathways regulate trafficking is less well understood. Here we use the mu opioid receptor (MOR), the primary target for opioid analgesics, to define a signaling pathway that dynamically regulates post-endocytic receptor recycling. By directly visualizing individual MOR recycling events, we show that agonist increases MOR recycling. Inhibition of Gβγ, Phospholipase-C, or Protein Kinase C mimicked agonist removal, while activation of Gβγ increased recycling even after agonist removal. Phosphorylation of serine 363 on the C-terminal tail of MOR was required and sufficient for agonist-mediated regulation of MOR recycling. Our results identify a feedback loop that regulates MOR recycling via Gβγ, Protein Kinase C, and receptor phosphorylation. This could serve as a general model for how signaling regulates post-endocytic trafficking of G protein-coupled receptors.

3.1 Introduction

The dynamic relationship between trafficking and signaling of receptors is currently being redefined by new paradigms that are emerging in the field. This is especially true in the case of G protein–coupled receptors (GPCRs), the largest class of signaling receptors in humans (Pierce et al., 2002; Sriram and Insel, 2018). Activated GPCRs signal via multiple signaling pathways, some of which cause receptors to be internalized and trafficked to endosomes. Internalized GPCRs may be either recycled back to the surface or degraded. Classically, this endocytic trafficking was thought to primarily control the desensitization and resensitization of signaling via G proteins by removing receptors from or returning receptors to the cell surface (Lefkowitz et al., 1997; Marchese et al., 2008). However, recent evidence shows that many GPCRs can signal from intracellular sites, and that intracellular signaling can have distinct downstream effects compared with signaling from the surface (Irannejad et al., 2013; Vilardaga et al., 2014; Thomsen et al., 2018). Intracellular signaling from endosomal microdomains might be a general characteristic of GPCRs, as the list of GPCRs that can signal from intracellular compartments is still growing (Caengprasath and Hanyaloglu, 2019; Weinberg et al., 2019). This supports the emerging idea that an equally important role of trafficking is to transfer receptors between distinct signaling environments within a cell.

In the endosome, receptors need to be localized to specific endosomal microdomains both to sort into specific recycling pathways and to signal (Ferrandon et al., 2009; Vistein and Puthenveedu, 2013; Bowman et al., 2016). The localization of receptors in these domains and their further intracellular sorting are mediated by specific sequences on the C-terminal tails of the receptors (Tanowitz and von Zastrow, 2003; Bowman and Puthenveedu, 2015; Bahouth and Nooh, 2017). For some of these sequences, interacting proteins that mediate this sorting and

recycling have been identified (Romero et al., 2011; Dunn and Ferguson, 2015; Broadbent et al., 2017). Nevertheless, how this sorting and recycling is dynamically regulated by signaling pathways is a fundamental question that is still not well understood.

The mu opioid receptor (MOR) is an excellent model GPCR that can be used to address this question. MOR is highly physiologically relevant, as it is the primary target for many currently used and abused opioid drugs. Endosomal sorting of MOR, based on a unique leucine-based sequence, can dynamically regulate its responses to different agonists at cellular and organismal levels (Williams et al., 2013; Bowman et al., 2015; Weinberg et al., 2017) MOR undergoes rapid phosphorylation and dephosphorylation in response to agonists, and heterologous manipulation of this phosphorylation regulates its plasma membrane localization, trafficking, and signaling (Feng et al., 2011; Just et al., 2012; Bowman et al., 2015; Halls et al., 2016; Arttamangkul et al., 2018).

In this study, we used a real-time live-cell-imaging assay that resolves MOR recycling at single-event resolution to study the homologous signals that allow self-regulation of endosomal sorting of MOR. We show that activation of MOR initiates downstream signaling cascades that enhance postendocytic receptor recycling back to the cell surface. The signaling cascade requires the G$\beta\gamma$-activated phospholipase C (PLC)/protein kinase C (PKC) signaling pathway, which results in the phosphorylation of serine 363 on MOR's C-terminal tail. This phosphorylation is required for increased MOR recycling. The positive feedback loop that regulates MOR endocytic trafficking that we describe here may serve as a template for similar adaptive self-regulatory mechanisms for many GPCRs.

3.2 Results

The Opioid Agonist DAMGO Increases Post-endocytic Recycling of MOR.

To determine if the signals downstream of activated MOR regulate its own post-endocytic recycling, we quantitated MOR recycling using a live cell imaging assay that resolves individual MOR recycling events without the confounding effects of endocytosis. To visualize recycling events, MOR was N-terminally tagged with a pH-sensitive GFP (SpH) (Sankaranarayanan et al., 2000). HEK293 cells stably expressing MOR that was N-terminally tagged with the pH-sensitive GFP superecliptic phluorin (SpH-MOR) were imaged using total internal reflection fluorescence microscopy. SpH-MOR on the cell surface is fluorescent and readily detectable. After activation, receptors are internalized into acidic endosomal compartments where the SpH fluorescence is quenched. When recycling vesicles containing receptors fuse back to the plasma membrane during an exocytic event, the SpH fluorescence is exposed to the neutral pH of the extracellular medium and is therefore dequenched. This coordinated dequenching generates a characteristic "puff" of fluorescence that is readily detectable (Supplemental Movie 1). We and others have extensively characterized these and similar puffs previously and confirmed that they represent individual vesicle fusion events during receptor recycling (e.g., Yudowski et al., 2006; Bowman et al., 2015; Logan et al., 2017).

Individual fusion events were readily observed after cells expressing SpH-MOR were treated with the opioid agonist DAMGO for 5 minutes (Figure 3.1A and B). Agonist-containing medium was washed out and replaced with medium containing naltrexone. Recycling movies were recorded 1 and 6 minutes after this washout (Figure 3.1C) and the number of individual events was normalized to the area in each cell. The raw recycling rate per cell area ± washout

was determined for each recycling movie (Figure 3.1D). This approach allowed us to follow changes in the same cells over time and to normalize the raw values to the baseline recycling rate in each condition for each cell (Figure 3.1E). When compared with cells continuously exposed to agonist for similar times (Figure 3.1D), the number of MOR recycling events decreases from baseline following agonist removal ($P < 0.0001$). Additionally, the normalized data matched at the same time points indicate statistically significant differences in recycling at 1 minute ($P < 0.0001$) and 6 minutes ($P < 0.0001$) for −washout versus +washout (Figure 3.1E). These results indicate that MOR signaling positively regulates MOR recycling.

Figure 3.1

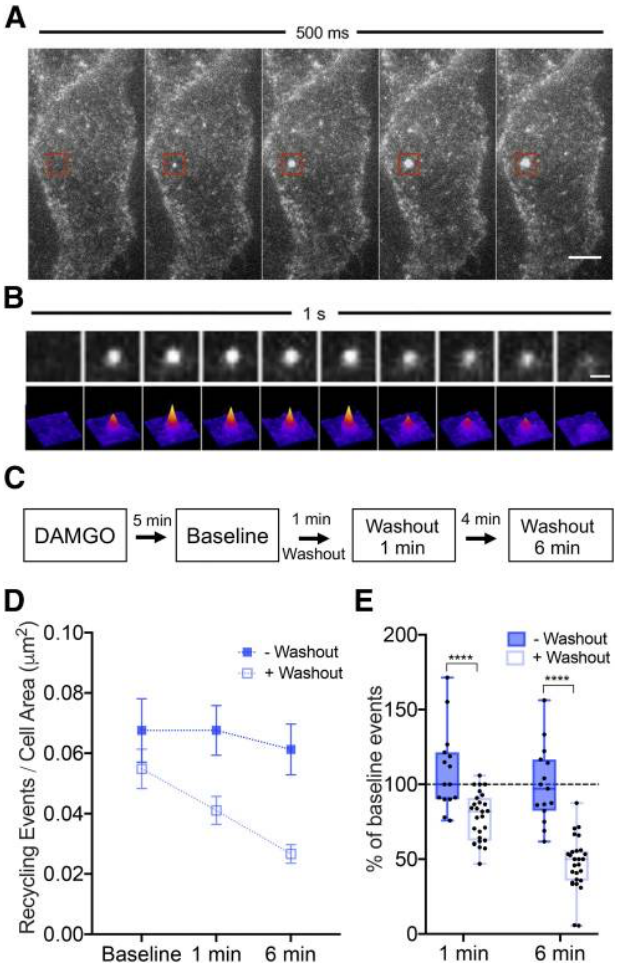

Figure 3.1. The opioid agonist DAMGO increases postendocytic recycling of MOR. (A) HEK293 cell expressing SpH-MOR imaged with total internal reflection fluorescence microscopy after DAMGO addition. The appearance of an individual exocytic recycling event is denoted by red boxes. Images are 100 ms apart. Scale bar, 5 μm. (B) Profile of an individual exocytic event (puff) over 1 s. Frames are 100 ms apart. Scale bar, 1 μm. The event begins as a defined spot of fluorescence intensity that appears suddenly. The fluorescence diffuses on the cell membrane as shown by the heat map surface plot. (C) Experimental paradigm to study MOR postendocytic recycling. (D) The number of recycling events normalized to cell area (square micrometer) over time ± DAMGO washout after the baseline recording. In the −washout condition, $P > 0.999$ for baseline versus +1 minute and $P = 0.306$ for baseline versus +6 minutes ($n = 15$ cells). In the +washout condition, ****$P < 0.0001$ for both baseline versus 1-minute washout and baseline versus 6-minute washout ($n = 27$ cells). Mean and S.E.M. are plotted for each time point. (E) The percentage of recycling events in each condition (±washout) was normalized to the baseline events for each condition. ****$P < 0.0001$ for −washout 1 minute versus +washout 1 minute. ****$P < 0.0001$ for −washout 6 minutes versus +washout 6 minutes (−washout: $n = 15$ cells; +washout: $n = 27$ cells.) Box and whisker plots are shown with all points from each condition.

The Agonist-Mediated Increase in MOR Recycling Rate Requires G Protein Signaling.

To address which signals downstream of receptor activation are involved in regulating postendocytic MOR recycling, we first probed the role of G proteins that couple to MOR by using the G protein inhibitor pertussis toxin (PTX). In SpH-MOR cells treated with PTX 14–16 hours before imaging, DAMGO-induced MOR clustering into endocytic domains was not inhibited (Figure 3.2A and B), consistent with previous studies (Halls et al., 2016; (Gondin et al., 2019)). Fluorescence values normalized to the first frames after DAMGO addition were quantified for control and PTX-treated cells as an index of receptor internalization. The decrease in fluorescence over the first 5 minutes after DAMGO addition was not different between control and PTX-treated cells, suggesting that endocytosis of the receptor was not altered due to PTX treatment (Figure 3.2C). When individual recycling events were quantified in the PTX condition, however, the baseline recycling rate was decreased compared with control ($P = 0.0064$), as shown in the summary data (Figure 3.2D). The full box plots and statistical comparisons are

shown in the corresponding panel of Supplemental Figure 3.2 (Supplemental Figure 3.2B). Following agonist washout, the recycling rate was unchanged compared with before washout in the PTX condition (Figure 3.2D). The normalized recycling for each baseline condition indicates a statistically significant change in the percentage of initial recycling between ±PTX at the time point 6 minutes after washout ($P = 0.0003$). These results show that agonist-mediated increase in MOR recycling requires G protein signaling.

Since $G\alpha_i$ negatively regulates protein kinase A (PKA) through its primary effector adenylate cyclase, we next tested whether PKA activity changed MOR recycling. PKA inhibition by KT5720, an acute PKA inhibitor, did not change MOR recycling compared with untreated cells (Figure 3.2F). Further, neither forskolin, which activates adenylate cyclase, thereby increasing cAMP and activating PKA, nor subsequent inhibition of PKA in the same cells changed MOR recycling rates (Figure 3.2F). These results suggest that, in our cells, cAMP and PKA signaling downstream of $G\alpha_i$ does not regulate MOR recycling.

Figure 3.2

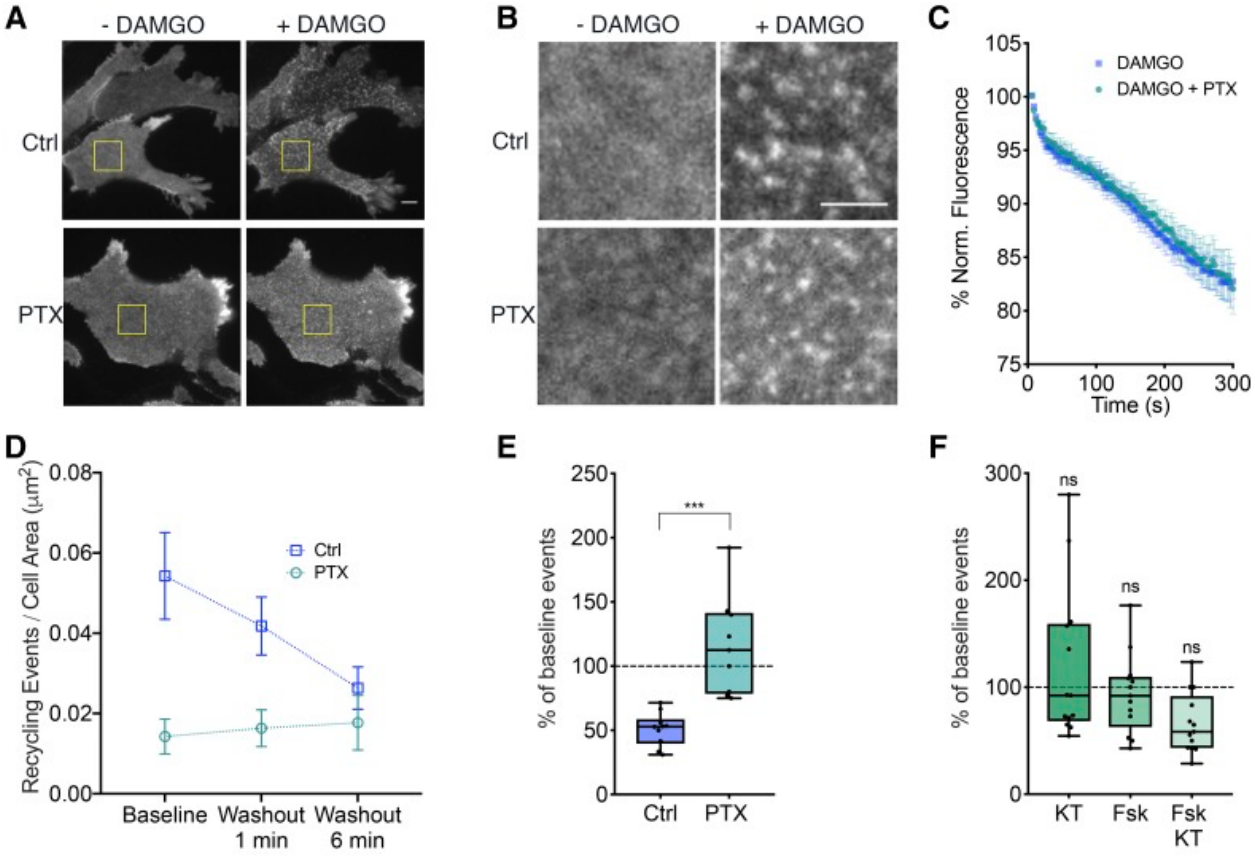

Figure 3.2. The agonist-mediated increase in MOR recycling requires G protein signaling. (A) Representative images of HEK293 cell expressing SpH-MOR imaged with total internal reflection fluorescence microscopy before and after DAMGO addition. Cells pretreated with PTX 14–16 hours before imaging. Scale bar, 5 μm. (B) Following DAMGO addition, SpH-MOR clusters on the cell surface before internalizing in both control (Ctrl) and PTX-treated cells. Scale bar, 2.5 μm. (C) Quantification of percentage of normalized fluorescence in control and PTX conditions for the first 5 minutes following DAMGO addition. Values are normalized to the first frames following DAMGO addition (Ctrl: n = 10 cells; PTX: n = 8 cells). (D) Number of recycling events per cell area (square micrometer) over time in response to DAMGO washout ± PTX. P = 0.0064 for control baseline versus PTX baseline (Ctrl: n = 10 cells; PTX: n = 8 cells). Mean and S.E.M. are plotted for each time point. (E) Percentage of baseline recycling events/min at washout 6 minutes for each condition; ***P = 0.0003 for control washout 6 minutes versus PTX washout 6 minutes (Ctrl: n = 10 cells; PTX: n = 8 cells). Box and whisker plots are shown with all points from each condition. (F) Percentage of baseline recycling events/min in response to KT5720 (KT; n = 14 cells), forskolin (Fsk; n = 14 cells), or Fsk + KT (n = 14 cells); treatment normalized to initial baseline recycling events (one-sample t test: P = 0.908 for baseline vs. +KT; P = 0.9758 for baseline vs. +Fsk; P = 0.7886 for baseline vs. +Fsk+KT). Box and whisker plots are shown with all points from each condition. ns, not significant.

Gβγ Signaling Is Required and Sufficient to Increase Post-endocytic Recycling of MOR.

We next tested whether G*βγ* activation regulates MOR recycling. To test whether G*βγ* activation was required, we inhibited G*βγ* using gallein, a small-molecule inhibitor of G*βγ* activation, and measured MOR recycling (Bonacci et al., 2006). In cells incubated with gallein 30 minutes prior to imaging, receptor-mediated clustering and endocytosis were not altered with gallein treatment (Supplemental Figure 3.1A), but baseline recycling decreased compared with that of untreated cells ($P = 0.0046$) (Figure 3.3A). Agonist washout in gallein-treated cells did not decrease recycling to the same extent compared with the control (Figure 3.3B), suggesting that the agonist-mediated increase in MOR recycling requires G*βγ* signaling. To test whether G*βγ* signaling was sufficient to increase MOR recycling, we activated G*βγ* in the absence of agonist and measured MOR recycling. We used mSIRK, a cell-permeable peptide activator of G*βγ*, and the compound 12155, a cell-permeable small-molecule activator of G*βγ* (Goubaeva et al., 2003; Lehmann et al., 2008; Surve et al., 2014), to activate G*βγ*. Both G*βγ* activators increased the rate of MOR recycling at 1 and 6 minutes after washing out DAMGO compared with control cells (Figure 3.3C and D). Interestingly, 12155 increased MOR recycling to a lesser degree than mSIRK, which may reflect different G*βγ* activation mechanisms by these two drugs (Bonacci et al., 2006; Surve et al., 2014). Together, these results indicate that G*βγ* signaling is required and sufficient to enhance MOR recycling back to the cell surface. Our results indicating that G*βγ* signaling is required and sufficient to enhance MOR recycling were also confirmed by measuring surface levels of SpH-MOR at an ensemble level in live cells over time. Since SpH is only fluorescent on the cell surface and not when the receptor is in endosomes, the fluorescence signal accurately measures surface levels of MOR (Yudowski et al., 2009; Vistein and Puthenveedu, 2013). After DAMGO addition, there is a significant decrease in

fluorescence intensity (~50%) as predicted due to receptor internalization. This level reaches a plateau around 10 minutes, which indicates a steady state between endocytosis and recycling. When agonist is removed in a washout, the steady state is shifted by removing the contribution of endocytosis. This results in an increase in fluorescence intensity, which allows us to capture the contribution of receptor recycling.

Multiple fields ($n > 15$) of cells expressing SpH-MOR were selected for each experiment. After collecting a 2-minute baseline signal for each field, DAMGO was added, and the fluorescence signal was recorded for 15 minutes until the signal plateaued. After 15 minutes, the medium containing DAMGO was washed out and replaced with fresh medium containing antagonist (naltrexone) and ±mSIRK or ±12155. The recovery of fluorescence signal was measured for 15 minutes after washout to determine a measurement of ensemble MOR recycling across cells (Figure 3.3E). In the G$\beta\gamma$-activating conditions, we observed an initial spike in fluorescence signal consistent with the increase we observed in the orthogonal puffs assay (Figure 3.3F and G). Overall the increase in fluorescence signal indicates an increase in the number of receptors recycled back to the cell surface in response to sustained G$\beta\gamma$ activation (Figure 3.3H). These results strongly support that G$\beta\gamma$ signaling is required and sufficient to increase MOR recycling.

Figure 3.3

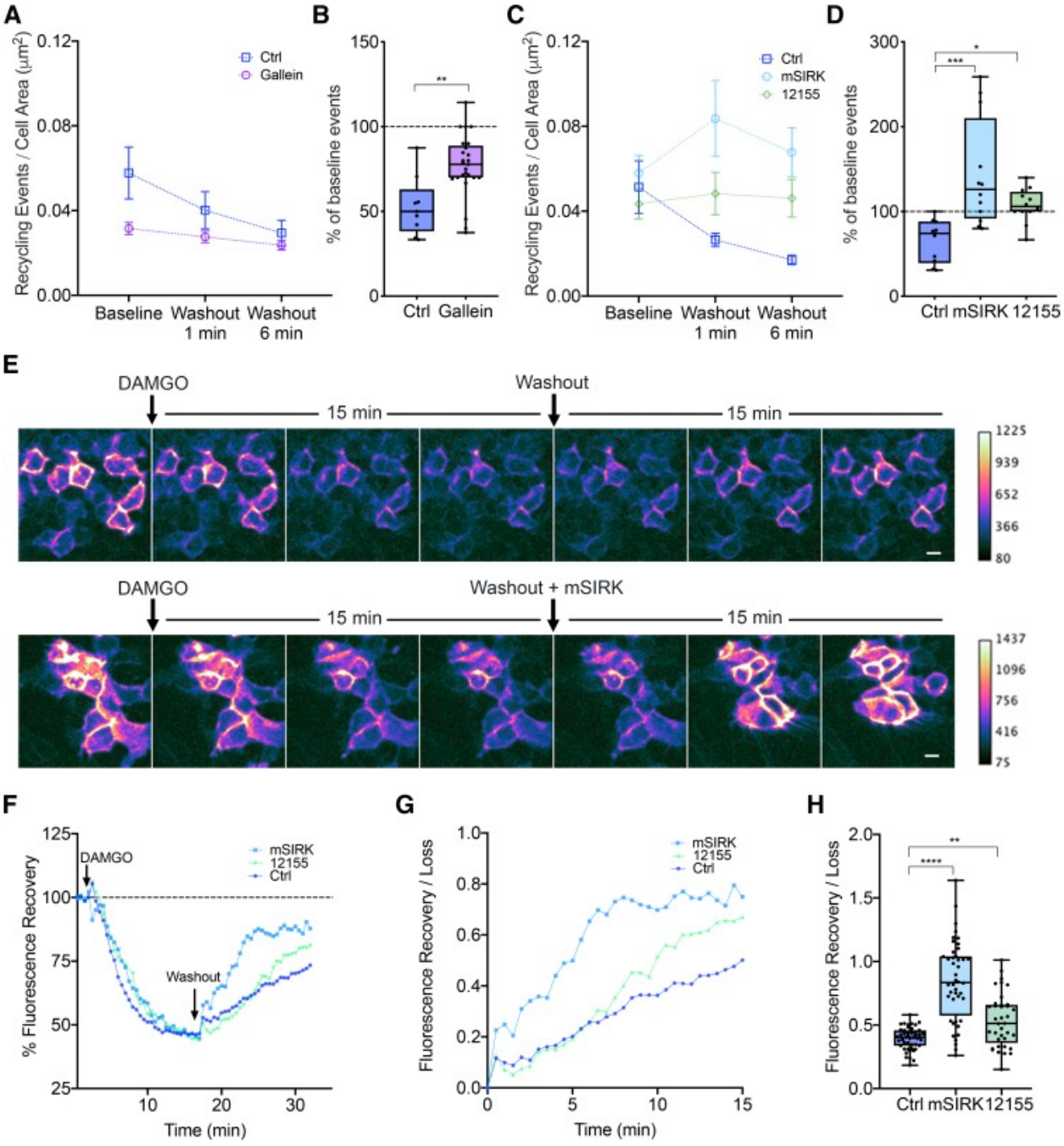

Figure 3.3. G*βγ* activation is required and sufficient to increase MOR recycling. (A) Number of MOR recycling events per cell area (square micrometer) over time in response to a DAMGO washout in control (Ctrl) and gallein conditions. Cells were treated with gallein 30 minutes prior to imaging. $P = 0.0046$ for control baseline versus gallein baseline (Ctrl: $n = 9$ cells; gallein: $n = 25$ cells). Mean and S.E.M. are plotted for each time point. (B) Percentage of baseline recycling events/min at washout 6 minutes for each condition: $P = 0.0015$ for control washout 6 minutes versus gallein washout 6 minutes (Ctrl: $n = 9$ cells; gallein: $n = 25$ cells). Box

and whisker plots are shown with all points from each condition. (C) Number of MOR recycling events per cell area (square micrometer) over time in response to a DAMGO washout in control, mSIRK, and 12155 conditions. Cells were treated acutely with mSIRK or 12155 during the washout. Mean and S.E.M. are plotted for each time point (Ctrl: $n = 10$ cells; mSIRK: $n = 12$ cells; 12155: $n = 12$ cells). (D) Percentage of baseline recycling events/min at washout 1 minute for each condition: ***$P = 0.0003$ for control washout 1 minute versus mSIRK washout 1 minute; *$P = 0.0488$ for control washout 1 minute versus 12155 washout 1 minute (Ctrl: $n = 10$ cells; mSIRK: $n = 12$ cells; 12155: $n = 12$ cells). Box and whisker plots are shown with all points from each condition. (E) Changes in surface MOR fluorescence over time measured after DAMGO addition and washout. MOR fluorescence decreased upon receptor internalization after DAMGO addition and returned upon recycling after DAMGO washout. G$\beta\gamma$ activation by either mSIRK or 12155 increased the rate of recovery of fluorescence. Scale bar, 10 μm. (F) Quantification of fluorescence recovery over 30 minutes following DAMGO treatment normalized to the baseline fluorescence. (G) Quantification of fluorescence recovery normalized to the fluorescence loss before washout for control, mSIRK, or 12155 conditions. (H) Box and whisker plots showing the fluorescence after 15 minutes of agonist washout in control, mSIRK, or 12155 conditions. G$\beta\gamma$ activation by either mSIRK or 12155 increased the receptors recycled; ****$P < 0.0001$ for control versus mSIRK, **$P = 0.0058$ for control versus 12155 (Ctrl: $n = 48$ fields; mSIRK: $n = 44$ fields; 12155: $n = 38$ fields, all across three independent experiments).

MOR Regulates Its Own Recycling via Phospholipase C, Protein Kinase C, and Serine 363.

To determine the signals downstream of G$\beta\gamma$ activation that regulated MOR recycling, we first examined the role of PLC, which is activated by G$\beta\gamma$. To test whether PLC inhibition changed DAMGO-mediated regulation of MOR recycling, we acutely inhibited PLC with U73122 and measured the change in MOR recycling from baseline recycling before PLC inhibition. U73122 decreased MOR recycling even in the presence of DAMGO, whereas U73343, an inactive control, did not change MOR recycling compared with baseline (Figure 3.4A). These results suggest that PLC activation is required for the DAMGO-mediated increase in MOR recycling. We next tested whether PKC signaling was required to increase MOR recycling in the presence of DAMGO. To do this, we acutely inhibited PKC by treating cells with chelerythrine or Gö6983 and measured the change in MOR recycling from baseline

recycling before PKC inhibition (Figure 3.4B). MOR recycling was reduced when PKC was inhibited, suggesting that PKC increased MOR recycling.

Because the C-terminal tail of MOR contains predicted PKC phosphorylation sites (Doll et al., 2011), we tested whether the receptor itself was a target of DAMGO-mediated regulation of MOR recycling. Specifically, we focused on serine 363, a putative PKC phosphorylation site, as a potential regulator of PKC signaling. To test whether serine 363 was required for DAMGO-mediated homologous regulation of MOR recycling, we mutated serine 363 on MOR to alanine. Receptor-mediated clustering and endocytosis were not different between S363A and wild-type (WT) MOR (Supplemental Figure 3.1B). In cells expressing this mutant construct (S363A), however, the number of recycling events was decreased compared with the cells expressing the wild-type MOR (Figure 3.4C). The reduction in recycling seen upon washout of drug was smaller for S363A compared with the wild-type MOR but was not fully abolished, suggesting that other residues or mechanisms may be involved in the regulation of DAMGO-mediated recycling (Figure 3.4D). Further, the recycling of S363A was also insensitive to G$\beta\gamma$ inhibition by gallein (Figure 3.4C and D) Together, these data indicate that phosphorylation at serine 363 is required to increase MOR recycling after activation.

To test if phosphorylation at serine 363 was sufficient to increase MOR recycling in the absence of MOR activation, we examined recycling in cells expressing a phosphomimetic MOR mutant where serine 363 was mutated to an aspartate (S363D). Baseline recycling was not different between the WT MOR and the S363D mutant. However, unlike WT MOR, recycling of the S363D mutant did not decrease from baseline after agonist washout (Figure 3.4C), suggesting that the phosphomimetic mutation was sufficient to keep MOR recycling at a high level even after agonist washout. Together, our results suggest a model of homologous regulation

of MOR recycling, where MOR activation phosphorylates the receptor at serine 363 via G$\beta\gamma$ signaling, PLC, and PKC and increases MOR recycling back to the cell surface (Figure 3.4E).

Figure 3.4

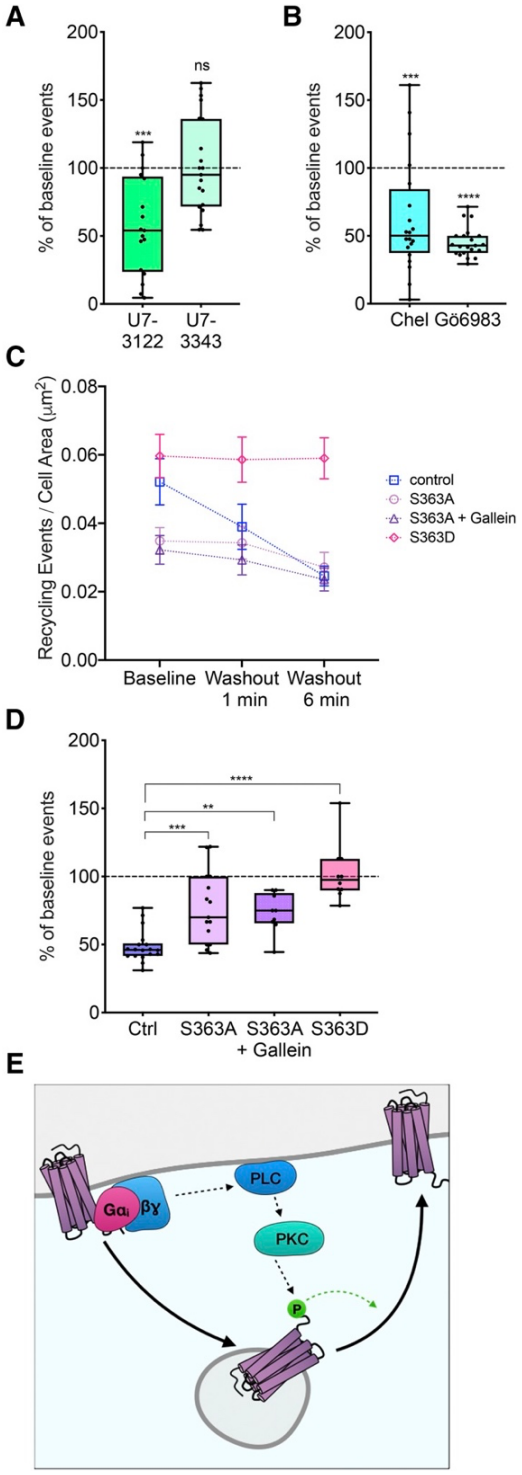
A
% of baseline events
200
150
100
50
0
***
ns
U7-3122
U7-3343
B
% of baseline events
***
****
Chel
Gö6983
C
Recycling Events / Cell Area (μm²)
0.08
0.06
0.04
0.02
0.00
Baseline
Washout 1 min
Washout 6 min
control
S363A
S363A + Gallein
S363D
D
% of baseline events
****
**
***
Ctrl
S363A
S363A + Gallein
S363D
E
Gαi
βγ
PLC
PKC
P

Figure 3.4. Homologous regulation of MOR recycling by MOR phosphorylation at serine 363. (A) Percentage of baseline recycling events/min in response to U73122 (n = 17 cells) or U73343 (n = 21 cells) treatment normalized to initial baseline recycling events. One-sample t test: ***P = 0.0002 for baseline versus U73122; P = 0.8910 for baseline versus U73343. Box and whisker plots are shown with all points from each condition. (B) Percentage of baseline recycling events/min in response to chelerythrine (n = 20 cells) or Gö6983 (n = 21 cells) treatment normalized to initial baseline recycling events. One-sample t test: ***P = 0.0007 for baseline versus chelerythrine; ****P < 0.0001 for baseline versus Gö6983. Box and whisker plots are shown with all points from each condition. (C) Number of recycling events per cell area (square micrometer) over time in response to DAMGO washout in control (Ctrl), S363A, S363A + gallein, or S363D conditions. P = 0.0392 for control baseline vs. S363A baseline; P = 0.0429 for control baseline vs. S363A + gallein baseline; P = 0.7203 for control baseline vs. S363D baseline; P = 0.9391 for S363D baseline vs. S363D washout 6 minutes (Ctrl: n = 18 cells; S363A: n = 15 cells; S363A + gallein: n = 19 cells; S363D: n = 10 cells). Mean and S.E.M. are plotted for each time point. (D) Percentage of baseline recycling events/min at washout 6 minute for each condition: ***P = 0.0003 for control washout 6 minute versus S363A washout 6 minutes; **P = 0.0077 for control washout 6 minutes versus S363A + gallein washout 6 minutes; ****P < 0.0001 for control washout 6 minutes versus S363D washout 6 minutes (Ctrl: n = 18 cells; S363A: n = 15 cells; S363A + gallein: n = 19 cells; S363D: n = 10 cells). Box and whisker plots are shown with all points from each condition. (E) Proposed model of self-regulation of postendocytic recycling of MOR. ns, not significant.

Supplemental Figure 3.1

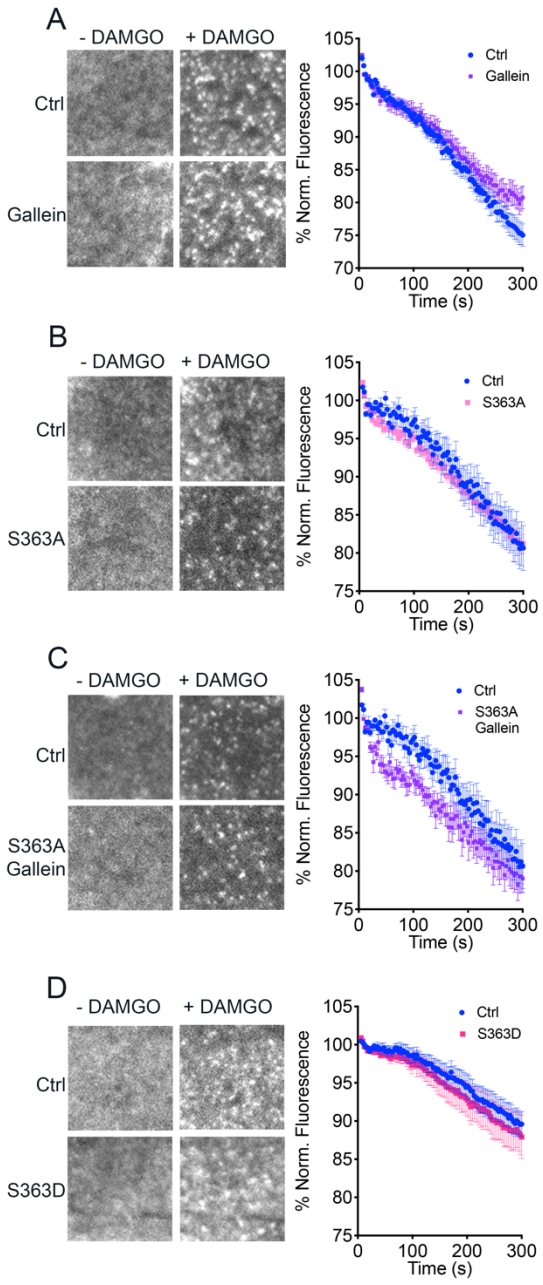

Supplemental Figure 3.1 Clustering and Internalization of MOR across conditions (A) 9.04 µm x 9.04 µm ROI of HEK293 cell expressing SpH MOR in TIRF +/- gallein and +/- DAMGO addition. SpH-MOR clusters on the cell surface in response to DAMGO before internalizing in both control and gallein treated cells. Right panel: Quantification of % normalized fluorescence in control and gallein conditions for the first 5 minutes following DAMGO addition. Values are

normalized to the first frame following DAMGO addition. n=15 cells for Ctrl; n=15 cells for gallein. (B) 9.04 µm x 9.04 µm ROI of HEK293 cell expressing SpH MOR WT or S363A in TIRF +/- DAMGO addition. SpH-MOR clusters on the cell surface in response to DAMGO before internalizing in both control and S363A conditions. Right panel: Quantification of % normalized fluorescence in control and S363A conditions for the first 5 minutes following DAMGO addition. Values are normalized to the first frame following DAMGO addition. n=6 cells for Ctrl; n=15 cells for S363A. (C) 9.04 µm x 9.04 µm ROI of HEK293 cell expressing SpH MOR WT or S363A(treated with gallein) in TIRF +/- DAMGO addition. SpH-MOR clusters on the cell surface in response to DAMGO before internalizing in both control and S363A + gallein conditions. Right panel: Quantification of % normalized fluorescence in control and S363A + gallein conditions for the first 5 minutes following DAMGO addition. Values are normalized to the first frame following DAMGO addition. n=6 cells for Ctrl; n=10 cells for S363A + gallein. (D)9.04 µm x 9.04 µm ROI of HEK293 cell expressing SpH MOR WT or S363D +/- DAMGO addition. SpH-MOR clusters on the cell surface in response to DAMGO before internalizing in both control and S363D conditions. Right panel: Quantification of % normalized fluorescence in control and S363D conditions for the first 5 minutes following DAMGO addition. Values are normalized to the first frame following DAMGO addition. n=5 cells for Ctrl; n=9 cells for S363D.

Supplemental Figure 3.2

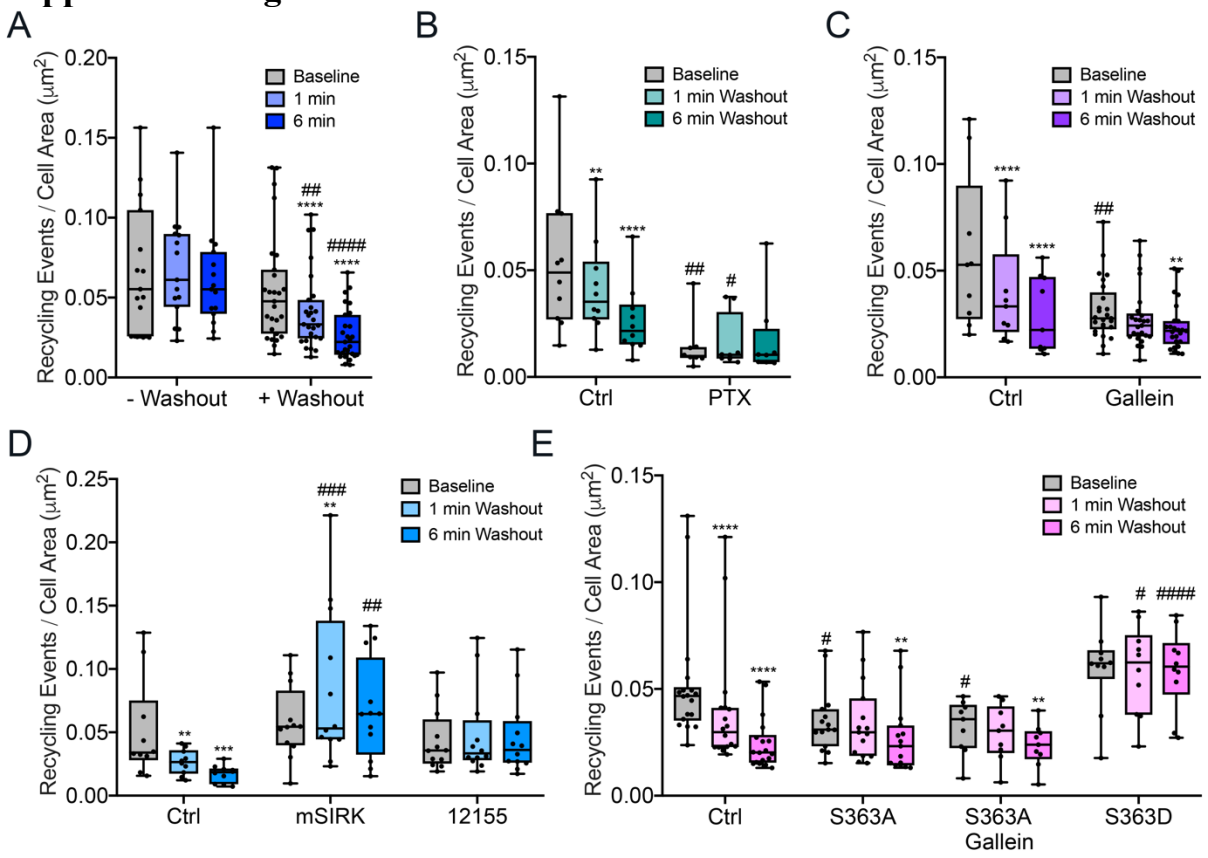

Supplemental Figure 3.2. Raw MOR recycling events across all conditions.
"*" denotes statistical significance ($p<0.05$) within family (condition) in Two-Way ANOVA.

"#" denotes statistical significance ($p<0.05$) between families at the same time points.
(A) Number of recycling events per cell area (μm^2) over time in response to DAMGO in +/- Washout conditions. $p>0.9999$ for - Washout baseline vs. - Washout 1 min; $p=0.3063$ for - Washout baseline vs. - Washout 6 min. $p<0.0001$ for + Washout baseline vs. + Washout 1 min; $p<0.0001$ for + Washout baseline vs. + Washout 6 min. Unpaired t test: $p=0.2854$ for - Washout baseline vs. + Washout baseline; $p=0.0042$ for - Washout 1 min vs. + Washout 1 min; $p<0.0001$ for - Washout 6 min vs. + Washout 6 min; - Washout: n=15 cells; + Washout: n=27 cells
(B) Number of recycling events per cell area (μm^2) over time in response to DAMGO washout in control or PTX conditions. $p=0.0090$ for Ctrl baseline vs. Ctrl 1 min; $p<0.0001$ for Ctrl baseline vs. Ctrl 6 min. $p=0.8650$ for PTX baseline vs. PTX 1 min; $p=0.6789$ for PTX baseline vs. PTX 6 min. Unpaired t test: $p=0.0064$ for Ctrl baseline vs. PTX baseline; $p=0.0127$ for Ctrl 1 min vs. PTX 1 min; $p=0.3216$ for Ctrl 6 min vs. PTX 6 min. Ctrl: n=10 cells; PTX: n=8 cells
(C) Number of recycling events per cell area (μm^2) over time in response to DAMGO washout in control or gallein conditions. $p<0.0001$ for Ctrl baseline vs. Ctrl 1 min; $p<0.0001$ for Ctrl baseline vs. Ctrl 6 min; $p=0.1561$ for gallein baseline vs. gallein 1 min; $p=0.0018$ for gallein baseline vs. gallein 6 min. Unpaired t test: $p=0.0046$ for Ctrl baseline vs. gallein baseline; $p=0.0778$ for Ctrl 1 min vs. gallein 1 min; $p=0.2675$ for Ctrl 6 min vs. gallein 6 min. Ctrl: n=9 cells; Gallein n=25 cells (D) Number of recycling events per cell area (μm^2) over time in response to DAMGO washout in control, mSIRK, or 12155 conditions. $p=0.0083$ for Ctrl baseline vs. Ctrl 1 min; $p=0.0002$ for Ctrl baseline vs. Ctrl 6 min; $p=0.0026$ for mSIRK baseline vs. mSIRK 1 min; $p=0.3378$ for mSIRK baseline vs. mSIRK 6 min; $p=0.7501$ for 12155 baseline vs. 12155 1 min; $p=0.9174$ for 12155 baseline vs. 12155 6 min. Sidak's multiple comparisons test: $p=0.8845$ for Ctrl baseline vs. mSIRK baseline; $p=0.8397$ for Ctrl baseline vs. 12155 baseline; $p=0.0005$ for Ctrl 1 min vs. mSIRK 1 min; $p=0.2760$ for Ctrl 1 min vs. 12155 1 min; $p=0.0021$ for Ctrl 6 min vs. mSIRK 6 min; $p=0.1079$ for Ctrl 6 min vs. 12155 6 min. Ctrl: n=10 cells; mSIRK: n=12 cells; 12155: n=12 cells (E) Number of recycling events per cell area (μm^2) over time in response to DAMGO washout in control, S363A, S363A + gallein, or S363D conditions. $p<0.0001$ for Ctrl baseline vs. Ctrl 1 min; $p<0.0001$ for Ctrl baseline vs. Ctrl 6 min; $p=0.9682$ for S363A baseline vs. S363A 1 min; $p=0.0047$ for S363A baseline vs. S363A 6 min; $p=0.1553$ for S363A + gallein baseline vs. S363A + gallein 1 min; $p=0.0093$ for S363A + gallein baseline vs. S363A + gallein 6 min; $p=0.9539$ for S363D baseline vs. S363D 1 min; $p=0.9391$ for S363D baseline vs. S363D 6 min; Sidak's multiple comparisons test: $p=0.0392$ for Ctrl baseline vs. S363A baseline; $p=0.0429$ for Ctrl baseline vs. S363A + gallein baseline; $p=0.7023$ for Ctrl baseline vs. S363D baseline; $p=0.8718$ for Ctrl 1 min vs. S363A 1 min; $p=0.5442$ for Ctrl 1 min vs. S363A + gallein 1 min; $p=0.0370$ for Ctrl 1 min vs. S363D; $p=0.9752$ for Ctrl 6 min vs. S363A 6 min; $p=0.9990$ for Ctrl 6 min vs. S363A + gallein 6 min; $p<0.0001$ for Ctrl 6 min vs. S363D 6 min. Ctrl: n=18 cells; S363A: n=15 cells; S363A + gallein: n=9 cells; S363D: n=10 cells.

3.3 Discussion

We identify a positive feedback mechanism that mediates homologous regulation of MOR recycling. Activation of MOR initiates a signaling cascade via G$\beta\gamma$ and PKC that increases the rate of MOR recycling. This increase in recycling requires the phosphorylation of MOR at serine 363, a site that can be directly phosphorylated by PKC.

Our results provide new information on how receptor phosphorylation can regulate MOR trafficking. Phosphorylation of MOR, mainly at the TSST (residues 354–357) and the STANT (residues 375–379) motifs, by multiple kinases, has been studied extensively for its role in receptor internalization and desensitization (Williams et al., 2013; Arttamangkul et al., 2018; Miess et al., 2018; Kliewer et al., 2019). PKC can phosphorylate MOR at multiple sites, but the residues that are phosphorylated in vivo and the role of PKC phosphorylation in regulating MOR trafficking and function are still being investigated (Doll et al., 2011; Feng et al., 2011; Yousuf et al., 2015). The serine 363 residue that we identified as critical for regulating MOR recycling can be phosphorylated in vitro by PKCε, although whether this is the primary enzyme that phosphorylates it in vivo is not clear (Doll et al., 2011; Feng et al., 2011). PKC activation by MOR on the plasma membrane varies between different agonists used (Halls et al., 2016). Further, activation of PKC downstream of G$\beta\gamma$ can regulate receptor localization to different domains on the plasma membrane (Halls et al., 2016). Once internalized, the phosphorylation of MOR at specific residues can determine receptor sorting between Rab4- and Rab11-dependent recycling compartments (Wang et al., 2008). In this context, the rate and extent of dynamic changes in phosphorylation at S363 of MOR is not clear. In biochemical

assays, the bulk levels of S363 phosphorylation do not change after agonist treatment (Lau et al., 2011; Moulédous et al., 2015). Considering our data, that this site is required and sufficient to mediate agonist-mediated increase in MOR recycling, it is possible that phosphorylation at this site is locally and transiently regulated in response to receptor activation.

Regulation of MOR recycling by G$\beta\gamma$-, PLC-, and PKC-mediated receptor phosphorylation is a novel example of homologous regulation of GPCR recycling. Receptor phosphorylation has been studied mainly in the context of receptor desensitization and endocytosis, but phosphorylation can regulate the recycling of other receptors such as the β adrenergic receptors. In the case of the β2-adrenoreceptor (β2AR), a prototypical Gα_s-coupled receptor, receptor recycling is regulated by receptor phosphorylation downstream of receptor signaling. However, unlike for MOR, agonist stimulation decreased the postendocytic recycling of β2AR. This decrease required PKA-mediated phosphorylation of β2AR on serine 345/346 (Yudowski et al., 2009; Vistein and Puthenveedu, 2013). PKA signaling, however, does not play a role in MOR recycling in our cells (Fig. 2F). MOR recycling in striatal neurons has been reported to be inhibited by forskolin, although PKA was not directly tested (Roman-Vendrell et al., 2012). This difference could reflect differences in mechanisms of recycling of β2AR and MOR, which might also differ between cell types. In HEK cells, β2AR recycles via a specialized set of endosomal tubules, termed ASRT tubules, characterized by the presence of an actin-SNX-retromer complex (Puthenveedu et al., 2010; Temkin et al., 2011). β2AR sorting into these tubules requires the interaction of a C-terminal post-synaptic density-95/disc large tumor suppressor/zonula occludens-1 (PDZ) ligand sequence with a set of PDZ-containing proteins, which ultimately link the receptor to the endosomal actin cytoskeleton (Temkin et al., 2011). MOR seems to recycle via a distinct mechanism, although the mechanism itself is not understood. MOR recycling

requires a unique "bileucine" sequence on the receptor C-terminal tail. There is no evidence that this sequence interacts with the PDZ-containing proteins or actin. Further, β2AR and MOR might also use different sets of Rab proteins to recycle (Wang et al., 2008). The use of both Gα- and G$\beta\gamma$-mediated pathways to phosphorylate receptor cargo via distinct kinases to regulate recycling of receptors through potentially distinct pathways suggests that homologous regulation of receptor recycling by modifying receptor phosphorylation states is a conserved mechanism on a global level, although the specific mechanisms might vary between different GPCRs.

The changes we observe in MOR recycling based on PKC-mediated receptor phosphorylation could have direct effects on MOR signaling and function. Many canonical GPCRs have been shown to signal from endosomes in the recent past, raising the idea that endosomal signaling is the norm rather than the exception (Calebiro et al., 2009; Vilardaga et al., 2014; Bowman et al., 2016; Jensen et al., 2017; Eichel and von Zastrow, 2018). When localized to specific microdomains on the endosome, β2AR activates the transcription of a complement of genes that are distinct from those activated by signaling from the plasma membrane (Tsvetanova and von Zastrow, 2014; Bowman et al., 2016). Endosomal signaling of the neurokinin-1 receptor in spinal neurons, or the calcitonin gene-related peptide-targeted calcitonin-like receptor, contributes to nociception (Jensen et al., 2017; Yarwood et al., 2017; Weinberg et al., 2019). Whether MOR signaling from endosomes has a distinct signaling consequence is less clear. However, increased recycling of MOR, induced by neurokinin-1 receptor signaling, can decrease acute tolerance to opioids, suggesting that the rate of recycling can regulate opioid physiology (Bowman et al., 2015). PKC-mediated phosphorylation of MOR could therefore serve as a convergence point for both homologous regulation of MOR recycling by G$\beta\gamma$ and heterologous regulation by other signaling pathways. Importantly, considering emerging data that the precise

location of receptors could dictate PKC-mediated phosphorylation of MOR, this could regulate both the rate of resensitization as well as the spatial encoding of opioid signaling, which has emerged as an exciting area of study in the recent past (Sorkin and von Zastrow, 2009; Tsvetanova and von Zastrow, 2014; Bowman et al., 2016; Eichel and von Zastrow, 2018). Similar feedback loops may serve as templates for adaptive self-regulation of signaling for many GPCRs, although the specific mechanisms may vary between different receptors. Understanding the regulation of GPCR trafficking, using assays that can directly detect and measure these dynamic events in real time, will allow us to better analyze the relationship between receptor trafficking and the spatiotemporal aspects of GPCR signaling.

3.4 Materials and Methods

Reagents, Constructs, and Cells.

[D-Ala2, N-MePhe4, Gly-ol]-enkephalin (DAMGO; used at 10 μM), naltrexone (10 μM), pertussis toxin (100 ng/ml, overnight treatment), forskolin (10 μM), KT5720 (1 μM), myr-SIRKALNILGYPDYD-OH (mSIRK; 10 μM), U73122 (10 μM), and chelerythrine (5 μM) were purchased from Sigma-Aldrich (St. Louis, MO). Gallein (20 μM, 30 minute treatment), U73343 (10 μM), and Gö6983 (5 μM) were purchased from Tocris Bioscience. Compound 12155 (10 μM) was provided by Dr. Alan Smrcka (University of Michigan). Stable nonclonal HEK293 cells (American Type Culture Collection CRL-1573) expressing superecliptic phluorin (SpH)-MOR were selected in Geneticin (Invitrogen) and grown in Dulbecco's modified Eagle's medium (Hyclone) + 10% fetal bovine serum (Gibco). The SpH-MOR-S363A point mutant thereof has been described previously (Soohoo and Puthenveedu, 2013; Bowman et al., 2015).

SpH-MOR-S363D was generated by Q5 Site-Directed Mutagenesis Kit (New England Biolabs) using ACAGCAAAACGATGCTCGAATCCG as the forward primer and TCGATTGTGGAG GAAGTTG as the reverse primer.

Live Cell Imaging.

Cells were passed to 25-mm glass coverslips coated with poly-D-lysine and imaged 2 days later. Cells were imaged live in Leibovitz L15 imaging medium (Gibco) and 1% fetal bovine serum at 37°C in a temperature- and CO_2-controlled chamber. A Nikon Eclipse Ti automated inverted microscope with a 60×/1.49 N.A. total internal reflection fluorescence objective and confocal 20×/0.75 N.A. objective was used for imaging. Images were acquired with an iXon+ 897 electron-multiplying charge-coupled device camera (Andor, Belfast, UK) with a solid-state laser of 488 nm as a light source. Images were scrambled using a scrambler.py script (https://gist.github.com/SavinaRoja/1629319) before analyzing them in FIJI (National Institutes of Health) (Schindelin et al., 2012).

Quantification of Individual Recycling Events.

HEK293 cells stably expressing SpH-MOR or its mutants were treated with DAMGO for 5 minutes to induce receptor clustering and internalization at 37°C. Receptor clustering was visualized by acquiring an image every 3 seconds for 5 minutes. A baseline recycling movie was acquired at 10 Hz for 1 minute using total internal reflection fluorescence microscopy, followed by a washout with antagonist (naltrexone). Subsequent movies were collected 1 and 6 minutes after washout. The number of individual exocytic recycling events in each movie was manually scored. The box plots display the median and the entire range with outliers excluded. To evaluate the effect of agonist washout on the frequency of recycling events between treatment conditions,

two-way repeated-measures ANOVAs were conducted on the raw recycling rates followed by post hoc comparisons of means within the treatment condition to the baseline recycling rate. These tests were conducted separately for each of the sets of conditions shown in Figs. 1D; 2D; 3, A and C; and 4C. Supplemental Figure 2. To compare the magnitude of the washout effect between treatment conditions, recycling events for each cell were normalized to that cell's recycling rate in the baseline movie. The mean normalized recycling rate was then compared between conditions of interest using either a one-way ANOVA followed by the indicated post hoc comparisons using Dunnett's multiple comparisons correction (Figures 3.1E, 3.3D, and 3.4D) or a single paired Student's *t* test when only two conditions were evaluated (Figures 3.2E and 3.3B). When testing whether a pharmacological treatment was able to perturb the basal rate of recycling, the normalized recycling events were compared with a theoretical mean of 100% using a single-sample Student's *t* test (Figures 3.2F, 3.3A and B).

Ensemble Recycling Assay.

To measure ensemble recycling, receptor surface levels were imaged using confocal microscopy with a 20× objective and 488-nm laser. Images were collected at 30-second intervals for 20 different fields. Baseline recordings for 2 minutes (four frames) were collected before the addition of DAMGO. After the addition of agonist, images were collected for 15 minutes. After 15 minutes, agonist was removed. The cells were rinsed with fresh imaging medium, and antagonist (naltrexone) was added to the new medium. After agonist washout, images were collected for another 15 minutes. Fluorescence intensities were corrected by a background threshold and normalized by the average fluorescence of the baseline four frames collected before DAMGO treatment. Surface fluorescence analysis was conducted using an ImageJ Macro automated script (National Institutes of Health) (https://zenodo.org/record/2645754).

Fluorescence recovery/loss ratios after washout were quantified by normalizing the fluorescence values after washout to the total fluorescence lost before washout. Cell fields that did not respond to DAMGO treatment were excluded from analysis. Statistical significance was determined by using a one-way ANOVA comparing endpoints of all conditions to the control condition, followed by post hoc comparisons between all means (Figure 3.3H).

3.5 References

Arttamangkul S, Heinz DA, Bunzow JR, Song X, and Williams JT (2018) Cellular tolerance at the m-opioid receptor is phosphorylation dependent. eLife 7:e34989.

Bahouth SW and Nooh MM (2017) Barcoding of GPCR trafficking and signaling through the various trafficking roadmaps by compartmentalized signaling networks. Cell Signal 36:42–55.

Bonacci TM, Mathews JL, Yuan C, Lehmann DM, Malik S, Wu D, Font JL, Bidlack JM, and Smrcka AV (2006) Differential targeting of Gbetagamma-subunit signaling with small molecules. Science 312:443–446.

Bowman SL and Puthenveedu MA (2015) Postendocytic sorting of adrenergic and opioid receptors: new mechanisms and functions. Prog Mol Biol Transl Sci 132: 189–206.

Bowman SL, Shiwarski DJ, and Puthenveedu MA (2016) Distinct G protein-coupled receptor recycling pathways allow spatial control of downstream G protein signaling. J Cell Biol 214:797–806.

Bowman SL, Soohoo AL, Shiwarski DJ, Schulz S, Pradhan AA, and Puthenveedu MA (2015) Cell-autonomous regulation of Mu-opioid receptor recycling by substance P. Cell Rep 10:1925–1936.

Broadbent D, Ahmadzai MM, Kammala AK, Yang C, Occhiuto C, Das R, and Subramanian H (2017) Roles of NHERF family of PDZ-binding proteins in regulating GPCR functions. Adv Immunol 136:353–385.

Caengprasath N and Hanyaloglu AC (2019) Hardwiring wire-less networks: spatially encoded GPCR signaling in endocrine systems. Curr Opin Cell Biol 57:77–82.

Calebiro D, Nikolaev VO, Gagliani MC, de Filippis T, Dees C, Tacchetti C, Persani L, and Lohse MJ (2009) Persistent cAMP-signals triggered by internalized G-protein- coupled receptors. PLoS Biol 7:e1000172.

Doll C, Konietzko J, Pöll F, Koch T, Höllt V, and Schulz S (2011) Agonist-selective patterns of m-opioid receptor phosphorylation revealed by phosphosite-specific antibodies. Br J Pharmacol 164:298–307.

Dunn HA and Ferguson SS (2015) PDZ Protein regulation of G protein–coupled receptor trafficking and signaling pathways. Mol Pharmacol 88:624–639.

Eichel K and von Zastrow M (2018) Subcellular organization of GPCR signaling. Trends Pharmacol Sci 39:200–208.

Feng B, Li Z, and Wang JB (2011) Protein kinase C-mediated phosphorylation of the m-opioid receptor and its effects on receptor signaling. Mol Pharmacol 79:768–775.

Ferrandon S, Feinstein TN, Castro M, Wang B, Bouley R, Potts JT, Gardella TJ, and Vilardaga JP (2009) Sustained cyclic AMP production by parathyroid hormone receptor endocytosis. Nat Chem Biol 5:734–742.

Gondin AB, Halls ML, Canals M, and Briddon SJ (2019) GRK Mediates m-Opioid Receptor Plasma Membrane Reorganization. Front Mol Neurosci 12.

Goubaeva F, Ghosh M, Malik S, Yang J, Hinkle PM, Griendling KK, Neubig RR, and Smrcka AV (2003) Stimulation of cellular signaling and G protein subunit dissociation by G protein betagamma subunit-binding peptides. J Biol Chem 278: 19634–19641.

Halls ML, Yeatman HR, Nowell CJ, Thompson GL, Gondin AB, Civciristov S, Bunnett NW, Lambert NA, Poole DP, and Canals M (2016) Plasma membrane localization of the m-opioid receptor controls spatiotemporal signaling. Sci Signal 9:ra16.

Irannejad R, Tomshine JC, Tomshine JR, Chevalier M, Mahoney JP, Steyaert J, Rasmussen SG, Sunahara RK, El-Samad H, Huang B, et al. (2013) Conformational biosensors reveal GPCR signalling from endosomes. Nature 495:534–538.

Jensen DD, Lieu T, Halls ML, Veldhuis NA, Imlach WL, Mai QN, Poole DP, Quach T, Aurelio L, Conner J, et al. (2017) Neurokinin 1 receptor signaling in endosomes mediates sustained nociception and is a viable therapeutic target for prolonged pain relief. Sci Transl Med 9.

Just S, Illing S, Trester-Zedlitz M, Lau EK, Kotowski SJ, Miess E, Mann A, Doll C, Trinidad JC, Burlingame AL, et al. (2012) Differentiation of Opioid Drug Effects by Hierarchical Multi-Site Phosphorylation. Mol Pharmacol 83 (3):633–639.

Kliewer A, Schmiedel F, Sianati S, Bailey A, Bateman JT, Levitt ES, Williams JT, Christie MJ, and Schulz S (2019) Phosphorylation-deficient G-protein-biased m-opioid receptors improve analgesia and diminish tolerance but worsen opioid side effects. Nat Commun 10:367.

Lau EK, Trester-Zedlitz M, Trinidad JC, Kotowski SJ, Krutchinsky AN, Burlingame AL, and von Zastrow M (2011) Quantitative encoding of the effect of a partial ag- onist on individual opioid receptors by multisite phosphorylation and threshold detection. Sci Signal 4:ra52.

Lefkowitz RJ, Pitcher J, Krueger K, and Daaka Y (1997) Mechanisms of B-adrenergic receptor desensitization. Advances in Pharmacology 42:416–420.

Lehmann DM, Seneviratne AMPB, and Smrcka AV (2008) Small molecule disruption of G protein b g subunit signaling inhibits neutrophil chemotaxis and in- flammation. Mol Pharmacol 73:410–418.

Logan T, Bendor J, Toupin C, Thorn K, and Edwards RH (2017) a-Synuclein pro- motes dilation of the exocytotic fusion pore. Nat Neurosci 20:681–689.

Marchese A, Paing MM, Temple BRS, and Trejo J (2008) G protein-coupled receptor sorting to endosomes and lysosomes. Annu Rev Pharmacol Toxicol 48:601–629. Miess E, Gondin AB, Yousuf A, Steinborn R, Mösslein N, Yang Y, Goldner M, Ruland

JG, Bunemann M, Krasel C, et al. (2018) Multisite phosphorylation is required for sustained interaction with GRKs and arrestins during rapid m-opioid receptor desensitization. Sci Signal 11.

Moulédous L, Froment C, Burlet-Schiltz O, Schulz S, and Mollereau C (2015) Phosphoproteomic analysis of the mouse brain mu-opioid (MOP) receptor. FEBS Lett 589:2401–2408.

Pierce KL, Premont RT, and Lefkowitz RJ (2002) Seven-transmembrane receptors. Nat Rev Mol Cell Biol 3:639–650.

Puthenveedu MA, Lauffer B, Temkin P, Vistein R, Carlton P, Thorn K, Taunton J, Weiner OD, Parton RG, and von Zastrow M (2010) Sequence-dependent sorting of recycling proteins by actin-stabilized endosomal microdomains. Cell 143:761–773.

Roman-Vendrell C, Yu YJ, and Yudowski GA (2012) Fast modulation of m-opioid receptor (MOR) recycling is mediated by receptor agonists. J Biol Chem 287: 14782–14791.

Romero G, von Zastrow M, and Friedman PA (2011) Role of PDZ proteins in regu- lating trafficking, signaling, and function of GPCRs: means, motif, and opportu- nity. Adv Pharmacol 62:279–314.

Sankaranarayanan S, De Angelis D, Rothman JE, and Ryan TA (2000) The use of pHluorins for optical measurements of presynaptic activity. Biophys J 79: 2199–2208.

Schindelin J, Arganda-Carreras I, Frise E, Kaynig V, Longair M, Pietzsch T, Pre- ibisch S, Rueden C, Saalfeld S, Schmid B, et al. (2012) Fiji: an open-source platform for biological-image analysis. Nat Methods 9:676–682.

Soohoo AL and Puthenveedu MA (2013) Divergent modes for cargo-mediated control of clathrin-coated pit dynamics. Mol Biol Cell 24:1725–1734, S1–S12.

Sorkin A and von Zastrow M (2009) Endocytosis and signalling: intertwining mo- lecular networks. Nat Rev Mol Cell Biol 10:609–622.

Sriram K and Insel PA (2018) G protein-coupled receptors as targets for approved drugs: how many targets and how many drugs? Mol Pharmacol 93:251–258.

Surve CR, Lehmann D, and Smrcka AV (2014) A chemical biology approach dem- onstrates G protein bg subunits are sufficient to mediate directional neutrophil chemotaxis. J Biol Chem 289:17791–17801.

Tanowitz M and von Zastrow M (2003) A novel endocytic recycling signal that dis- tinguishes the membrane trafficking of naturally occurring opioid receptors. J Biol Chem 278:45978–45986.

Temkin P, Lauffer B, Jäger S, Cimermancic P, Krogan NJ, and von Zastrow M (2011) SNX27 mediates retromer tubule entry and endosome-to-plasma membrane traf- ficking of signalling receptors. Nat Cell Biol 13:715–721.

Thomsen ARB, Jensen DD, Hicks GA, and Bunnett NW (2018) Therapeutic tar- geting of endosomal G-protein-coupled receptors. Trends Pharmacol Sci 39: 879–891.

Tsvetanova NG and von Zastrow M (2014) Spatial encoding of cyclic AMP signaling specificity by GPCR endocytosis. Nat Chem Biol 10:1061–1065.

Vilardaga JP, Jean-Alphonse FG, and Gardella TJ (2014) Endosomal generation of cAMP in GPCR signaling. Nat Chem Biol 10:700–706.

Vistein R and Puthenveedu MA (2013) Reprogramming of G protein-coupled receptor recycling and signaling by a kinase switch. Proc Natl Acad Sci USA 110: 15289–15294.

Wang F, Chen X, Zhang X, and Ma L (2008) Phosphorylation state of mu-opioid receptor determines the alternative recycling of receptor via Rab4 or Rab11 pathway. Mol Endocrinol 22:1881–1892.

Weinberg ZY, Crilly SE, and Puthenveedu MA (2019) Spatial encoding of GPCR signaling in the nervous system. Curr Opin Cell Biol 57:83–89.

Weinberg ZY, Zajac AS, Phan T, Shiwarski DJ, and Puthenveedu MA (2017) Sequence-specific regulation of endocytic lifetimes modulates arrestin-mediated signaling at the m opioid receptor. Mol Pharmacol 91:416–427.

Williams JT, Ingram SL, Henderson G, Chavkin C, von Zastrow M, Schulz S, Koch T, Evans CJ, and Christie MJ (2013) Regulation of m-opioid receptors: desensitization, phosphorylation, internalization, and tolerance. Pharmacol Rev 65:223–254.

Yarwood RE, Imlach WL, Lieu T, Veldhuis NA, Jensen DD, Klein Herenbrink C, Aurelio L, Cai Z, Christie MJ, Poole DP, et al. (2017) Endosomal signaling of the receptor for calcitonin gene-related peptide mediates pain transmission. Proc Natl Acad Sci USA 114:12309–12314.

Yousuf A, Miess E, Sianati S, Du YP, Schulz S, and Christie MJ (2015) Role of phosphorylation sites in desensitization of m-opioid receptor. Mol Pharmacol 88:825–835. Yudowski GA, Puthenveedu MA, Henry AG, and von Zastrow M (2009) Cargo- mediated regulation of a rapid Rab4-dependent recycling pathway. Mol Biol Cell

20:2774–2784.
Yudowski GA, Puthenveedu MA, and von Zastrow M (2006) Distinct modes of regulated receptor insertion to the somatodendritic plasma membrane. Nat Neurosci 9:622–627.

Chapter 4: Regulation of Mu Opioid Receptor Trafficking and Signaling via receptor Phosphorylation

Abstract

Dynamic phosphorylation of the mu opioid receptor (MOR) is an important regulatory mechanism for receptor trafficking and signaling. Specifically phosphorylation sites on the c-terminal tail have been implicated in changing receptor sorting in response to agonist activation. Here we investigate how two key phosphorylation sites serine363 (S363) and threonine370 (T370) may affect MOR hierarchal sorting and signaling in response to opioid peptide activation.

4.1 Introduction

Post-translational modifications of G protein-coupled receptors (GPCRs) are key determinants for receptor function. Agonist-dependent phosphorylation of the C-terminus is one major regulatory post-translational modification. The physiologically relevant, mu opioid receptor (MOR) contains several phosphorylation sites in the C-terminal cytoplasmic tail located in the conserved ^{370}TREHPSTANT^{379} sequence (Mann et al., 2015). Previous work from our lab suggests hierarchical sorting of MOR based on its phosphorylation state. As mentioned previously, phosphorylation at S363 regulates recycling back to the cell surface in an initial G$\beta\gamma$-dependent mechanism (Kunselman et al., 2019). As another example of phosphoregulatory sorting, T370A receptors sort primarily into actin-positive domains, suggesting a role for C-

terminal tail phosphorylation in receptor endosomal distribution (Bowman, 2016). In light of previous work highlighted above with the kappa opioid receptor (KOR) and for the B2AR intracellular signaling (Kunselman et al., 2021; Bowman et al., 2016), we wanted to test the role phosphorylation had in regulating MOR signaling profiles and its activity in endosomes.

4.2 Results

To assess the role of phosphorylation at sites S363 and T370 on MOR recycling, we tested recycling in three stable HEK293 cell lines that express either wildtype (WT), S363A, and T370A SpH-MOR, which have been previously reported in Kunselman et al., 2019 and Bowman et al., 2015. We imaged cells using TIR-FM. After 5 min of DAMGO treatment, we photobleached the cell surface and recorded movies for 1 min at 10Hz. The number of exocytic events were recorded for each condition and normalized by cell area to determine the initial recycling rate. The initial rates of recycling were not statistically different between WT and T370A recycling, while S363A had decreased recycling (Figure 4.1A). Additionally, cells expressing the T370A receptor showed decreased recycling when treated with a G$\beta\gamma$ inhibitor, gallein, (Figure 4.1B) similarly to the WT receptor, while S363A showed gallein insensitivity as reported in Kunselman et al., 2019.

Figure 4.1

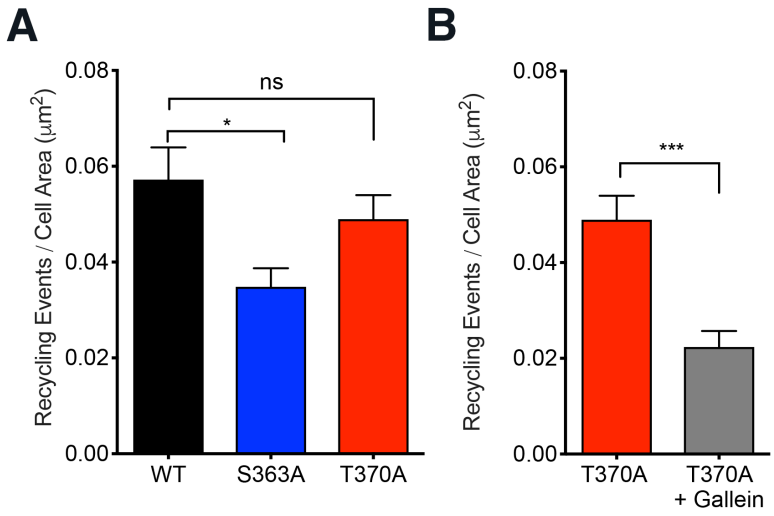

Figure 4.1. Recycling rates for wildtype MOR and phosphodeficient mutants S363A and T370A in HEK293 cells.

(A) HEK293 cells stably expressing WT, S363A, or T370A SpH-MOR. Number of recycling events per cell area (square micrometer) over time in response to 5 min DAMGO treatment. (B) Number of recycling events per cell area (square micrometer) over time in response to 5 min DAMGO treatment in cells expressing T370A SpH-MOR treated with or without 30 min Gallein pretreatment.

Next we wanted to test if these phosphodeficient mutants were capable of signaling from intracellular compartments. To do this we used three stable HEK293 cells expressing either WT, S363A, or T370A FLAG-MOR. We transfected Nb39-YFP, a nanobody that recognizes that active conformation into each cell line to examine if MOR was in the activate conformation after DAMGO treatment. After 20 minutes of DAMGO, Nb39 colocalizes to endosomal receptor in all three conditions (Figure 4.2A). To quantify colocalization, we scored the total number of MOR positive endosomes using an Image J macro "Object Picker" to determine the percent colocalization with Nb39, which showed that all conditions had similar Nb39 recruitment (Figure 4.2B).

Figure 4.2

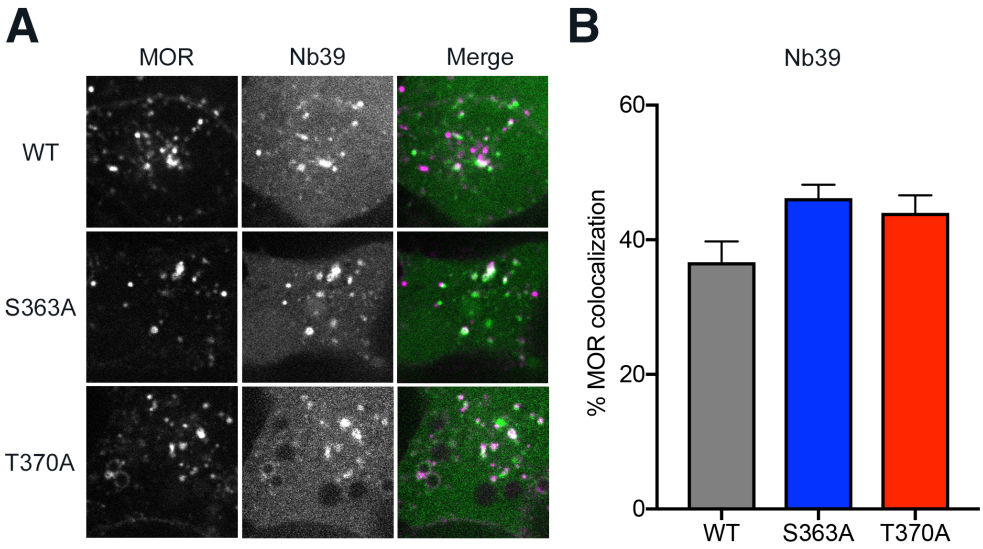

Figure 4.2. Endosomal recruitment of active conformation biosensor (Nb39) for wildtype MOR and phosphodeficient mutants S363A and T370A in HEK293 cells.
(A) HEK293 cells stably expressing WT, S363A, or T370A FLAG-MOR transfected with Nb39-YFP. Representative images show endosomal FLAG-MOR colocalized with Nb39 after 20 min DAMGO treatment. (B) The percent colocalization of Nb39 with total MOR endosomes is quantified for each WT, S363A, and T370A expressing cells.

We next wanted to test if the phospho-deficient mutants had altered extracellular signal-regulated kinases (ERK) signaling, based on previous data, which shows that different opioid ligands and the bileucine receptor sequence regulate lifetimes at the cell surface and ERK signaling (Weinberg et al., 2017). To do this we used three stable HEK293 cells expressing either WT, S363A, or T370A FLAG-MOR. We treated cells with +/- DAMGO for 5 minutes and then blotted for phosphoERK and total ERK to measure activation of ERK signaling. The S363A mutant showed increased phosphoERK in comparison to the T370A mutant and WT receptor (Figure 4.3A and B).

Figure 4.3

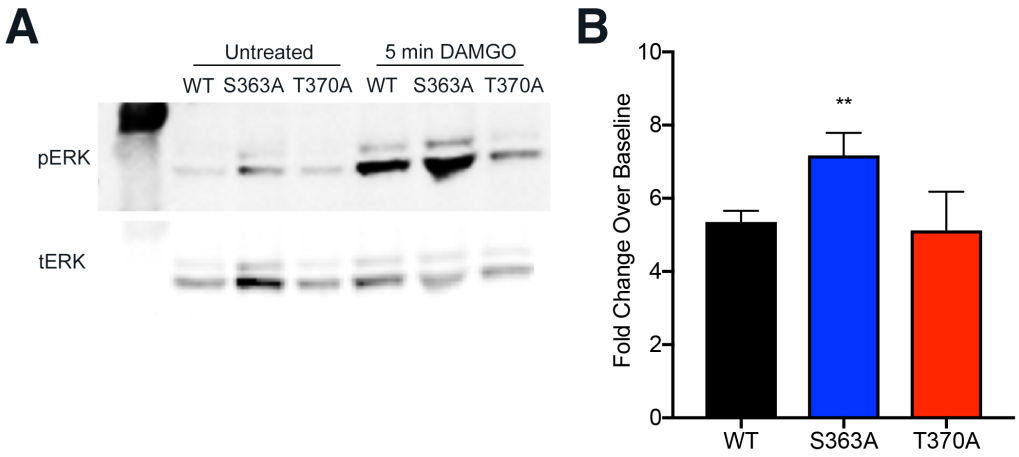

Figure 4.3. Phosphorylated ERK after activation of wildtype MOR and phosphodeficient mutants S363A and T370A in HEK293 cells.
(A) HEK293 cells stably expressing WT, S363A, or T370A FLAG-MOR were treated with 5 min DAMGO and phosphoERK (pERK) levels were probed in an immunoblot. The membrane was stripped and reprobed with totalERK (tERK). (B) Fold change over baseline was calculated for each receptor condition by normalizing the pERK signal over the tERK signal for DAMGO treated conditions to the untreated conditions.

4.3 Discussion

These experiments suggest that there are some key differences in trafficking and signaling between the phosphorylation mutants. The S363A mutant shows decreased initial recycling and increased ERK signaling, while the T370A mutant is more similar to the wildtype receptor in readouts for recycling and ERK signaling. Wildtype MOR, S363A, and T370A all show similar levels of Nb39 recruitment to endosomal compartments after 20 minutes of DAMGO treatment. However, there may be differences detected under other conditions, such as different cell-types or changes in the signaling environment. Interestingly, T370A receptors appear to sort primarily into actin-positive domains, which further suggests that phosphorylation may regulate hierarchical receptor sorting (Bowman, 2016).

Another interesting question to address is the stage at which receptor phosphorylation is occurring during endocytosis and whether that correlates with distinct sorting throughout the endolysosomal pathway. Previous studies that used phospho-antibodies developed to recognize these specific sites showed that S363 is constitutively phosphorylated, while T370 phosphorylation is dependent on the agonist (Doll et al., 2011). However, phosphorylation at S363 does occur in a homologous mechanism regulated by DAMGO activation (Kunselman et al., 2019), suggesting that these sites could be dynamically regulated at different points after receptor activation and at steady-state. The kinases involved in phosphorylation may also change depending on the cell-type. For example, previous evidence suggests that T370 is phosphorylated by GRK 2/3 in addition to PKC (Mann et al., 2015).

Taken together these findings support additional layers of regulation through changes in MOR phosphorylation. The combination of homologous and heterologous signaling resulting in distinct spatial and temporal phosphorylation may be a mechanism of cellular resensitization in response to numerous external stimuli.

4.4 Materials and Methods

Live Cell Imaging

Cells were imaged using a Nikon TE-2000E inverted microscope with a 60X 1.49 NA TIRF objective, Andor Revolution XD spinning disk confocal system, and 488 and 647 nm solid-state lasers. Cells were imaged in Leibowitz's L15 medium (Gibco), 1% FBS, at 37˚C. Images were acquired using an Andor iXon+ EM-CCD camera using Andor IQ.

Quantification of Individual Recycling Events.

HEK293 cells stably expressing SpH-MOR or its mutants were treated with DAMGO for 5 minutes to induce receptor clustering and internalization at 37°C. Receptor clustering was visualized by acquiring an image every 3 seconds for 5 minutes. A baseline recycling movie was acquired at 10 Hz for 1 minute using total internal reflection fluorescence microscopy, followed by a washout with antagonist (naltrexone). Subsequent movies were collected 1 and 6 minutes after washout. The number of individual exocytic recycling events in each movie was manually scored. The box plots display the median and the entire range with outliers excluded

Immunoblotting

HEK293 cells stably expressing FLAG-MOR (WT, S363A, or T370A) were grown in a PDL coated 12-well plate for 2 days at 37˚C. Cells were for four hours in serum-free media and then treated with 10 μM DAMGO for 5 min. Cells were placed on ice and rinsed twice with PBS containing calcium and magnesium. Cells were directly lysed in the plate using 2 RSB (Bio-Rad, Hercules, CA). Lysates were placed on ice for 5 min and then placed at 95˚C for 5 min. Lysates were run on 10% stain-free gels (BioRad), which were then transferred to nitrocellulose membrane overnight. Membranes were blocked in 5% BSA and then probed with phosphoERK(CST) to detect phosphorylated ERK 1/2 levels in each condition. Blots were developed using the iBright imager for chemiluminescence signal and quantified using FIJI software. Membrane was stripped and probed with total ERK 1/2 (CST) to determine total levels of ERK 1/2 present in the samples. The phospho-ERK signal was normalized to the total ERK signal for each condition. All samples were then normalized to the no treatment control to determine the fold change over baseline for each condition. Five biological replicates were performed. Statistical analysis was performed using two-way ANOVA across time and drug treatment.

4.5 References

Bowman SL (2016) Regulation of G protein-coupled receptor trafficking by downstream signaling kinases, Dissertation

Bowman SL, Shiwarski DJ, and Puthenveedu MA (2016) Distinct G protein-coupled receptor recycling pathways allow spatial control of downstream G protein signaling. J Cell Biol 214:797–806.

Bowman SL, Soohoo AL, Shiwarski DJ, Schulz S, Pradhan AA, and Puthenveedu MA (2015) Cell-autonomous regulation of Mu-opioid receptor recycling by substance P. Cell Rep 10:1925–1936.

Doll, C., Konietzko, J., Pöll, F., and Koch, T., Hollt, V, Schulz, S. (2011). Agonist- selective patterns of μ-opioid receptor phosphorylation revealed by phosphosite-specific antibodies. Br J Pharmacol 164, 298-307.

Kunselman, J. M., Gupta, A., Gomes, I., Devi, L. A., & Puthenveedu, M. A. (2021). Compartment-specific opioid receptor signaling is selectively modulated by Dynorphin peptides. *eLife,* 10, e60270.

Kunselman, J. M., Zajac, A. S., Weinberg, Z. Y., & Puthenveedu, M. A. (2019). Homologous regulation of mu opioid receptor recycling by Gβγ, Protein Kinase C, and receptor phosphorylation. *Molecular Pharmacology*, 96(6), 702-710.

Mann, A., Illing, S., Miess, E., & Schulz, S. (2015). Different mechanisms of homologous and heterologous μ-opioid receptor phosphorylation. *British journal of pharmacology*, *172*(2), 311–316.

Weinberg ZY, Zajac AS, Phan T, Shiwarski DJ, and Puthenveedu MA (2017) Sequence-specific regulation of endocytic lifetimes modulates arrestin-mediated signaling at the m opioid receptor. Mol Pharmacol 91:416–427.

Chapter 5: Conclusions and Future Directions

Together, the data presented in this thesis highlight the mechanisms regulating G protein-coupled receptor (GPCR) function via modulation of receptor trafficking and signaling. Specifically, I investigated the mechanisms underlying differential opioid receptor activity in response to endogenous opioid peptide ligands. In chapter one, I reviewed regulators of GPCR endocytic trafficking and biosynthetic trafficking, which showcased various points of regulation from lipid membrane composition to post-translational modifications of the receptor itself. Additionally, agonist-dependent sorting is an area of particular interest in this dissertation.

In chapter two, I examined kappa opioid receptor (KOR) trafficking and signaling in response to different, yet highly-related, dynorphin peptides. Interestingly, we observed that dynorphin A localizes KOR to lysosomes and drives degradation, while dynorphin B localizes KOR into recycling endosomes and drives recycling. Strikingly, KOR activated by dynorphin A, but not dynorphin B, remains in an active conformation on lysosomes and causes sustained cAMP signaling. This study shows that different endogenous opioid peptides fine-tune KOR signaling by regulating receptor localization to and signaling from different endosomal compartments.

Currently, I am investigating changes in gene expression in the context of spatial signaling in response to different dynorphin treatments. Additionally, changes in the phosphoproteome in response to different agonists may provide insight for functional differences in signaling profiles between peptides. Since many of these peptides are thought to be released from the same vesicles, I am also interested in testing combinatorial effects of several co-released

peptides on receptor trafficking and signaling. Overall this work suggests that physiological systems generate diversity in signaling by inducing different subcellular spatial and temporal profiles of receptors, which should be an important consideration in drug development.

In chapter three, I investigated the relationship between receptor signaling and trafficking by examining mu opioid receptor (MOR) recycling. My findings show that DAMGO-activated MOR initiated downstream signaling via a G$\beta\gamma$, PLC, and PKC pathway, resulting in the phosphorylation of serine 363, which increased MOR recycling. Interestingly, this is in contrast to the mechanism regulating agonist-dependent recycling for the β-2 adrenergic receptor (B2AR), where agonist washout actually increases recycling for B2AR (Vistein and Puthenveedu, 2013). It is unknown if receptor phosphorylation at serine 363 occurs at the plasma membrane or at the endosome. The timing and location of this phosphorylation may play a significant regulatory role in the receptor's post-endocytic sorting and its ability to interact with downstream signaling complexes. This example again highlights the unique trafficking profiles of various GPCRs.

Moreover, previous work from the lab studied the role of serine 363 and threonine 370 in a heterologous PKC signaling model, which further emphasizes the importance of these phosphorylation sites on MOR with respect to receptor trafficking (Bowman et al., 2015). In chapter four, we explored how these sites contributed to endosomal signaling and ERK signaling. I did not observe statistically significant differences between phosphodeficient mutants S363A and T370A in endosomal recruitment of a biosensor that recognizes an active conformation of MOR. However, there may be differential coupling to G proteins and other signaling complexes in addition to differential sorting into endosomal compartments and

microdomains (Crilly et al., 2021; Bowman, 2016). Future studies should investigate how the spatial encoding of signals differs between relevant cell types.

Overall my thesis work provides additional evidence for a hierarchical sorting model for GPCRs leading to spatially distinct signaling outcomes and increases our understanding of receptor physiology.

References

Bowman SL, Soohoo AL, Shiwarski DJ, Schulz S, Pradhan AA, and Puthenveedu MA (2015) Cell-autonomous regulation of Mu-opioid receptor recycling by substance P. Cell Rep 10:1925–1936.

Bowman SL (2016) Regulation of G protein-coupled receptor trafficking by downstream signaling kinases, Dissertation

Crilly, S. E., Ko, W., Weinberg, Z. Y., & Puthenveedu, M. A. (2021). Conformational specificity of opioid receptors is determined by subcellular location irrespective of agonist. *Elife*, *10*, e67478.

Vistein R, Puthenveedu MA: Reprogramming of G protein- coupled receptor recycling and signaling by a kinase switch. Proc Natl Acad Sci USA 2013, 110:15289–15294.